The University of Manitoba

VAPOR PRESSURES AND VAPOR LIQUID EQUILIBRIA IN THREE BINARY MIXTURES UP TO THE CRITICAL REGION

A Thesis
Presented to
The Faculty of Graduate Studies
In Partial Fulfilment
of the Requirements for the Degree of
Doctor of Philosophy

by

Goolam Mohamed Musbally

Winnipeg, Canada

December 1969

c Goolam Mohamed Musbally 1969

TO MY PARENTS

ACKNOWLEDGEMENTS

It is my pleasure to acknowledge my debt of gratitude to Professor A. N. Campbell for his invaluable advice and help during the course of this research. My sincere thanks go to Dr. E. M. Kartzmark for her interest, the many helpful discussions and the encouragement she provided during this period.

I wish to thank Mr. G. Epp, Mr. Howard Griffiths and Mr. B. Easterbrook who fabricated all the glass apparatus. The assistance of Mr. G. Trider and his staff of the Central Instrument Service who showed great patience during the construction of the metal bombs and the shaking mechanism is gratefully acknowledged.

Dr. R. M. Chatterjee's help during the course of this work is gratefully acknowledged. My sincere thanks also go to Mr. S. Y. Lam for his interest and the many helpful discussions we had during the last three years that we shared the same laboratory in the Parker Chemistry Building.

The financial help in the form of a Graduate Assistantship by the University of Manitoba is gratefully acknowledged.

ABSTRACT

The saturation vapor pressure of ten mixtures of the binary systems (1)Acetone-Chloroform, (2)Acetone-Carbon Tetrachloride and (3)Benzene-Carbon Tetrachloride have been determined, from a temperature of 100°C to 230°C for system (1) and from 100°C up to the highest temperature at which liquid and vapor coexist for systems (2) and (3). The system Acetone-Chloroform could not be studied at higher temperatures because of decomposition.

The gas-liquid critical temperatures of the three binary systems have been determined by the disappearance of the meniscus method.

The orthobaric compositions of the vapor-liquid equilibria of the binary systems have been independently measured from 100°C to 180°C for system (1) and from 100°C to the critical region for systems (2) and (3) using a specially designed glass bomb enclosed in a stainless steel bomb.

From the vapor liquid composition curves and the vapor pressure curves at fixed temperatures (100°C, 150°C, 160°C, 170°C and 180°C) the existence of an azeotope in the system Acetone-Chloroform at these temperatures with a composition of 36.2 mole per cent acetone at 100°C was confirmed. It was observed that the composition of the azeotope shifted towards lower acetone content as the temperature was raised. No azeotope was found in the systems Acetone-Carbon Tetrachloride and Benzene-Carbon Tetrachloride in the range of temperature and pressure studied in this research.

The data of the binary systems were treated thermodynamically to yield the liquid phase activity coefficients, and the Redlich-Kwong equation in a modified form, as suggested by Chueh and Prausnitz was used to obtain the fugacity coefficient of a component in the vapor mixture.

Several binary liquid phase parameters, such as the binary interaction constant, Henry's constant and dilation constant have been calculated using the equation of van Laar as modified by Chueh and Prausnitz.

GLOSSARY OF SYMBOLS

a, b	-	constants in van der Waals' equation and Redlich Kwong equation.
Cv, Cp	-	specific heat at constant volume and constant pressure.
f_i	-	fugacity of component i.
f_i^o	-	reference fugacity of component i.
G^E	-	excess Gibbs free energy.
H	-	enthalpy.
$H_{2(1)}$	-	Henry's constant for solute 2 in solvent 1.
K_{ij}	-	characteristic constant for i-j interaction.
n_i	-	number of moles of component i.
N	-	number of components.
P	-	total pressure.
P_c	-	critical pressure.
P^r	-	constant reference pressure.
P^s	-	saturation vapor pressure.
P^o	-	constant reference pressure of zero pressure.
q	-	effective molal volume defined by equations 58 and 59.
R	-	gas constant.
S	-	entropy.
T	-	temperature.
T_c	-	critical temperature.
T_{cM}	-	pseudocritical temperature of a mixture.
T_{cT}	-	true critical temperature of a mixture.
T_M	-	temperature of disappearance of meniscus.
T_R	-	reduced temperature.

v	-	molal volume of the liquid phase or vapor phase.
V_c	-	critical volume.
V_R	-	reduced volume.
$\bar{V}_i^L$	-	partial molal volume of component i in the liquid mixture.
V	-	total volume.
x	-	mole percent in the liquid phase.
y	-	mole percent in the vapor phase.

Subscripts

c	-	critical.
g	-	gas.
i	-	component i.
ij	-	i-j interaction.
L	-	liquid
R	-	reduced property.

Superscripts

E	-	excess property.
id	-	ideal property.
L	-	liquid phase.
(Po)	-	constant reference pressure of zero.
P^r	-	constant reference pressure.
o	-	reference state.
∞	-	infinite dilution.

Greek Letters

α, β, γ	-	critical exponents.
α_{12}	-	interaction constant of molecules 1 and 2.

$\alpha_{22(1)}$	-	self-interaction constant of molecules 2 in the environment of molecules 1.
γ_i	-	activity coefficient of component i.
$\eta_{2(1)}$	-	dilation constant of solute 2 in solvent 1.
θ	-	surface fraction.
ν_{ij}	-	correlating parameter for critical volume.
ρ	-	density.
τ_{ij}	-	correlating parameter for critical temperature.
ϕ_i	-	fugacity coefficient of component i in vapor phase.
Φ	-	volume fraction.
ω	-	acentric factor.
$\Omega a, \Omega b$	-	dimensionless constants in Redlich-Kwong equation.

TABLE OF CONTENTS

CHAPTER PAGE

LIST OF FIGURES

LIST OF TABLES

THEORETICAL INTRODUCTION

I. CRITICAL PHENOMENA

I(a). The Critical Point

The critical point of a liquid, whether it be a single compound or a mixture, is a property of considerable practical as well as theoretical importance. This is because the critical point defines the temperature and pressure where the liquid and vapor phases have identical properties and is, therefore, a key point in the construction of the phase diagram as well as in the development of a theory of the liquid state. Also in some cases a knowledge of the critical temperature and pressure makes possible, by van der Waals' theorem of corresponding states, the prediction of the thermodynamic properties of the compound when these properties have not been determined experimentally.

Evidence for the existence of a critical point was first presented in 1822 by de la Tour (1) who observed that upon heating a liquid in a stationary sealed tube, at a certain temperature the meniscus between the liquid and vapor phases disappeared without ebullition, yielding what appeared by ordinary light to be one homogeneous phase. The meniscus again appeared on cooling the tube but the temperature of reappearance did not exactly coincide with the temperature of disappearance.

It was not however, until the quantitative measurements of Andrews on carbon dioxide (2) that the nature of the transition was understood. Prior to that time many investigators had tried unsuccessfully to liquefy gases by the application of pressure and had come to the erroneous conclusion that there existed certain "permanent" gases

which could not be liquefied. Andrews was the first to apply the term "critical point" to the phenomenon associated with the liquid-vapor transition and he used the disappearance of the meniscus as the criterion for the critical temperature.

From his studies on the gaseous and liquid states of carbon dioxide under various conditions of temperature and pressure, Andrews concluded that above this critical temperature, a gas phase exists which cannot be liquefied by pressure, but below this critical temperature, the vapor is condensable by pressure. The critical temperature may be defined, in terms of Andrews' classical experiments, as the temperature at which the meniscus disappears (it being understood that experimentally it is the average of the temperatures at which the meniscus disappears and reappears), or as the minimum temperature above which a gas cannot, as evidenced by the appearance of a meniscus, be liquefied. The pressure (vapor pressure) required to liquefy a gas at this critical temperature is called the critical pressure.

In 1879 van der Waals (3) proposed his now famous equation of state from which it follows that there is but one temperature at which the pressure and the volume of a gas equal those of the liquid. Besides its success in explaining the deviation of gas behaviour from the ideal gas law, the isothermal lines plotted from this equation reproduce well the experimentally determined isotherms. Successful and widely accepted, the van der Waals' equation has been the starting point for most subsequent papers dealing with equations of state (4).

On the basis of this theory, it was concluded, that at the critical point no discontinuity exists, both liquid and gas phases

becoming identical in all properties. The critical temperature, the temperature at which the meniscus disappears may be interpreted, in terms of the above theory, as the temperature at which the density of the liquid becomes equal to the density of the vapor, or as the temperature at which the properties of the liquid and gas become identical, i.e., a homogeneous phase exists at this point.

The conclusion drawn from Andrew's work and the van der Waals' equation was that the critical point was a unique point at which the meniscus separating the vapor and liquid disappeared and the two phases became a single homogeneous phase.

The work of Andrews and of van der Waals seemed not only to establish the identity of phases at the critical point but to yield the additional deduction that there could be no liquid above the critical temperature. These two deductions may be said to represent what has come to be known as the classical theory of the critical state. But evidence which conflicted with the van der Waals' continuity theory was obtained around the turn of the century by several investigators and the concept of a critical region in contrast to a critical point was used to explain various anomalous critical phenomena.

I(b). The Critical Region

It was mainly the work of Maass (5) that first raised serious doubts about the validity of the classical description though many earlier workers, for example, Cailletet and Colardeau (6), Harnay and Hogarth (7), and Hagenbach (8) (to mention a few) had produced what seemed

to be evidence that the liquid state may persist above the critical temperature, i.e., that the critical temperature does not mark the end of the liquid state. The belief grew that the observed vapor phase was really only largely vapor with liquid mixed with it and that the observed liquid phase contained some vapor mixed with it. At the critical point the two mixtures became identical. Liquid, according to these observers, persisted far above the critical temperature and gradually disappeared.

Many different methods were employed to show the persistence of liquid above the critical point. Harnay and Hogarth (7) added coloring matter to the liquid and found that above the critical temperature the substance in the lower part of the tube was more strongly colored than that in the upper portion of the tube. Others added salt to the liquid to make it electrically conducting and found that above the critical temperature the lower part of the tube remained more strongly conducting than the upper part.

Kuenen (9) stated that nearly all the phenomena observed may be regarded as transition phenomena which would or do disappear upon stirring, and that if final states after stirring are dealt with, most of the abnormalities disappear. Moreover, it has been shown by many investigators that when the substance is agitated or if time enough is allowed, nearly all of the abnormalities do disappear.

Maass found that on heating a fluid of two phases through the critical point, the density gradient persisted after the meniscus had disappeared. This gradient could not be removed by mechanical stirring

but disappeared if the lower end of the tube was heated to a temperature higher than that of the upper end. The temperatures at which the meniscus appeared and disappeared did not always coincide.

It is now very doubtful if any of these observations are correct descriptions of the true equilibrium behaviour of a real fluid in a negligible gravitational field. Kuenen (9) in his review of the older literature discussed the effect of gravity and of impurities on the critical phenomena. Schneider and coworkers (13) have shown that gravitational effects could account for a large part of the flat-topped segment of the coexistence curve. In their studies on xenon and sulphur hexafluoride they used "bombs" of different lengths, 19 cm. and 1.2 cm. in both vertical and horizontal positions. They found that the co-existence curves in the vertical position are flatter than those found when the "bombs" were in the horizontal position. The latter are undoubtedly the more "correct" curves, that is, they represent the behaviour of the fluids in a negligible gravitational field, as no density gradient can be set up in a tube of zero height. Whiteway and Mason (14) have confirmed this behaviour in their studies on ethylene and ethane.

Apart from the experimental results, Porter (10) furnished a theoretical basis for a critical region instead of a critical point. He showed that a surface tension may become zero before the densities of a liquid and its saturated vapor are the same. Mayer (11) has calculated on a statistical mechanical basis the general form of the pressure-volume curve for a number of temperatures in the region of the critical temperature. A review of Mayer's arguments, which are based on the fugacity and virial expansions, is given in a monograph by Mayer and

Mayer (12). The type of P-V diagram obtained for a pure liquid saturated vapor system is given in Figure I. Two critical or characteristic temperatures T_m and T_c may thus exist. T_m is interpreted to correspond to the temperature at which the meniscus disappears and the surface tension becomes zero. This temperature is lower than the true critical temperature T_c, the temperature at which the P-V curve has an inflexion point for only one volume. At and above T_c no differences exist between gas and liquid. Below T_m a definite meniscus exists and the condensed phase has a surface tension.

Although the existence of a critical region is still controversial, that is, that T_m and T_c are two distinct and separate characteristic temperatures, sufficient experimental and theoretical results are available to substantiate the view that the molecular state of the liquid and the vapor is certainly not always identical at the temperature at which the meniscus disappears. This would be untrue if sufficient time is allowed for equilibrium to be reached. At this temperature the liquid and vapor states may be regarded as miscible, the lower phase in the sealed tube consisting of the liquid molecular species saturated with the vapor molecular species and the upper phase consisting of the vapor saturated with the liquid, the line of demarcation between the two phases not being visible with ordinary light. Since a liquid possesses a more definite structure (order) than a gas, this structure persists beyond T_m and is not completely broken (disorder) until T_c is reached, at which temperature the complete disorder, or complete random molecular arrangement, characteristic of the gas state, is finally attained.

In recent years, considerable attention has been drawn to the phenomena which occur very near critical points. Several recent conferences (15,16) have presented new experimental and theorectical results which

FIGURE I. Plot of Pressure against Volume at Different Temperatures near the Critical Point

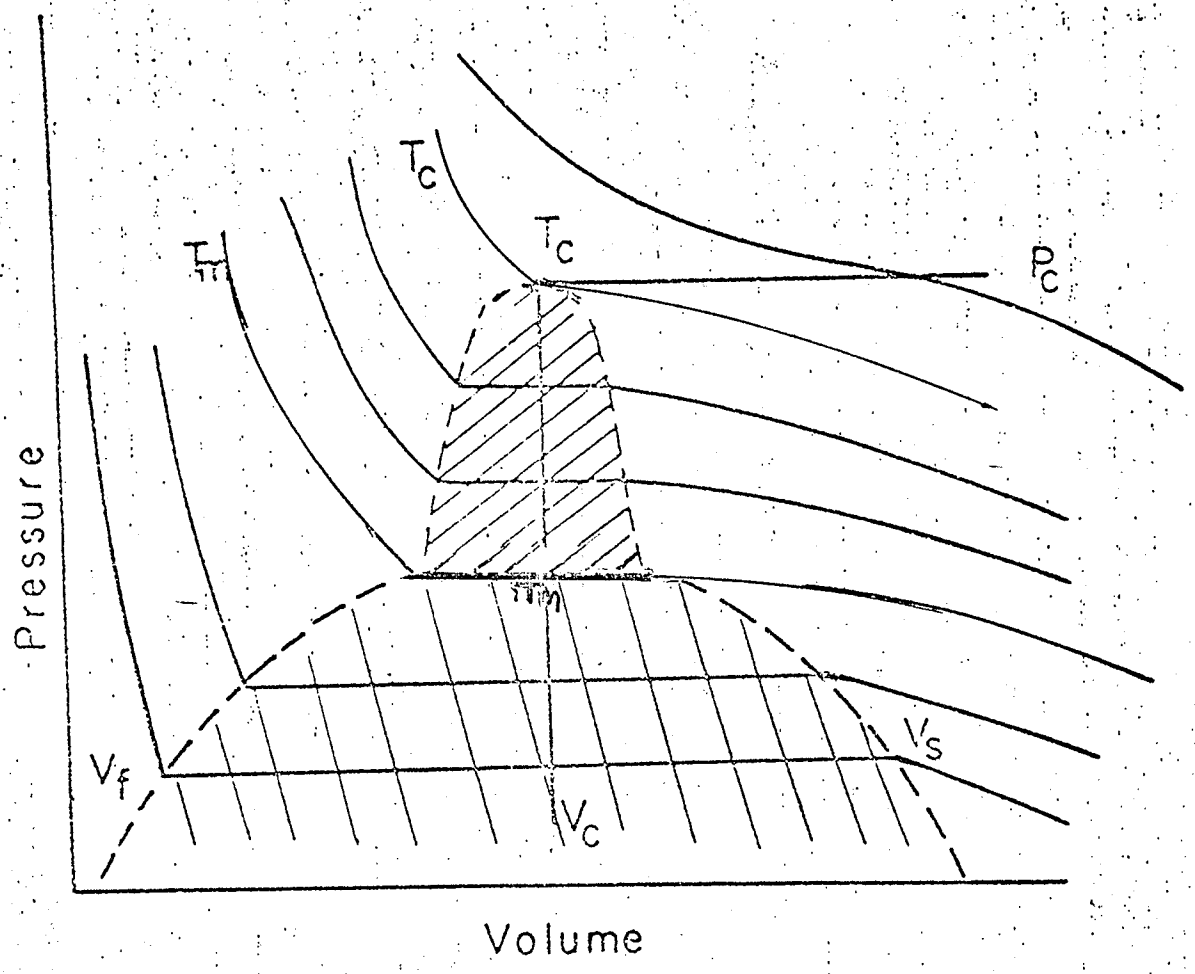

Figure. Plot of pressure against volume at different temperatures near the critical temperature.

Reproduced from Harrison & Mayer (11)

have established the fact that certain phase transitions, apparently very different, are in fact very similar to each other. Rice (17,18) has reviewed the field of critical phenomena several times. A very thorough discussion of the classical thermodynamics of the coexistence curve and the critical region has been given by Rowlinson (19).

I(c). Classical Theories

Various early attempts were made to understand the occurrence of phase transitions and the anomalies in the vicinity of the critical point. The fact that gases can be condensed to liquids requires that the picture of gases as given by the perfect gas law (PV = RT) be modified considerably. The formation of liquids can be accounted for only by the assumption that attractive forces exist between the molecules, and moreover, since the volume does not go to zero, the volume occupied by the molecules themselves must be appreciable. Correction for the volume occupiedby the molecules themselves was first made by Clausius (20) in connection with mean path studies. He deduced the equation $p(v-b) = RT$ for one mole of gas where b is four times the volume of the molecules themselves.

In 1854 Rankine (21) suggested the equation $(p + \frac{a}{V^2T})V = RT$ to allow for the attractive forces between the molecules. The greatest advance in the subject was made by van der Waals (22) in 1873 when he took account of both of the effects mentioned above and proposed his celebrated equation $(p + \frac{a}{V^2})(v - b) = RT$. This equation represented quite accurately the conditions at the critical point and represented qualitatively the behaviour of fluids at other points. Specifically

the van der Waals' equation predicts that the coexistence curve should have a rounded top, that the compressibility should diverge as $(T-T_c)^{-1}$ and that the critical isotherm $(p-p_c)$ is of the third degree in the density $\rho-\rho_c$. The specific heat at constant volume increases linearly with temperature in the two phase region and drops to the perfect gas value when the one phase region is entered.

It can be shown that all the above facts, viz., (1) the coexistence curve is quadratic (2) the critical isotherm is of the third degree and (3) the compressibility diverges linearly are a consequence of a very general assumption -- that the free energy behaves analytically around the critical point, and not just consequences of the particular form of the van der Waals' equation. This means that the free energy is assumed to have a Taylor series expansion in density and temperature.

In 1907, Weiss with more or less the same reasonings and assumptions as van der Waals, gave a theoretical explanation of the ferromagnetic phase transition using the notion of the inner field. The third inner field theory was proposed in 1934 by Bragg and Williams for the order-disorder transitions of binary alloys.

These three classical theories (van der Waals, Weiss and Bragg-Williams) are very similar to each other though the derivations are quite different. The first two theories are based on the assumption that the attractive forces between the molecules which produce the cooperative effects have a very long range. As a result, the type of singularity which the critical point represents is in all the theories exactly the same. For example, as pointed out by Fisher (23), the following theoretical predictions are similar: (1) At the critical point, the specific heat

makes a finite jump and then decreases. For a van der Waals gas at the critical density we have

$$\Delta C_v = C_v - \frac{3k}{2} = \begin{cases} 0 \text{ for } T > T_c \\ \frac{9}{2}K \left\{1 - \frac{28}{25}\frac{T_c - T}{T_c} + \ldots\right\} \end{cases}$$

For a Weiss ferromagnet

$$\Delta C_v = \begin{cases} 0 \text{ for } T > T_c \\ \frac{5}{2} K \left\{1 - \frac{13}{5}\frac{T_c - T}{T_c} + \ldots\right\} \end{cases}$$

For a Bragg-Williams binary alloy

$$\Delta C_v = \begin{cases} 0 \text{ for } T > T_c \\ \frac{3}{2} K \left\{1 - \frac{8}{5}\frac{T_c - T}{T_c} + \ldots\right\} \end{cases}$$

(2) At the critical point the coexistence curve is parabolic.

(3) At the critical point the compressibility or the susceptibility becomes infinite as $(T - T_c)^{-1}$.

As can be deduced from the above, the classical theories represented well, at least qualitatively, the observed critical phenomena but then, since little was known about the intermolecular forces, it was always thought that the attractive forces had a very long range.

Later developments showed more and more clearly that the cooperative forces were not of a very long range and that each atom was influenced by at best a few shells of neighbouring atoms. This necessitated the elucidation of the nature of the van der Waals attractive forces by London and of the Weiss inner field by Heisenberg which came in the late twenties as a byproduct of the quantum mechanical

revolution. Partly because of this fact and also because the classical theories, although qualitatively correct, could not be modified so as to give a precise quantitative description of the phenomena, the classical theories became more and more discredited in the thirties.

I(d). Recent Developments in Critical Phenomena

The failures of the classical theories were many. For instance, by the early 1900's it was known that gas-liquid coexistence curves were roughly of the third degree, in contrast to the parabola predicted by van der Waals' equation. The best value of the exponent β in $|\rho - \rho_c| \propto |T - T_c|^{\beta}$ is 0.35 for a large variety of gases, including even ^3He and ^4He. In binary liquid mixtures, the precise measurements of Rice and coworkers (18) indicate that β is close to 0.33. The behaviour of the spcific heat yielded the most dramatic example of the failure of the classical theory. It was showed that near the λ - point the specific heat of helium varies with temperature as $\log |T - T_\lambda|$, both above and below T_λ. For the gas-liquid transition, specific heats at constant volume, calculated from PVT data, as well as the few directly measured C_v data, show a large increase of C_v near the critical point, unexplained by the classical theory.

The first step towards modifying the classical theory of van der Waals was made by Kamerlingh Onnes who represented the experimental data by a series expansion in the density, the so-called virial expansion. And the inner field theory of ferromagnetism was replaced by the Ising model, when it was realized that interactions between magnetic spins were short range exchange forces rather than long range magnetic dipole forces. Ising assumed the spins to be localized on the lattice sites

of a regular array and capable of only two orientations in opposite directions, so that the interaction is only between neighbouring pairs. All interactions beyond those between nearest neighbours are neglected. The Ising model can be applied to the other models for phase transitions. For example, when upward pointing spins are replaced by molecules and downward pointing spins by "holes" or empty sites, the ferromagnetic Ising model is transformed into a model for the gas$\rightleftharpoons$liquid transition, the so-called lattice gas.

The summaries of the results of the Ising model theories as well as the theoretical and experimental values of the critical point exponents are given in recent reviews by Fisher (23,24), Heller (25), and Sengers and Levelt-Sengers (26).

A landmark in the history of the Ising model was Onsager's presentation (27) in 1944 of an exact solution for the two-dimensional model in zero field. This solution predicts a logarithmically diverging specific heat, which implies that a Taylor expansion of the free energy is impossible at the critical point.

The droplet (physical cluster) picture of condensation for a fluid (L$\rightleftharpoons$V) has been used by Fierz (28) and de Boer (29) to develop a theory of the critical region. Fisher and coworkers (30, 31) have extended their ideas to describe the critical point of liquids. Rice (17) had earlier considered the process of condensation of a vapor from the point of view of associating molecules. That involves the consideration of the equilibrium between single molecules, double molecules, triples, and higher clusters or droplets; the molecules within a cluster being held together by van der Waals' or, possibly, dipole forces. As the

system is compressed to smaller volumes, and more and more of the larger clusters are formed and, if it is compressed sufficiently, clusters of macroscopic size suddenly become stable, that is, condensation begins.

Recently there has been considerable discussion about the shape of the coexistence curve in the neighbourhood of the critical point. As has been mentioned before, according to the classical van der Waals' theory $|T_c - T|$ should be proportional to $(\rho_L - \rho_V)^2$ near the critical point, ρ_L and ρ_V being the densities of liquid and vapor respectively, T being the temperature, and T_c being the critical temperature. Guggenheim (32), however, has collected data on a number of liquid vapor equilibria, and has found that $|T_c - T|$ is more nearly proportional to $(\rho_L - \rho_V)^3$. (As indicated previously (page 10)).

Rice (33,34) has discussed the shape of the coexistence curve near the critical point very thoroughly, dealing with both the liquid⇌ liquid equilibrium and the liquid⇌vapor equilibrium. In the case of the liquid ⇌ vapor equilibrium the experimental difficulties are many -- the effect of gravity being of great importance. Many workers, for example Murray and Mason (35), have investigated the properties of different systems near the critical point, taking very special precautions, but the data which come nearest to penetrating the critical region are those published by Lorentzen (36) who has claimed a temperature control within about 0.0001°, and who has made measurements within about 0.001° of the critical temperature for carbon dioxide. Using an optical method for his measurements of density, Lorentzen has concluded that there is no evidence for a truly flat top on the

coexistence curve.

Widom and Rice (37) and Widom (38) have given a mathematical treatment of the critical isotherm and the equation of state of liquid vapor systems. They analysed PVT data on xenon, carbon dioxide and hydrogen in the region fairly close to, but not in the immediate neighbourhood of, the critical point. They have shown that in each case the critical isotherm is of the fourth degree, one degree higher than that of the coexistence curve, as required by the theorem of Rice (33).

Recently Davis and Rice (39) have deduced two different Taylor series for pressure to account for a cubic coexistence curve and for behaviour in the gas and liquid single phase regions. Though their treatment agrees to a satisfactory degree with the experimental results, it is still believed that no ordinary Taylor series is valid near the critical point and that a more general equation of state such as that proposed by Widom (38) might prove to be correct or nearly correct for any "non-classical" region which may exist close to the critical point.

Experimentally, it has proved very difficult to say with certainty whether the coexistence curve is horizontal or not. There is no limit to the accuracy of temperature control to which the measurements should be made. Rice (40) has made measurements up to $0.0001^{\circ}C$ of the critical point and has concluded that there is no truly horizontal portion of the coexistence curve.

II. THERMODYNAMIC PROPERTIES FROM P-V-T DATA

It is well known that the thermodynamic properties of a pure fluid can be computed with reference to a particular standard state

from the usual thermodynamic differential equations provided that (1) the heat capacity at constant pressure (or volume) is known as a function of temperature for some one pressure (or density) and, (2), an equation of state exists with determined values of the parameters, or there are available extensive pressure-volume-temperature or equivalent data over the entire range of temperatures and pressures involved. The properties of a fluid mixture of invariant composition can be evaluated with reference to a particular standard state of the mixture from the same relations used for pure fluids provided thermal and compressibility data of that particular mixture are given.

However, the problem of importance to be solved in the treatment of the thermodynamic properties of mixtures, is the computation of the properties of all possible mixtures from thermal and compressibility data of the pure constituents alone, and a knowledge of certain integration constants of the pure components. The solution of the problem involves the use of both thermodynamic and statistical methods.

The thermodynamic properties calculated from PVT data are obtained in the form of deviations of these properties in dimensionless form from ideal behaviour. For example, the dimensionless form of volume is given by $\frac{P}{RT}(V - V_o^{id})$*; that of enthalpy by $(H - H_o^{id})/RT$ etc.

Thermodynamic functions as function of pressure can be written down making use of the compressibility factor Z. A single chart of the compressibility factor Z defined by $Z = \frac{PV}{RT}$, in terms of reduced quantities, represents adequately the behaviour of most pure gases. The fugacity coefficient ϕ defined by $\phi = \frac{f}{p}$ is obtained by integrating the equation

$$\ln \phi = \int_o^p \frac{Z - 1}{P} dp \qquad (1)$$

* which is $\frac{PV}{RT} - 1 = Z - 1$

P-V-T data will give values of Z as a function of P_R at a given T_R.

Using the equation

$$\frac{H - H_o^{id}}{RT} = - T \int_o^P \left(\frac{\partial Z}{\partial T}\right)_p / P \, dp \qquad (2)$$

the enthalpy deviation, that is the difference between the enthalpy of an ideal gas and that of an actual gas, can be obtained.

Once the values of $\ln \phi$ and $H - H_o^{id}$ are obtained the other thermodynamic functions are calculated from well known thermodynamic relationships. Table I gives a summary of the thermodynamic functions.

Table I.

Summary of Reduced Thermodynamic Functions Pertaining to:

Volume	$Z - 1$
Fugacity Coefficient	$\exp \int_o^P \frac{Z-1}{P} \, dp$
Enthalpy	$- T \int_o^P \frac{\left(\frac{\partial Z}{\partial T}\right)_P}{P} \, dp$
Gibbs Free Energy	$\int_o^P \frac{Z-1}{P} \, dp$
Entropy	$- T \int_o^P \frac{\left(\frac{\partial Z}{\partial T}\right)_P}{P} \, dp - \int_o^P \frac{Z-1}{P} \, dp$
Internal Energy	$- T \int_o^P \frac{\left(\frac{\partial Z}{\partial T}\right)_P}{P} \, dp - (Z-1)$

All the above equations apply to gases from zero pressure to the pressure at which condensation occurs, that is, the dew point. When this pressure

is reached along an isotherm, the thermodynamic property changes from that observed for the vapor phase to that observed for the liquid phase. The Clapeyron equation for example

$$\frac{dp}{dT} = \frac{\Delta H^{vap}}{T\Delta V^{vap}} \tag{3}$$

gives the enthalpy of vaporization of a pure material. In equation (3) $\frac{dp}{dT}$ is the slope of the vapor pressure curve at the temperature considered; ΔH^{vap}, the latent heat of vaporization is given by

$$\Delta H^{vap} = H_g - H_L \tag{4}$$

and ΔV^{vap}, the volume change of vaporization is given by

$$\Delta V^{vap} = V_g - V_L \tag{5}$$

Hence from PVT data and certain equations of statistical mechanics the thermodynamic properties of pure fluids in the gaseous and liquid regions can be calculated.

III. VAPOR-LIQUID EQUILIBRIA

Although it has been common practice for many years to subject vapor-liquid equilibrium data to thermodynamic analysis, in the past this practice has been largely confined to low or moderate pressures. While many experimental studies of high pressure vapor-liquid equilibria have been published, little work has been reported on the reduction of such data to thermodynamic functions, but such a reduction is necessary for interpreting and correlating experimental data; thermodynamic analysis is the essential tool whereby experimental data can be generalized to

FIGURE II. Plot of Equilibrium Mole Fraction of Low Boiler in the Vapor, y, against Mole Fraction in the Liquid x.

Curve	System	Conditions
A	Chloroform-Ethyl Alcohol	$35^{o}C$
B	Acetone-Chloroform	$35.17^{o}C$

FIG. II : EQUILIBRIUM MOLE FRACTION OF LOW BOILER IN THE VAPOR y_1 vs MOLE FRACTION IN THE LIQUID x_1 .

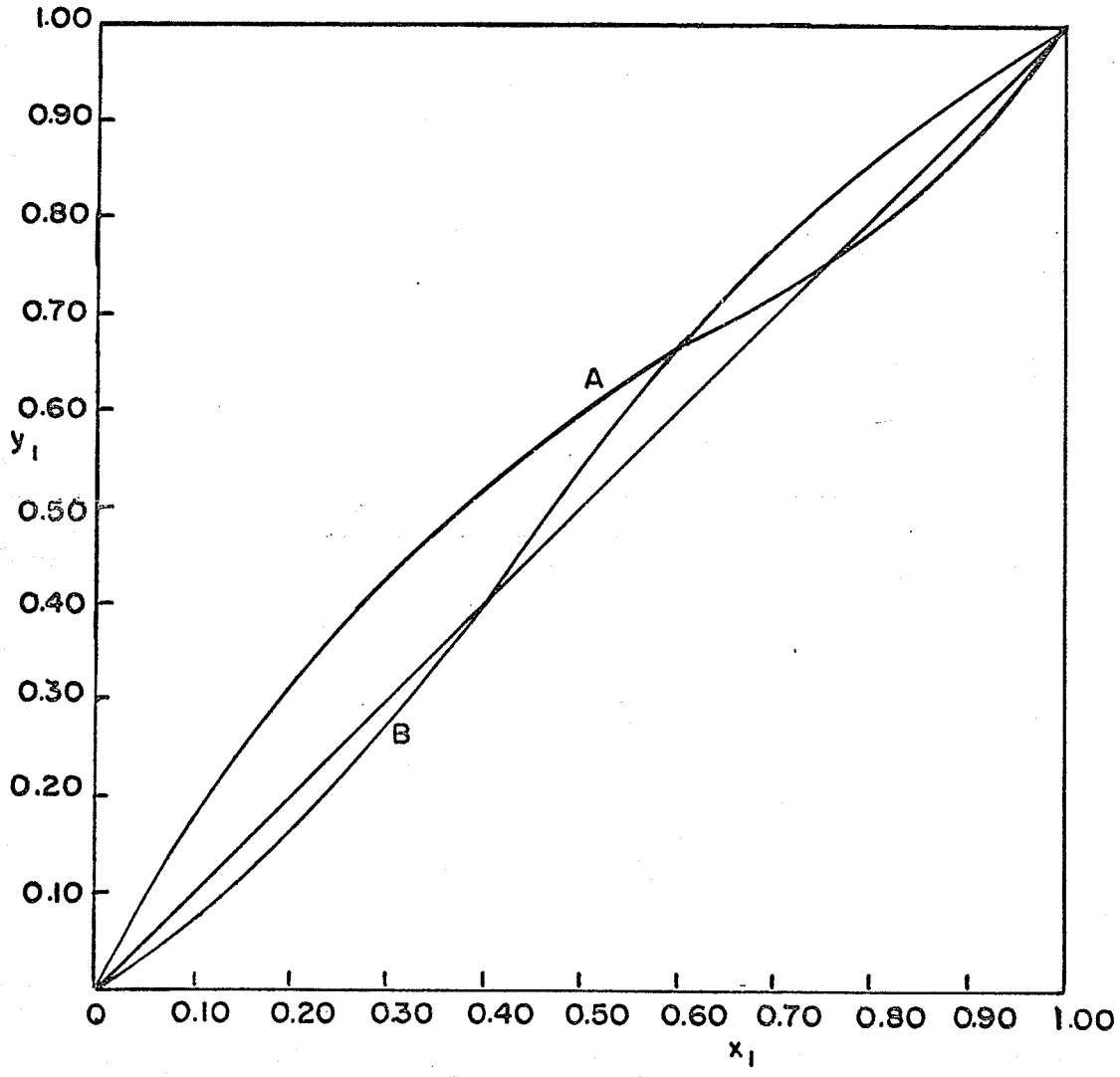

the same data are calculated in terms of deviation factors from Raoult's law by the equations

$$\gamma_1 = \frac{Py_1}{P_1 x_1} \quad \text{and} \quad \gamma_2 = \frac{Py_2}{P_2 x_2} \tag{5}$$

where P = total pressure

P_1 = partial pressure of component 1

and P_2 = partial pressure of component 2,

and the deviation factors are plotted on semilog paper against the composition of one of the components in the liquid, characteristic curves like those in Figure III are obtained.

These plots are orderly, consistent and more valuable than a mere graphical representation. The term introduced as deviation factor from Raoult's law is equivalent to the thermodynamic property, activity coefficient. There is a definite relation between the values for the several components, which, according to Lewis and Randall (41) follows from the Gibbs relation between the partial molal free energies $\bar{G}_1$, $\bar{G}_2$, etc.

$$x_1\left(\frac{\partial \bar{G}_1}{\partial x_1}\right)_{P,T} + x_2\left(\frac{\partial \bar{G}_2}{\partial x_1}\right)_{P,T} + \ldots = 0 \tag{6}$$

Since $\bar{G}_1 = RT \ln f_1 + K_1$, at constant temperature $\partial \bar{G}_1 = RT\, \partial \ln f_1$ and equation (6) becomes

$$x_1\left(\frac{\partial}{\partial x_1} \ln f_1\right)_{P,T} + x_2\left(\frac{\partial}{\partial x_1} \ln f_2\right)_{P,T} + \ldots = 0 \tag{7}$$

In this equation f_1 the fugacity, can be regarded as the "ideal" partial pressure, and is identical with the partial pressure P for conditions under which the ideal gas laws hold.

FIGURE III. Plot of Activity Coefficients against Mole Fraction.

Curve	System	Conditions
A	Isopropyl ether-Isopropyl Alcohol	Atmospheric pressure
B	n-Propyl alcohol-water	Atmospheric pressure.

FIG. III. ACTIVITY COEFFICIENTS

vs MOLE FRACTION.

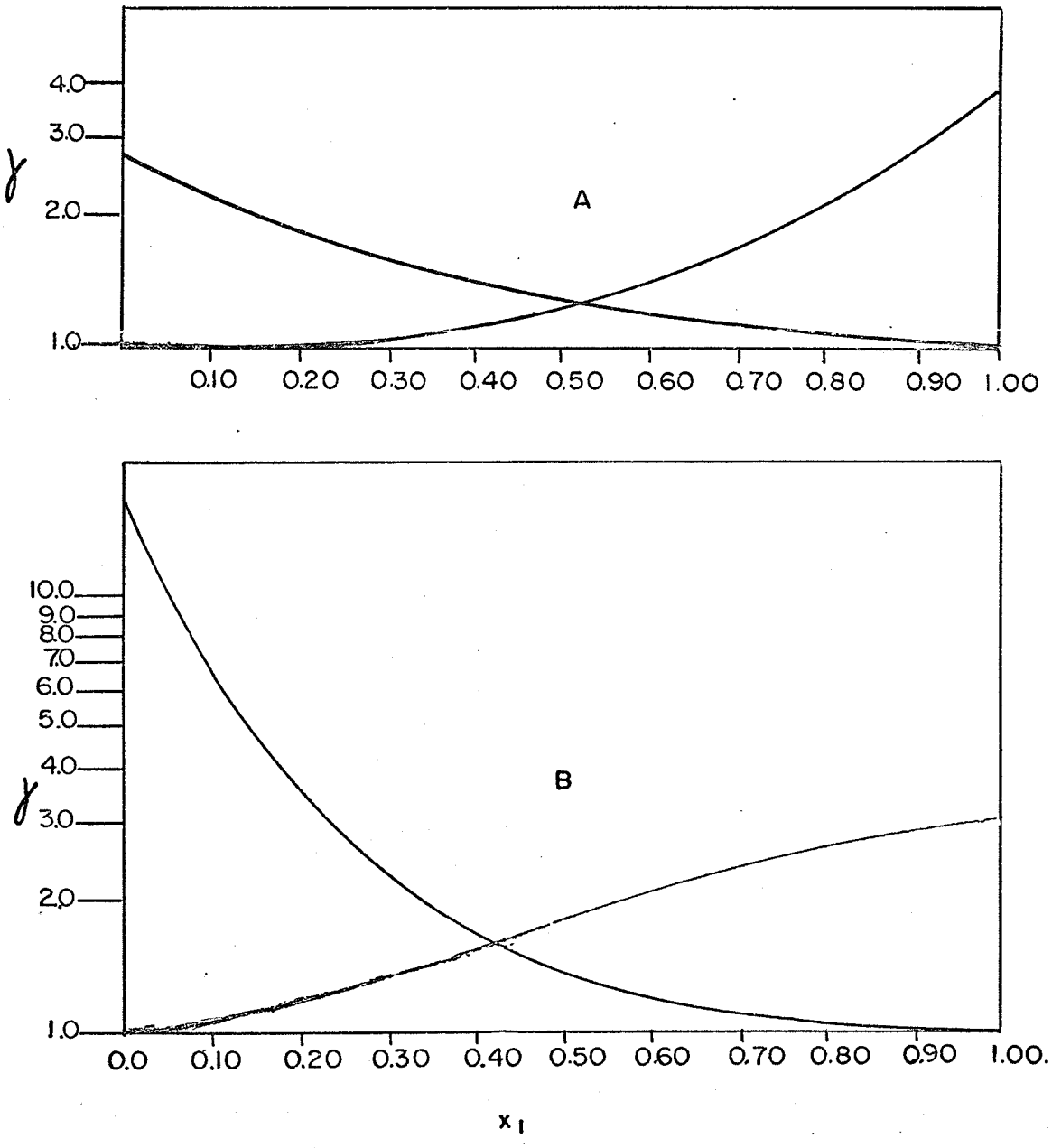

Lewis and Randall (41) define activity a as the relative fugacity, or the ratio between the fugacity of the substance in solution and its fugacity as a pure liquid. Thus, $a_1 = \frac{f_1}{f_1^o}$ and $a_2 = \frac{f_2}{f_2^o}$ where a_1 and a_2 are the activities of components 1 and 2 respectively and f_1^o and f_2^o are the fugacities of the pure liquids.

The Gibbs-Duhem equation (7) can be more conveniently used in terms of activity coefficients.

$$x_1\left(\frac{\partial}{\partial x_1} \ln \gamma_1\right)_{T,P} + x_2\left(\frac{\partial}{\partial x_1} \ln \gamma_2\right)_{T,P} + \ldots + = 0 \qquad (8)$$

For binary mixtures $\partial x_1 = -\partial x_2$ so that

$$x_1\left(\frac{\partial}{\partial x_1} \ln \gamma_1\right)_{T,P} = x_2\left(\frac{\partial}{\partial x_2} \ln \gamma_2\right)_{T,P} \qquad (9)$$

Equations (9) and (8) are of immediate value in studying experimental data on vapor-liquid equilibria by relating the slopes of such curves as those of Figure III. Since the magnitudes of the slopes are difficult to determine precisely, studies have been made to obtain convenient mathematical solutions of this differential equation.

Van Laar Equations

Perhaps the most useful of the solutions are the equations derived by van Laar (42) from a thermodynamic study.

$$\log \gamma_1 = \frac{A}{\left(1 + \frac{Ax_1}{Bx_2}\right)^2} \qquad (10)$$

$$\log \gamma_2 = \frac{B}{\left(1 + \frac{Bx_2}{Ax_1}\right)^2} \qquad (11)$$

In this symmetrical form, constants A and B have the property of being equal to the terminal values of log γ of the two curves. Thus,

at $x_1 = 0$, $\log \gamma_1 = A$ and at $x_1 = 1$ when $x_2 = 0$ $\log \gamma_2 = B$. At $x_1 = 0$ $\log \gamma_2 = 0$ or $\gamma_2 = 1$ and at $x_1 = 1$ $\log \gamma_1 = 0$ or $\gamma_1 = 1$, and these satisfy the limiting condition that Raoult's law holds for a component whose concentration approaches 100 mole per cent.

Margules Equations

Margules (43) integrated the Gibbs-Duhem equation in terms of a pair of exponential series with unlimited numbers of terms and then derived the constants for one of the equations from those of the other by applying equation (9). The Margules two-term equations are

$$\log \gamma_1 = (2B - A)x_2^2 + 2(A - B)x_2^3 \tag{12}$$

$$\log \gamma_2 = (2A - B)x_1^2 + 2(B - A)x_1^3 \tag{13}$$

The Margules equations become identical with those of van Laar when A = B.

Scatchard Equations

Scatchard and Hamer (44) extended the methods of van Laar to obtain equations which can be represented by

$$\log \gamma_1 = A\left(\frac{2BV_1}{AV_2} - 1\right)z_2^2 - 2A\left(\frac{BV_1}{AV_2} - 1\right)z_2^3 \tag{14}$$

$$\log \gamma_2 = B\left(\frac{2AV_2}{BV_1} - 1\right)z_1^2 - 2B\left(\frac{AV_2}{BV_1} - 1\right)z_1^3 \tag{15}$$

where V_1, V_2 are molar volumes.

and, z_1 and z_2 are volume fractions of the components given by

$$z_1 = \frac{V_1x_1}{V_1x_1 + V_2x_2} \quad \text{and} \quad z_2 = \frac{V_2x_2}{V_1x_1 + V_2x_2} \tag{16}$$

III B. General Equilibrium Equation

A vapor phase and a liquid phase are in equilibrium when both are at the same temperature and when f_i, the fugacity of any component i in the vapor phase, is equal to that in the liquid phase, that is,

$$f_i^V = f_i^L \tag{17}$$

where superscript V stands for vapor and superscript L stands for liquid. Equation (17) will not be very useful unless the fugacity of each component is related to the temperature, pressure and composition; f_i^V must be written as a function of T,P and y, where y is the vapor phase composition in mole fractions. Similarly, f_i^L must be written as a function of T,P and x, where x is the liquid phase composition in mole fractions. Three auxiliary functions are required to enable us to achieve the above relations: (1)the vapor phase fugacity coefficient ϕ, (2)the liquid phase activity coefficient γ and (3) the liquid phase standard state fugacity f^o. The fugacity coefficient ϕ relates the vapor phase fugacity f_i^V to the mole fraction y; and to the total pressure P. Itis defined by

$$\phi_i \equiv \frac{f_i^V}{y_i P} \tag{18}$$

The activity coefficient γ relates the liquid phase fugacity f_i^L to the mole fraction x_i and to a standard-state fugacity f_i^{oL}; itis defined by

$$\gamma_i \equiv \frac{f_i^L}{x_i f_i^{oL}} \tag{19}$$

But for phase equilibrium $f_i^V = f_i^L$ (Equation 17); therefore, the equation of equilibrium for any component i is given by

$$\phi_i y_i P = \gamma_i x_i f_i^{oL} \tag{20}$$

As indicated in equation (19) the activity coefficient is completely defined only if the standard state fugacity f_i^{oL} is clearly specified. The definition of f_i^{oL}, however, is quite arbitrary and is dictated only by convenience but it must apply to the same temperature as that of the solution and to some arbitrary but fixed composition and pressure. It is desirable that γ_i be of the order of unity and therefore the standard state should be chosen accordingly. To ensure that γ_i be near unity, the standard state fugacity f_i^o should be chosen such that to a first approximation $f_i^L \simeq x_i f_i^o$. It is common practice to define f_i^o for every component i as the fugacity of pure liquid i at the temperature and pressure of the solution. When this definition is adopted for all components, the activity coefficients are normalized symmetrically; for every component i

$$\gamma_i \longrightarrow 1 \text{ as } x_i \longrightarrow 1 \qquad (21)$$

While the above definition is useful for mixtures of liquids at low pressures, it has serious disadvantages for high pressure vapor-liquid equilibria. First, whenever the system temperature T exceeds T_{c_i}, the critical temperature of componenti, the fugacity of pure liquid i at T is a hypothetical quantity which is experimentally inaccessible; it must be found by arbitrary extrapolation. The next disadvantage comes when we consider the relation between activity coefficients as given by the Gibbs-Duhem equation. This leads to the definition and use of adjusted or pressure independent activity coefficients (I have more to say about them in the section "The Liquid Phase").

Because of the above difficulties the equation for characterization of vapor-liquid equilibrium (Equation 20) at high pressures was obtained by using fugacity coefficients only for the vapor phase and activity coefficients for the liquid phase. The fugacity coefficient represents the deviation of gases from ideal behaviour and is by definition dependent on pressure, vapor composition and temperature. Its values are practically always derived from an equation of state.

III C. The Vapor Phase

When well removed from critical conditions, the vapor phase is characterized by relatively low density. It is then a common simplification to assume that all the non-ideality in vapor-liquid equilibria exists in the liquid phase and that the vapor phase can, to a very close approximation, be treated as an ideal gas. This simplification is most attractive because then the fugacity of i is given by the product of y_i, mole fraction of i in the vapor and P, the total pressure, but unfortunately this simplification is limited to moderate pressures and, as mentioned before, the fugacity coefficient ϕ_i is introduced to account for the deviation from ideal behaviour $\left(\phi_i = \frac{f_i}{y_i P}\right)$.

The fugacity coefficient is a function of pressure, temperature and gas composition; it is related to the volumetric properties of the gas mixture by either of the two exact relations (45, 46).

$$RT \ln \phi_i = \int_0^P \left[\left(\frac{\partial V}{\partial n_i} \right)_{T,P,n_j} - \frac{RT}{P} \right] dP \qquad (22)$$

$$RT \ln \phi_i = \int_V^\infty \left[\left(\frac{\partial P}{\partial n_i} \right)_{T,V,n_j} - \frac{RT}{V} \right] dV - RT \ln Z \qquad (23)$$

Where V is the total volume of the gas mixture and Z is the compressibility factor of the gas mixture at T and P; n_i stands for the number of moles of component i.

To obtain numerical results from equations (22) and (23) an equation of state is needed. Since most equations of state are explicit in pressure, equation (23) is more convenient than equation (22).

III C. (I) Equation of State

Since the classical work of van der Waals in 1873 a large number of equations of state have appeared in the literature. Their degree of complexity, as indicated by the number of constants, has been deliberately increased to represent better the PVT behaviour of substances over wide ranges of temperature and pressure. For example, the equation of state proposed by Martin and Hon (47) requires nine constants to predict the PVT behaviour of a substance.

One of the main reasons why so much work has been done to obtain a well-behaved equation of state concerns the exceptional power and utility of an equation of state. When combined with appropriate thermodynamic relations, a well-behaved equation can predict with precision, isothermal changes in heat capacity, enthalpy, entropy and fugacity, vapor pressure, latent heat of vaporization, activity coefficients, and vapor liquid equilibria in mixtures. Unfortunately, even though the useful applications of an equation of state are so extensive and attractive, the development of a high performance equation proves to be so involved that to date no one has come close to discovering a single relation which is truly good over a wide range of density.

There are two main approaches to the development of an equation of state. One is the theoretical approach based on either kinetic theory or statistical mechanics involving intermolecular forces and the other is the empirical approach. A thorough review is given by Martin (47A). It has been proved that the empirical or semitheoretical approach has the greatest success in representing data with high precision over a wide range of density.

There are three decisions to be made before embarking on the task of finding an equation of state. The first concerns the amount and kind of data that will be required to obtain the parameters in the equation, the second concerns the range of density to be covered and the third concerns the precision with which the PVT data are to be represented. For some applications, it is desirable to have an equation which can be obtained from a minimum of data, that is, the critical temperature, pressure, and volume, or the boiling point, or some molecular parameter.

The merits and limitations of fourteen of the most common equations of state have been thoroughly discussed by Shah and Thodos (48) for the subcritical, critical and hypercritical regions.

The Redlich-Kwong equation proposed by Redlich and Kwong (49) in 1949 was found to be quite satisfactory and is the one adopted by Chueh and Prausnitz (50) in their calculation of vapor phase fugacity coefficients. The Redlich-Kwong equation is somewhat empirical in nature and no rigorous justification can be made in its presentation.

The Redlich-Kwong equation is

$$P = \frac{RT}{v-b} - \frac{a}{T^{0.5}V(V+b)} \tag{24}$$

where, according to R-K -

$$a = \frac{\Omega_a R^2 T_{c_i}^{2.5}}{P_{c_i}} \tag{25}$$

$$b = \frac{\Omega_b R T_{c_i}}{P_{c_i}} \tag{26}$$

i.e., a and b are adjustable constants.

The dimensionless constants Ω_a and Ω_b are 0.4278 and 0.0867 respectively if the first and second isothermal derivatives of pressure with respect to volume are set equal to zero at the critical point. But in vapor-liquid equilibria one is interested in the volumetric behaviour of saturated vapors over a relatively wide range of temperature, rather than in the critical region only. Therefore, Ω_a and Ω_b for each component are evaluated by fitting equation (24) to the volumetric data of the saturated vapor.

The Redlich-Kwong equation has been shown by Shah and Thodos (48) to be quite satisfactory up to a reduced pressure of $P_R = 50$ for certain substances but the eight parameter equation of Benedict, Webb and Rubin (51) does have advantages. The B-W-R equation is of the following form

$$P = RTd + (B_oRT - A_o - \frac{C_o}{T^2})d^2 + (bRT - a)d^3 + a\alpha d^6 + cd^3\frac{1+\gamma d^2}{T^2}e^{-\gamma d^2} \tag{27}$$

where the empirical constants A_o, B_o etc. are different for different substances.

In an effort to improve the two parameter Redlich-Kwong equation, Redlich et al (52) introduced Pitzer's acentic factor (53) as a third parameter but because of their inflexible mixing rules the equation failed for mixtures.

Though only the virial equation has a sound theoretical foundation for representing the properties of pure and mixed gases, Chueh and Prausnitz (50) have shown that for application at densities higher than the critical density, the Redlich-Kwong equation (24) is quite reliable. The mixing rules for a mixture containing N components are

$$b = \sum_{i=1}^{N} y_i b_i \tag{28}$$

$$\text{where } b_i = \frac{\Omega_{b_i} R T_{c_i}}{P_{c_i}} \tag{29}$$

$$\text{and } a = \sum_{i=1}^{N} \sum_{j=1}^{N} y_i y_j a_{ij} \quad (a_{ij} \neq \sqrt{a_{ii} a_{jj}}\ ) \tag{30}$$

$$\text{where } a_{ii} = \frac{\Omega_{ai} R^2 T_{ci}^{2.5}}{P_{ci}} \tag{31}$$

$$a_{ij} = \frac{(\Omega_{ai} + \Omega_{aj}) R^2 T_{cij}^{2.5}}{2P_{cij}} \tag{32}$$

$$P_{cij} = \frac{z_{cij} R T_{cij}}{V_{cij}} \tag{33}$$

$$V_{cij}^{1/3} = \frac{1}{2}(V_{ci}^{1/3} + V_{cj}^{1/3}) \tag{34}$$

$$z_{cij} = 0.291 - 0.08\ \frac{(\omega_i + \omega_j)}{2} \tag{35}$$

where ω is the acentric factor.

$$T_{cij} = \sqrt{T_{cii}\, T_{cjj}}\ (1 - K_{ij}) \qquad (36)$$

The binary constant K_{ij} is a constant characteristic of the i-j interaction and represents the deviation from the geometric mean for T_{cij} . K_{ij} must in general be obtained from some experimental information about the binary interaction and is, to a good approximation, independent of the temperature, density and composition. Information about K_{ij} is provided by second virial cross coefficients (54) or by saturated liquid volumes of binary systems (55). Chueh and Prausnitz (50) have reported the best estimates of K_{ij} for 115 binary systems. There are two aspects in which the mixing rule for A_{ij} proposed by Chueh and Prausnitz differs from that proposed by Redlich. The first one is the introduction of the binary constant K_{ij} and the second one is the combination of critical volumes and compressibility factors to obtain a_{ij} according to equations (32) through (35).As a result of the latter, the proposed mixing rule does not reduce to Redlich's original rule even when $K_{ij} = 0$, except when V_{ci}/V_{cj} is close to unity.

A comparison of Chueh and Prausnitz's correlation with a few others which have been discussed recently shows that the former, because it takes account of the deviation from the geometric mean rule, is the most satisfactory. Fender and Halsey (56) for example, suggested a harmonic mean combination which has been used by Dantzler, Knobler and Windsor (57). They obtained too weak an interaction with the harmonic mean combination and too strong an interaction with the geometric mean rule.

III C. (2) Fugacity Coefficient

As mentioned earlier (equations (22) and (23)) the fugacity coefficient, which is a function of pressure, temperature and gas composition, is related to the volumetric properties of the gas mixture by either of the two exact relations (45,46):

$$RT \ln \phi_i = \int_0^P \left[\left(\frac{\partial V}{\partial n_i}\right)_{T,P,n_j} - \frac{RT}{P} \right] dp \qquad (22)$$

$$RT \ln \phi_i = \int_V^{OO} \left[\left(\frac{\partial P}{\partial n_i}\right)_{T,V,n_j} - \frac{RT}{V} \right] dv - RT \ln z \qquad (23)$$

where V is the total volume of the gas mixture and z is the compressibility of the gas mixture at T and P. Equation (23) is the one used more often since most equations of state are explicit in pressure.

If sufficient volumetric data are available for a gas mixture, the fugacity coefficient of component i in the gas mixture can be calculated from either equation (22) or equation (23). Unfortunately, such volumetric data are lacking, especially for multicomponent systems and therefore calculations of fugacity coefficients are most often performed using an extension of the theorem of corresponding states or with an equation of state.

I will discuss only the calculation of fugacity coefficients using an equation of state -- the Redlich-Kwong equation in particular. The method based on corresponding states has been discussed thoroughly by Joffe (58) and Leland et al (59).

The Redlich-Kwong equation has been found to be satisfactory for fugacity coefficient calculations though it is well known that only the virial equation has a sound theoretical foundation for representing the properties of pure and mixed gases. When truncated after the third term, the virial equation is often useful up to a density just slightly less than the critical density. Methods for estimating second and third virial coefficients of mixtures have been extensively discussed (60,61, 62,63,64,65).

Substitution of the mixing rules (28) to (36) in the Redlich-Kwong equation (24) yields the following expression for the fugacity coefficient of component $\underline{K}$ in the mixture.

$$\ln \phi_{\underline{K}} = \ln \frac{V}{V-b} + \frac{b_K}{V-b} - \frac{2 \sum_{i=1}^{N} Y_i a_{iK}}{RT^{3/2} b} \ln \frac{V+b}{V} + \frac{ab_K}{RT^{3/2} b^2} \left[\ln \frac{V+b}{V} - \frac{b}{V+b} \right] - \ln \frac{PV}{RT} \qquad (37)$$

where V, the molar volume of the gas mixture, is obtained by solving equation (24) and taking the largest real root of V.

Chueh and Prausnitz (50) have carried out calculations for various systems (for example, nitrogen-n-butane at 310°F, carbon dioxide-n-butane at 340°F, n-pentane-hydrogen sulphide at 160°F) and the very satisfactory agreements obtained between calculated and experimental fugacity coefficients at high pressures led them to conclude that the revised Redlich-Kwong equation can be used for mixtures containing non-polar or slightly polar gases.

III D. The Liquid Phase

The thermodynamic properties of liquid mixtures have been investigated for many years, the basic problem being to relate the properties of a mixture to those of its components with a minimum amount of experimental information on the mixture itself. The final goal is to predict the properties of the mixture using only pure component data. This goal has not been reached, even for the simplest mixtures, but for a few types of mixtures it is now possible to make good estimates of mixture properties using approximate theories of solutions. These theories have been developed and discussed by Rowlinson (19), Guggenheim (66) and others.

As mentioned before, in the case of liquids a new function, the activity coefficient γ is introduced. For any component i in solution, the activity coefficient γ_i relates the fugacity f_i^L at mole fraction x_i, temperature T and pressure P, to that at some other condition where its value is known accurately, that is, the standard state, which must be at the same temperature as that of the solution and at some arbitrary but fixed composition and pressure. At this time a discussion of reference states seems appropriate.

III D. (1) Reference States

The case for condensable (subcritical) components, that is for components whose critical temperatures are above the temperature of the solution has been discussed earlier (see section III B). For every component i we have

$$\gamma_i \longrightarrow 1 \quad \text{as} \quad x_i \longrightarrow 1 \tag{38}$$

In such a case we say that the activity coefficients are normalized symmetrically.

The above definition fails at high temperatures because whenever the system temperature T exceeds Tc_i, the critical temperature of component i, the fugacity of pure liquid i at T is a hypothetical quantity which is experimentally inaccessible and must be found by arbitrary extrapolation. If the component in question is not excessively above its critical temperature, extrapolation is allowable, but for a highly supercritical component the concept of a hypothetical liquid is of little use since the extrapolation of pure liquid properties in this case is so excessive as to lose all its physical significance. We therefore have a different normalization for a non-condensable component:

$$\gamma_i^* \longrightarrow 1 \quad \text{as} \quad x_i \longrightarrow 0 \tag{39}$$

From equation (39) the fugacity of component i becomes equal to the mole fraction times the standard state fugacity of i when component i is infinitely dilute. The concentration region where the activity coefficient of a dilute component is equal to unity is called the ideal dilute solution or Henry's law region. The characteristic constant for the ideal dilute solution is Henry's constant H which is defined by

$$H \equiv \underset{x_i \longrightarrow 0}{\text{Limit}} \quad \frac{f_i^L}{x_i} \tag{40}$$

In a binary liquid solution containing one non-condensable and one condensable component, the first is referred to as the solute and the second as the solvent. Equation (38) is used for the normalization of

the solvent activity coefficient. The standard-state fugacity of the solvent is the fugacity of the pure liquid and the standard state fugacity of the solute is Henry's constant.

The use of Henry's constant for a standard state fugacity means that the standard state fugacity for a non-condensable component depends not only on the temperature but also on the nature of the solvent. Since H depends on the solvent, a difficulty arises in the case of a mixed solvent. The most convenient correlation and the one adopted by Chueh and Prausnitz (50) is to define the standard state fugacity of a non-condensable component as Henry's constant for that component in a pure reference solvent r which is a constituent of the solvent mixture. Thus, in a multicomponent solution, for each condensable component

$$\gamma_i \longrightarrow 1 \quad \text{as} \quad x_i \longrightarrow 1 \quad \text{and} \quad f_i^{oL} = \text{fugacity of pure liquid i,}$$

and for each non-condensable component

$$\gamma_i^* \longrightarrow 1 \quad \text{as} \quad x_i \longrightarrow 0 \quad \text{and} \quad x_r \longrightarrow 1 \qquad \text{and} \quad f_i^{oL} = H_i \text{ (in pure r)}$$

$$\text{where } H_i \text{(in pure r)} \equiv \lim_{\substack{x_i \longrightarrow 0 \\ x_r \longrightarrow 1}} \frac{f_i^L}{x_i}$$

The second disadvantage of equation (38) concerns the effect of pressure on the thermodynamic properties of condensed phases. At low pressures the effect of pressure on the thermodynamic properties of condensed phases is negligible but at higher pressures this is no longer the case.

The pressure at which standard state fugacities are most conveniently evaluated is suggested by considerations based on the

Gibbs-Duhem equation, which says that at constant temperature and pressure

$$\sum_i x_i \, d \ln \gamma_i = 0 \tag{41}$$

If, however, we wish to vary the composition of a two-phase mixture over all possible composition values at a constant temperature, the pressure will not remain constant. Therefore, if integrated forms of the Gibbs-Duhem equation are to be used to correlate isothermal activity coefficient data, it is necessary that all activity coefficients be evaluated at the same pressure. Hence, experimentally obtained isothermal activity coefficients must be corrected from the experimental total pressure P to some constant reference pressure P^r.

When the standard state fugacity is defined at a constant pressure, for any component i, the pressure dependence of the activity coefficient γ_i is given by

$$\left(\frac{\partial}{\partial P} \ln \gamma_i\right)_{T,x} = \frac{\bar{V}_i}{RT} \tag{42}$$

where $\bar{V}_i$ = partial molal volume of component i.

By integration of equation (42) experimentally obtained activity coefficients are corrected to the constant reference pressure P^r, thatis,

$$\gamma_i^{(Pr)} = \gamma_i^P \exp \int_P^{Pr} \frac{\bar{V}_i}{RT} \, dP \tag{43}$$

The above leads to the introduction of constant pressure activity coefficients.

III D.(2) Constant-Pressure Activity Coefficients

Consider a binary liquid mixture at temperature T such that

$Tc_1 > T > Tc_2$; component 1 is the (liquid) solvent and component 2 is the (normally gaseous) solute. For component 1 $\gamma_1^{(P^r)}$ is defined by

$$\gamma_1^{(P^r)} = \frac{f_1}{x_1 f_1^{o(P^r)}} \exp \int_P^{P^r} \frac{\bar{V}_1^{L}}{RT} dP \qquad (44)$$

where P^r is a fixed reference pressure, $\bar{V}_1^{L}$ is the partial molar volume of component 1 in the liquid mixture at system temperature T_1 and $f_1^{o(P^r)} = f_{\text{pure } 1}^{(P^r)}$, the fugacity of pure liquid 1 at reference pressure P^r and temperature T.

For component 2, $\gamma_2^{*(P^r)}$ is defined by

$$\gamma_2^{*(P^r)} = \frac{f_2}{x_2 H_{2(1)}^{(P^r)}} \exp \int_P^{P^r} \frac{\bar{V}_2^{L}}{RT} dP \qquad (45)$$

where P^r is the same reference pressure as that used in equation (44), $\bar{V}_2^{L}$ is the partial molar volume of component 2 in the liquid mixture at system temperature T_1 and $H_{2(1)}^{(P^r)}$ is Henry's constant for solute 2 in solvent 1 at reference pressure P^r and temperature T.

The reference fugacity $H_{2(1)}^{(P^r)}$ depends on the solvent 1 and is defined by

$$H_{2(1)}^{(P^r)} = \left[\underset{x_2 \to 0}{\text{Limit}} \frac{f_2}{x_2} \right] \exp \int_{P_1^s}^{P^r} \frac{\bar{V}_2^{\infty}}{RT} dP \qquad (46)$$

where P_1^s is the saturation (vapor) pressure of solvent 1 and $\bar{V}_2^{\infty}$ is the partial molar volume of solute 2, infinitely dilute in solvent 1, both at system temperature T.

At constant temperature, constant-pressure activity coefficients $\gamma_1^{(P^r)}$ and $\gamma_2^{*(P^r)}$ are functions of composition only; they do not depend

on the total pressure. At constant temperature, these constant-pressure activity coefficients satisfy the Gibbs-Duhem equation

$$x_1 \, d \ln \gamma_1^{(P^r)} + x_2 \, d \ln \gamma_2^{*(P^r)} = 0 \tag{47}$$

where for the solvent, component 1

$$\gamma_1^{(P^r)} \longrightarrow 1 \text{ as } x_1 \longrightarrow 1 \tag{48}$$

and for the solute, component 2

$$\gamma_2^{*(P^r)} \longrightarrow 1 \text{ as } x_2 \Longrightarrow 0 \tag{49}$$

The reference pressure P^r is arbitrary and is most conveniently set equal to zero.

III D. (3) Excess Gibbs Energy

Constant-pressure activity coefficients depend on temperature, and on composition; the composition dependence is conveniently expressed through the molar excess Gibbs energy g^{E^*} defined by

$$\frac{g^{E^*}}{RT} = \sum_{\substack{\text{All solvent} \\ \text{components}}} x_i \ln \gamma_i^{(P^r)} + \sum_{\substack{\text{All solute} \\ \text{components}}} x_i \ln \gamma_i^{*(P^r)} \tag{50}$$

The individual activity coefficients are related to g^{E^*} by

$$RT \ln \gamma_i^{(P^r)} = \left(\frac{\partial n_T}{\partial n_i} g^{E^*}\right)_{T,P,n_j} \text{ for solvents} \tag{51}$$

$$\text{or } RT \ln \gamma_i^{*(P^r)} = \left(\frac{\partial n_T}{\partial n_i} g^{E^*}\right)_{T,P,n_j} \text{ for solutes} \tag{52}$$

where n_i is the number of moles of component i, n_T is the total number of moles and the subscript n_i denotes that all mole numbers except n_i are held constant.

In view of the unsymmetric normalization, g^{E^*} vanishes at infinite dilution with respect to component 2 but not with respect to component 1, that is,

$$\begin{aligned} & g^{E^*} \longrightarrow 0 \text{ as } x_2 \longrightarrow 0 \\ \text{but} \quad & g^{E^*} \not\longrightarrow 0 \text{ as } x_1 \longrightarrow 0 \end{aligned} \tag{53}$$

With the above definition, the ideal solution ($g^{E^*} = 0$) is one where at constant temperature and pressure, the fugacity of the light component is given by Henry's law and that of the heavy component by Raoult's law.

In a manner analogous to that used by Wohl (67) the excess Gibbs energy can be represented by summing interactions of molecules:

$$\frac{g^{E^*}}{RT(x_1q_1 + x_2q_2)} = - \alpha_{22(1)} \Phi_2^2 \tag{54}$$

where Φ_2 is the effective volume fraction given by

$$\Phi_2 = \frac{x_2q_2}{x_1q_1 + x_2q_2} \tag{55}$$

where q_1 is the effective size of molecule 1 and $\alpha_{22(1)}$ is the self-interaction constant for molecules 2 in the environment of molecules 1.

Activity coefficients can be found from the exact relations

$$\ln \gamma_1^{(P,r)} = \left(\frac{\partial n_T}{\partial n_1} g^{E^*}/RT\right)_{T,P,n_2} \tag{56}$$

$$\ln \gamma_2^{*(P,r)} = \left(\frac{\partial n_T}{\partial n_2} g^{E^*}/RT\right)_{T,P,n_1} \tag{57}$$

where n_1 stands for the number of moles of component 1 and n_T is the total number of moles.

A dilated van Laar model is used to express g^{E*} as a function of composition and temperature. The van Laar model provides a good description of the effect of composition for mixtures of non-polar or slightly polar components up to the critical region. Since the effect of temperature is not given explicitly by the dilated van Laar model, it is absorbed in the temperature dependent parameters which appear in that model.

III D. (4) A Dilated Van Laar Model for Binary Liquid Mixtures

Equations (54) and (55) yield the classical van Laar equations for unsymmetric normalization. It has been shown by Muirbook (68) that these equations, containing two adjustable parameters, are unsatisfactory for describing the properties of some systems which are at a temperature much above the critical temperature of the light component, or near the critical temperature of the heavy component.

Van Laar's assumption that q_1 and q_2 are constants independent of composition is one of the reasons for the failure of the classical treatment. The q's are parameters which reflect the cross-sections, or sizes, or spheres of influence of the molecules. At conditions remote from the critical region it is reasonable to assume that the q's are composition independent since then the liquid molar volume is close to a linear function of the mole fraction, but for a mixture of a non-condensable component and a subcritical liquid near the critical point, the molar volume of the mixture is a non-linear function of the mole fraction and hence the classical van Laar treatment has to be modified.

Chueh and Prausnitz (50) in their modification of the van Laar

equations assumed that whereas q_1 and q_2 depend on composition, their ratio does not. Assuming that q_1 and q_2 are given by a quadratic function of the effective volume fraction of the solute, we have

$$q_1 = Vc_1 \ (1 + \eta_2(1) \ \Phi_2^2) \tag{58}$$

$$q_2 = Vc_2 \ (1 + \eta_2(1) \ \Phi_2^2) \tag{59}$$

where Φ_2 is defined by equation A*.

From equations (58) and (59) it can be deduced that at infinite dilution when $\Phi_2 = 0$, $q_1 = Vc_1$ and $q_2 = Vc_2$, that is, the molecular cross sections at infinite dilution are equal to the pure component critical volumes. The dilation constant $\eta_2(1)$ is a measure of how effectively the light component dilates (swells) the liquid solution.

Solving equation (54) with the help of equations (58) and (59), the constant pressure activity coefficients are given by:

$$\ln \gamma_1^{(Pr)} = A \ \Phi_2^2 + B \ \Phi_2^4 \tag{60}$$

$$\ln \gamma_2^{*(Pr)} = A \ \frac{Vc_2}{Vc_1} \ (\Phi_2^2 - 2 \ \Phi_2) + B(\frac{Vc_2}{Vc_1}) \ (\Phi_2^4 - \frac{4}{3} \ \Phi_2^3) \tag{61}$$

$$\text{where } A \equiv \alpha_{22(1)} \ Vc_1 \tag{62}$$

$$B \equiv 3\eta_2 \ (1) \ \alpha_{22(1)} \ Vc_1 \tag{63}$$

Equation (60) can be deduced from Wohl's treatment (67) for the dependence of g^{*E} on the composition of the liquid phase. The final form of the Wohl equation of the third order for a binary system is

$$\ln \gamma_1 = \Phi_2^2 \quad A + 2 \ \Phi_1 \ (B \ \frac{q_1}{q_2} - A) + ... \tag{64}$$

$$\ln \gamma_2^* = \Phi_1^2 \quad B + 2 \ \Phi_2 \ (A \ \frac{q_2}{q_1} - B) + ... \tag{65}$$

If now we introduce the assumption that $\frac{q_1}{q_2} = \frac{A}{B}$ we obtain the

A* $$\Phi_2 = \frac{x_2 Vc_2}{x_1 Vc_1 + x_2 Vc_2}$$

van Laar equation for γ_1 as

$$\ln \gamma_1 = A \Phi_2^2 + \ldots . \qquad (66)$$

where, as seen, the cubic term Φ_2^3 disappears and only even powers are left.

Chueh and Prausnitz (50) did not use the Gibbs-Duhem equation (47) to find $\ln \gamma_2^{*(Pr)}$ but they observed that equations (60) and (61) provide accurate representation of the pressure-independent activity coefficients of non-polar binary mixtures from the dilute region up to the critical composition.

III D. (5) Partial Molar Volume from an Equation of State

As indicated by equation (42) the effect of pressure on liquid phase activity coefficients is given by the partial molar volumes in the liquid mixture through the equation

$$\left(\frac{\partial}{\partial P} \ln \gamma_i\right)_{T,X} = \frac{\bar{V}_i}{RT} \qquad (42)$$

At high pressures in the critical region, $\bar{V}_i$ is usually a strong function of composition, especially for heavy components where $\bar{V}_i$ frequently changes sign as well as magnitude. There are very few experimental data for partial molar volumes of binary systems and, because thermodynamic analysis of high pressure phase equilibria requires partial molar volumes, a reliable method for calculating them from a minimum of experimental information is needed.

The partial molar volume of component K in a mixture of N components is defined by

$$\bar{V}_K = \left(\frac{\partial V}{\partial n_K}\right)_{P,T,n_i (i \neq K)} \qquad (67)$$

Given a suitable equation of state, the partial molar volume can be calculated from equation (67). Equation (67) is transformed to

$$\bar{V}_K = - \frac{\left(\frac{\partial P}{\partial n_K}\right)_{T,V,n_i (i \neq K)}}{\left(\frac{\partial P}{\partial V}\right)_{T,n_i}} = f\,(x,T,V)$$

since most equations of state are explicit in pressure rather than in volume. In vapor-liquid equilibria what is required is partial molar volumes at saturation; that is, we need the saturated molar volume of the liquid mixture. This can be calculated by extending to mixtures, the corresponding-states correlation of Lyckman and Eckert (69) who revised Pitzer's tables (70) for the saturated liquid volume of pure substances for the reduced temperature region 0.56 - 1.00. Before discussing equation (68) thoroughly, attention is turned to a method for calculating the molar volume of a saturated liquid mixture.

III D. (5) a. Saturated Molar Volume of Liquid Mixtures Up to a Reduced Temperature of 0.93

The corresponding-states correlation developed for saturated liquids by Lyckman and Eckert (69) gives the following expression for the reduced saturated volume

$$V_R = V_R^{(0)} + \omega V_R^{(1)} + \omega^2 V_R^{(2)} \tag{69}$$

where ω is the acentric factor (70,71) and $V_R^{(0)}$, $V_R^{(1)}$ and $V_R^{(2)}$ are functions of the reduced temperature which have been tabulated for T_R ranging from 0.560 to 0.990 (69).

Chueh and Prausnitz (50) modified equation (69) so that the calculations can be facilitated using an electronic computer.

Their relation is

$$V_R^{(j)} = A^{(j)} + B^{(j)}T_R + C^{(j)}T_R^2 + D^{(j)}T_R^3 + \frac{E^{(j)}}{T_R} + F^{(j)} \ln (1 - T_R) \tag{70}$$

where $A^{(j)}$ to $F^{(j)}$ are coefficients for $V_R^{(0)}$, $V_R^{(1)}$ and $V_R^{(2)}$ and are tabulated in their publication (50)

Relatively good agreement has been observed between tabulated values of $V_R^{(0)}$, $V_R^{(1)}$ and $V_R^{(2)}$ and those calculated from equation (70). For pure components, equations (69) and (70) may be used from a reduced temperature of 0.56 to a reduced temperature of 0.995. For reduced temperatures above 0.995, the reduced volume may be obtained by first calculating the reduced volumes at T_R of 0.990 and 0.995 and then interpolating to $T_R = 1.0$; by definition $V_R = 1.0$ and $T_R = 1.0$.

For application of equations (69) and (70) to mixtures, mixing rules for the pseudo-critical volume and temperature have been suggested (55,54,59,72,73,74).

$$V_{CM} = \sum_i x_i V_{c_i} \tag{71}$$

$$T_{CM} = \sum_i \sum_j \Phi_i \Phi_j T_{cij} \tag{72}$$

$$\omega_M = \sum_i \Phi_i \omega_i \tag{73}$$

where $$\Phi_K = \frac{x_K V_{cK}}{\sum_i x_i V_{ci}} \tag{74}$$

and $$T_{cij} = \sqrt{T_{cii} T_{cjj}} \; (1 - K_{ij}) \tag{75}$$

In equations (72) and (73) volume fractions rather than mole fractions are used since, because of the small separation between molecules, molecular size is a more important factor in the liquid phase than in the vapor phase.

We now have a reliable method for calculating the volumes of saturated liquid mixtures. With the help of an equation of state and

equation (68) we should be able to calculate partial molar volumes.

III D. (5) b. Equation of State for Liquid Mixtures

The Redlich-Kwong equation (24), with certain alterations, has been found to provide a reasonable description of volumetric properties of liquids. The universal constants $\Omega_a = 0.4278$ and $\Omega_b = 0.0867$ are not used since adoption of these values is equivalent to fitting the equation of state to derivates in the critical region which, although the most sensitive, does not provide the best fit over a wide range of conditions. It has been proposed (50) for each pure liquid to fit the Redlich-Kwong equation to the P-V-T data of the saturated liquid and to evaluate the best Ω_a and Ω_b values for each component.

For application to mixtures, the same mixing rules as given by equations (28) to (36) are used except that the cube root average for V_{cij} is replaced by the arithmetic mean of V_{ci} and V_{cj} so as to weight the larger molecule slightly more heavily in the liquid phase.

III D. (5) c. Partial Molar Volumes

Using equations (24) and (68) and the mixing rules (28) to (36), the partial molar volume is obtained in the following form:

$$\bar{V}_K = \frac{\dfrac{RT}{(V-b)}\left(1+\dfrac{b_K}{V-b}\right) - 2\sum_i^N x_i a_{K_i} - ab_K/V + b}{V(V+b)T^{\frac{1}{2}}}}{\dfrac{RT}{(V-b)^2} - \dfrac{a}{T^{\frac{1}{2}}}\left[\dfrac{2V+b}{V^2(V+b)^2}\right]} \qquad (76)$$

where V is the saturated liquid molar volume of the mixture. Once the partial molar volumes are known, the effect of pressure on liquid-

phase activity coefficients can be taken into account.

IV. Critical Properties of Mixtures

Much attention has been given to the critical properties of pure fluids both theoretically and experimentally (2,75) but the critical properties of mixtures are not known nearly as well, although experimental data are available for a large number of binary mixtures (19).

Thermodynamic analysis of vapor-liquid equilibria is difficult in the critical region because thermodynamic properties in that region are strongly sensitive to small changes in temperature, pressure and composition. To establish rational methods for calculating vapor-liquid equilibria, including the critical region, it is necessary to know where the critical region is or, more precisely, to express the critical temperature, critical volume and critical pressure as a function of composition. The literature reports several correlations (76,78,78,79) of the critical temperature or critical pressure of mixtures but these have been largely confined to a particular chemical class of substances (usually paraffins).

IV A. Critical Temperatures

Rowlinson (19) has shown that the true critical temperature T_{CT} of a binary mixture is, to a good approximation, a simple quadratic function of the mole fraction x, provided components 1 and 2 consist of simple, spherically symmetric molecules of nearly the same size. Rowlinson suggests the following expression:

$$T_{CT} = x_1 T_{C_1} + x_2 T_{C_2} + 2x_1 x_2 \Delta T_{12} \qquad (77)$$

where ΔT_{12} is a known function of T_{C1}, T_{C2}, V_{C1} and V_{C2} and a parameter which depends on the two exponents used in the potential function for describing the intermolecular forces.

Rowlinson's treatment is not useful for mixtures whose components differ appreciably in molecular size. The thermodynamic properties of such mixtures are quadratic functions of the mole fraction only at moderate densities; at liquid-like densities the thermodynamic properties of such mixtures are commonly expressed in terms of volume fractions. It has been suggested by Chueh and Prausnitz (50) that experimentally determined critical temperatures could be correlated as a quadratic function of the surface fraction θ, defined by

$$\theta_i = \frac{x_i V_{c_i}^{2/3}}{\sum_i^N x_i V_{c_i}^{2/3}} \tag{78}$$

For a binary mixture, the critical temperature is then given by

$$T_{CT} = \theta_1 T_{C1} + \theta_2 T_{C2} + 2\theta_1\theta_2\tau_{12} \tag{79}$$

where τ_{12} is a parameter characteristic of the 1-2 interaction.

IV B. Critical Volumes

The critical volume of a mixture can be expressed as a quadratic function of the composition if it is assumed that the configurational thermodynamic properties of a dense system are due to two-body nearest neighbour interactions, but, as in the case of the critical temperatures it has been found that the surface fraction is the best parameter for components of significantly different molecular size. The critical

volume of a binary mixture is therefore written as

$$V_{CT} = \theta_1 V_{C_1} + \theta_2 V_{C_2} + 2\theta_1\theta_2\nu_{12} \qquad (80)$$

where ν_{12}, is a correlating parameter characteristic of the 1,2 binary system.

IV C. Critical Pressures

The critical pressure cannot be correlated as quadratic functions of the surface fraction because it has been observed (79) that the dependence of the critical pressure on composition is much more strongly non-linear than that of the critical temperature and the critical volume. Both critical temperatures and critical volumes can be related directly to the intermolecular potential but critical pressure can be related to the intermolecular potential only indirectly through critical temperature and critical volume.

It is proposed to use the correlations for critical temperature and critical volume coupled with the Redlich-Kwong equation of state to express the critical pressure as a function of composition. The dimensionless parameters Ω_a and Ω_b are determined from experimental data available in the region of temperature and density where the equation of state is to be used. The mixing rules are the same as given by equations (28) to (36). Good agreement has been observed for several binary systems between experimental and calculated results.

CHAPTER II

NATURE OF THE PROBLEM AND REVIEW OF THE LITERATURE

Although most of the common liquids have been investigated at high temperatures, thermodynamic treatment of their mixtures has been limited to a particular class of substances, such as for example, the paraffins at relatively low temperatures and pressures. This has been so because the problems in high pressure, vapor liquid equilibrium thermodynamics are different from those encountered in phase equilibria at pressures near or below atmospheric.

Acetone, chloroform, benzene and carbon tetrachloride were chosen in this study because these materials have been intensively investigated at low temperatures (the vapor liquid equilibrium compositions at temperatures ranging from 10°C to 55°C have been determined for the binary systems and the vapor pressures of several mixtures of the binary systems have been determined at 25°C) and recently Chatterjee (80) has determined the orthobaric densities and vapor pressures of the pure liquids up to the critical region.

As well as the vapor pressures and the vapor liquid equilibrium compositions of the binary systems, I also determined the gas liquid critical temperature of each system as a function of composition since as pointed out by Rowlinson (19) the critical temperature of a simple mixture (L V) is one of the most direct sources of information on the energy of interaction of two unlike molecules.

The System Acetone-Chloroform

This system has been thoroughly investigated at low temperatures.

Campbell et al (81), who reported H^E values for this binary system at 25°C, also showed (82) the existence of a compound between acetone and chloroform in the liquid state and calculated the energy of the hydrogen bond from the heats of mixing data. The vapor pressure and the vapor liquid equilibrium compositions at temperatures ranging from 15°C to 55°C have been studied by many workers including Zawidzki (83), Röck and Schröder (84). A complete review of the work done on this binary system has been compiled by Chatterjee (85).

The System Benzene-Carbon Tetrachloride

The vapor liquid equilibrium compositions of this binary system at temperatures ranging from 25°C to 45°C have been determined by at least twelve different investigators including Young (86), Scatchard et al (87) and Fowler and Lim (88) and each has reported a somewhat different result. The existence or non-existence of an azeotrope has been a question for more than 50 years. Young (86) first suspected the formation of an azeotrope in this system and gave its composition as 91.65 mole percent carbon tetrachloride at 760 mm H_g. Scatchard et al (87) investigated the system under isobaric and isothermal conditions at 760 mm H_g and at 40°C but failed to find an azeotrope. Campbell and Dulmage (89) have stated definitely that the vapor phase is never richer in benzene than the liquid phase, over a range from 1 to 99 percent benzene; that is, there is no reversal of composition as there would be in passing through an azeotropic point.

The System Acetone-Carbon Tetrachloride

Vapor-liquid equilibrium compositions on the system Acetone-

Carbon Tetrachloride have been measured at 0°C by Gerritz (90), at 50°C by Severns et al (91) and by many other workers at relatively low temperatures. Brown and Smith (92) carried out vapor liquid equilibria measurements at 45°C and concluded that there exists an azeotrope at a mole fraction of acetone 0.964 and a pressure of 513.2 mm H_g. Ellis and Rose (93) have measured the vapor pressure of this binary system over a temperature range of 5 - 25°C.

CHAPTER III

EXPERIMENTAL PROCEDURE AND APPARATUS

I. Purification of the Materials

A. Acetone

Spectranalysed Acetone (ACS) from the Fisher Scientific Company was dried with anhydrous calcium sulphate and distilled to remove any water present. Calcium Chloride could not be used as a drying agent because it forms an addition compound. Organic impurities were removed from the distillate by treating it with silver nitrate solution, followed by sodium hydroxide solution. The solution was shaken vigorously, filtered and then distilled over anyhdrous calcium sulphate. The portion distilling between 56.1 to 56.2^{o}C under an atmospheric pressure of 746 mm H_g was collected. A fresh sample was prepared every week.

B. Chloroform

A fresh sample of chloroform was prepared every three days because it reacts slowly with oxygen when exposed to air and light. The principal products of this decomposition are carbonyl chloride (phosgene), chlorine and hydrogen chloride. Chloroform (ACS) from the Fisher Scientific Company was treated, to remove ethanol, by repeated extraction with concentrated sulphuric acid and final washing with distilled water. The chloroform was then dried with calcium chloride and distilled over phosphorus pentoxide. The final distillate was stored in a brown container wrapped in black paper and kept in a closed cupboard to prevent decomposition by light.

C. Benzene

Thiophene free Benzene (ACS) from the Fisher Scientific Company was shaken successively with concentrated sulphuric acid until the yellow color in the acid layer disappeared, then with water, dilute sodium hydroxide and finally with two portions of water. It was then dried over phosphorus pentoxide and distilled over pieces of sodium.

D. Carbon Tetrachloride

Carbon tetrachloride (ACS) from the Fisher Scientific Company was boiled with dilute alkali, potassium hydroxide to remove carbon disulfide. It was then shaken with a mixture of sodium hydroxide solution and potassium permanganate solution and distilled over barium oxide.

The physical constants, refractive index, and density of the purified materials compare well with the literature values. Table II gives a comparison between measured values and a few literature values.

TABLE II

Substance	Refractive Index at 25°C	Density at 25°C	Investigation
Acetone	1.3561	0.7880	This research
	1.3562	0.78799	Schwers (94)
	1.35609	0.7880	Rosin (95)
Chloroform	1.4433	1.4805	This research
	1.4433	1.4806	Campbell et al (96)
	1.4431	1.4789	Reinders and de Minjer (97)
Benzene	1.4979	0.8734	This research
	1.4980	0.8738	Reinders and de Minjer (97)
	--	0.87365	Brown and Smith (98)
Carbon Tetrachloride	1.4576	1.5842	This research
	--	1.5840	Rosin (95)
	1.4576	1.5843	Fowler and Lim (88)

II. Method of Analysis

Generally the analysis of the compositions of the liquid mixtures is made from physical properties like density, refractive index, viscosity, etc. The determining factors for the suitability of a certain physical property for analytical purposes are (1)the accuracy and reproducibility of the measurement, (2) the degree of variance of the property with concentration and, (3)the requirement of small amount of the sample in order to finish the measurement.

I tried analysing the vapor liquid compositions using gas chromatography, since only a very small amount of sample was required, but I abandoned this procedure for various reasons,for example,tailing encountered. Refractive index measurements using an Abbe Refractometer maintained at 25.00 ± 0.05^{o}C and the monochromatic light of a sodium lamp (5893A^{o}) were found to be the most suitable. The accuracy of the refractometer made by Officine Galileo of Italy is ±0.0001 unit of refractive index. An uncertainty of ±0.0001 in refractive index means an uncertainty of 0.001 in the values of mole fraction.

III. Determination of Temperature at which Meniscus Disappears

The critical temperature, being the easiest to measure of the three critical constants (T_c, P_c, and V_c) has been measured for at least 200 pure substances. A very thorough review has been made by Kobe and Lynn (99). Most of these measurements have been carried out by observing the temperature at which the meniscus disappears in a system maintained at an overall density nearly equal to the critical.

If a sealed tube containing liquid and vapor is heated uniformly, then, depending on the conditions, one of three things may occur.

If the overall density is less than the critical, then the liquid evaporates and the meniscus falls. If the overall density is greater than the critical, then the meniscus rises and liquid completely fills the tube. And finally, if the density is nearly equal to the critical then the meniscus becomes flatter and fainter until the critical temperature is reached when the meniscus disappears at the centre of the tube. It has been observed by many workers including myself that the overall density does not have to be exactly that of the critical to observe the fluctuating striae characteristic of critical phenomena.

The above method was the one I chose for the study of the three binary systems (1)Acetone-Chloroform (2)Benzene-Carbon Tetrachloirde and (3)Acetone-Carbon Tetrachloride. The experimental tubes were 15 cm long and had an internal diameter of 2mm. They were sealed at one end and had a slight constriction, to permit easy sealing off, near the open end.

The apparatus for degassing the samples and for transferring a degrassed sample to the experimental tube is shown in Figure IV. A mercury diffusion pump B backed by a mechanical oil pump A was used to produce a vacuum with a residual non-condensable gas pressure of less than 10^{-5} mm of mercury. The samples were degassed by a series of operations which included freezing with liquid nitrogen and pumping off the residual gas over the frozen liquid. The freeze-pump-thaw operation was carried out several times to remove as much dissolved air as possible.

FIGURE IV. Apparatus for Degassing and Preparing Mixtures.

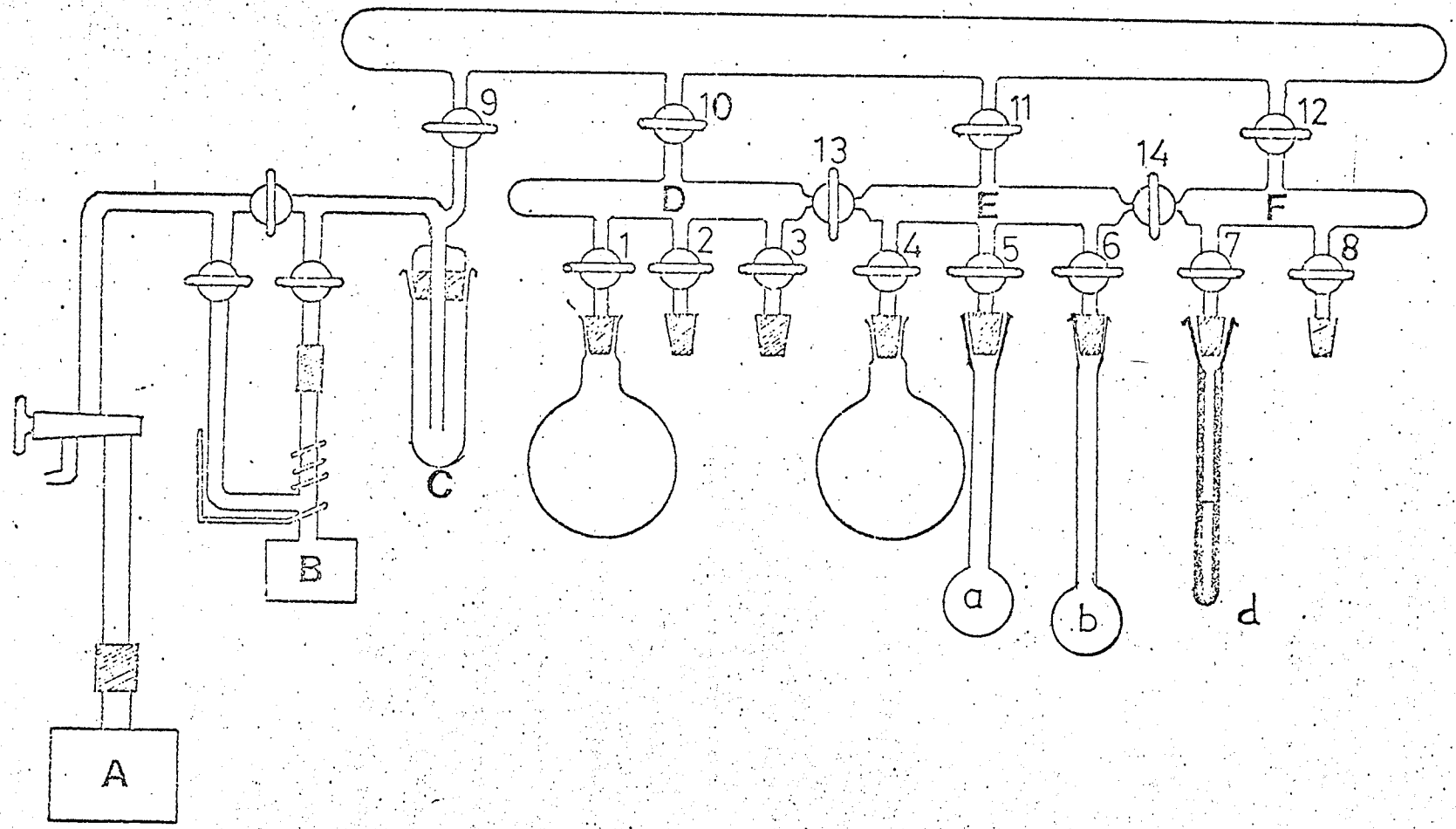
9
10
11
12
13
14
D
E
F
1
2
3
4
5
6
7
8
A
B
C
a
b
d

Pure liquid 1 was contained in flask b which was attached to the vacuum line by means of a ground joint. The sample was frozen in liquid nitrogen and the air above the frozen liquid was pumped off with stopcock 6 open. After half an hour, when the pressure would be less than 10^{-5}mm H_g, stopcock 6 was closed and the frozen liquid melted when entrapped bubbles of air escaped. Flask b was again put in liquid nitrogen to freeze the sample and stopcock 6 opened so that the flask could be evacuated. This process was carried out several times to ensure that most of the air had been removed from the sample. Then a calibrated 1 mm internal diameter capillary tube d was connected to stopcock 7. With all stopcocks except 6, 14 and 7 closed, flask b was warmed and the tip of the capillary tube d was cooled with liquid nitrogen so that liquid 1 would distil into d. Using a cathethometer (accurate to 0.05 mm) to measure the length of the tube occupied by liquid 1 at room temperature and knowing the density of the liquid at that temperature, the mass of component 1 was determined. The sample tube was connected to stopcock 8 and compartment F and the sample tube were evacuated. The material in d was then totally vacuum distilled into the sample tube. Stopcock 8 was then closed.

Flask b was then removed and cleaned thoroughly. Component 2 was then introduced in b and the same process as described for component 1 was carried out. Finally a known length of component 2 from d was distilled into the sample tube. Knowing the weight of each component in the sample tube, the composition was calculated. The sample tube was then sealed off at the constriction with the sample kept frozen in liquid nitrogen.

The tube with a sample of known composition was then placed in the thermostat (for a description of the thermostat see section III (a)) which was initially kept at 200°C. A rough guess of the critical temperature of a mixture could be made, and for the final few degrees before reaching it, the rate of heating of the sample was very slow (a very small heater was used to heat the silicone bath). The meniscus which becomes faint and hazy as the temperature is raised was observed through the glass window by means of a telescope placed two metres away from the thermostat. As soon as the meniscus disappeared, the temperature, measured by a copper constantan multiple junction thermocouple, was noted. The thermostat was allowed to cool down slowly and the temperature at which the meniscus reappeared was noted. The mean of the two temperatures was taken as the correct reading. The reproducibility of the observations of the critical points was 0.05°C to 0.10°C for the mixtures. The above procedure was carried out over the whole range of concentration for each binary system.

III a. The Thermostat

The thermostat is shown in Figure V. It consists of a glass jar of 5 litres capacity lagged with vermiculite and contained in a metal container except for a glass window 3 inches wide by 9 inches high. A bulb placed directly behind the window in the vermiculite insulator illuminates the thermostat and allows clear observation of the sample tubes. The thermostat liquid was stirred by a paddle rotated by a powerful motor and the temperature was controlled by a solid state Proportional Temperature Controller manufactured by Athena Controls Inc.,

FIGURE V. The Thermostat.

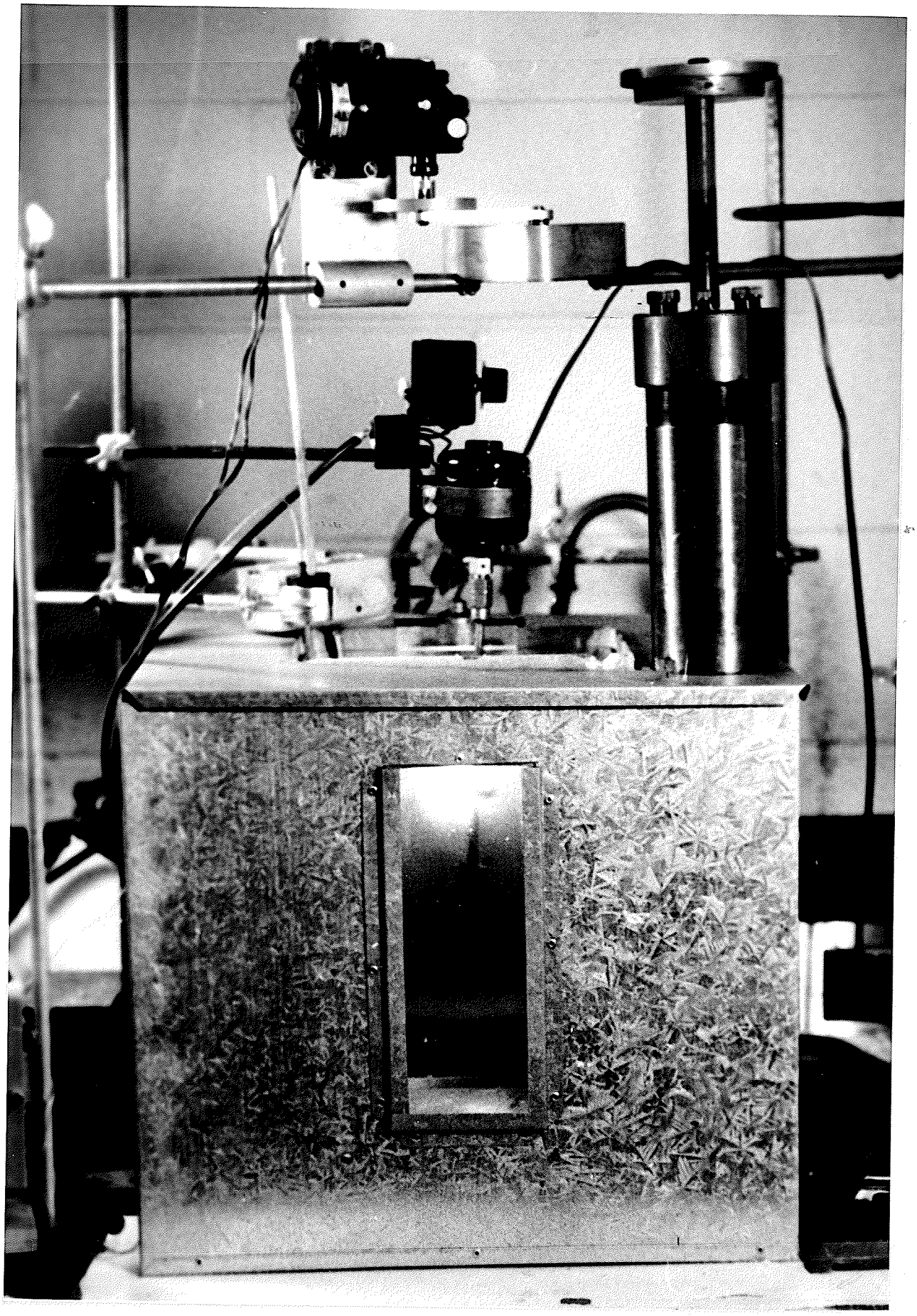

Pennsylvania. To prevent corrosion by the thermostat liquid the temperature sensor was a thermistor sheathed in stainless steel and the heating element was encased in non-corrosive "Nickel-Chrome-Iron" alloy. The temperature was measured using a multiple junction copper constantan thermocouple in conjunction with a Tinsley vermier potentiometer (Type 4363A) measuring to a microvolt for the emf measurements. The thermocouple was calibrated with the standard temperatures of the ice point, steam point, melting points of tin, bismuth and cadmium with the cold junction in a bath of melting ice.

The thermostat liquid was Dow Corning Silicone Oil 550 up to a temperature of 225^{o}C and a eutectic mixture of potassium, sodium and lithium nitrates was used for temperatures higher than 225^{o}C. When using the fused salt bath the glass container had to be changed every month or so because of corrosion. The temperature control was better than ±0.03^{o}C up to 225^{o}C and ±0.03^{o}C above that.

IV. Measurement of Vapor-Liquid Compositions

In the measurement of vapor-liquid equilibrium compositions one is interested in separating the vapor and liquid phases and determining their compositions at equilibrium. This can be achieved by the following methods (a)Distillation Method, (b)Circulation Method, (c)Static Method, (d)Dew and Bubble Point Method and, (e)Flow Method.

I used the static method, which is very satisfactory at high pressures and temperatures, in my study of the three binaries. The apparatus used is shown in Figure VI. The cylindrical glass bomb, 16 cms. long and 5 cms diameter, made from thick walled pyrex was divided into two compartments by a ring seal such that the upper

FIGURE VI. Sectional View of the Glass and Metal Bombs for Vapor-Liquid Equilibrium Composition Determination.

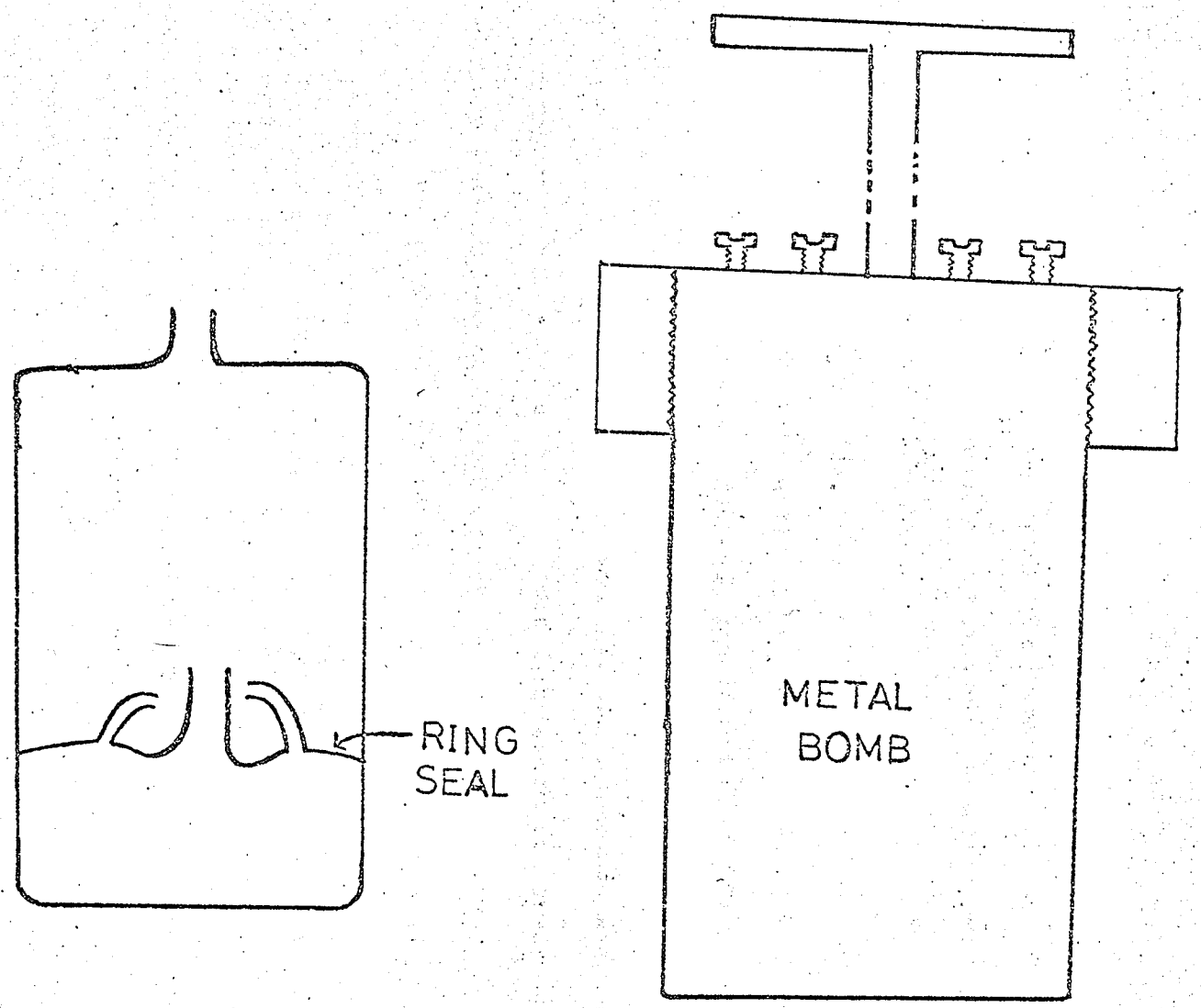
RING
SEAL
METAL
BOMB

compartment was twice as large as the lower one. The liquid could initially be introduced into the lower compartment through the centre tube. The ring seal had vents through which the vapor could escape to the upper compartment. These vents were bent so that there was no possibility of the condensed vapor mixing with the liquid phase.

A sample of about 30 ml volume, whose composition was made up by weighing, was introduced into the lower compartment and frozen using liquid nitrogen. The centre tube was attached to the vacuum pump and the glass bomb was evacuated. After a couple of hours the centre tube was sealed off so that a closed system was obtained. The bomb was allowed to warm up to room temperature and then placed in a metal container which had a glass sleeve, containing some of the sample, in the inside. This was done so that the pressure inside the glass bomb could be equalised by the outside pressure and hence prevent explosion. The glass sleeve was used because the organic materials underwent extensive decomposition when heated, with the metal.

The metal container had a screw cap which fitted tightly on the cylinder. To get a very good seal a copper O ring was used between the cap and the collar of the cylinder. The Allenhead bolts were then screwed down so that the O ring sat tightly on the groove made on the collar of the cylinder. A pressure-tight system was thus obtained.

The metal container was then attached to a shaking device and lowered into the thermostat which was kept at a required temperature. The shaking device is shown in Figure VII. It consists of a powerful motor mounted in a horizontal position and bearing on its shaft an

FIGURE VII. The Metal Bomb in the High Temperature Bath with the Shaking Mechanism.

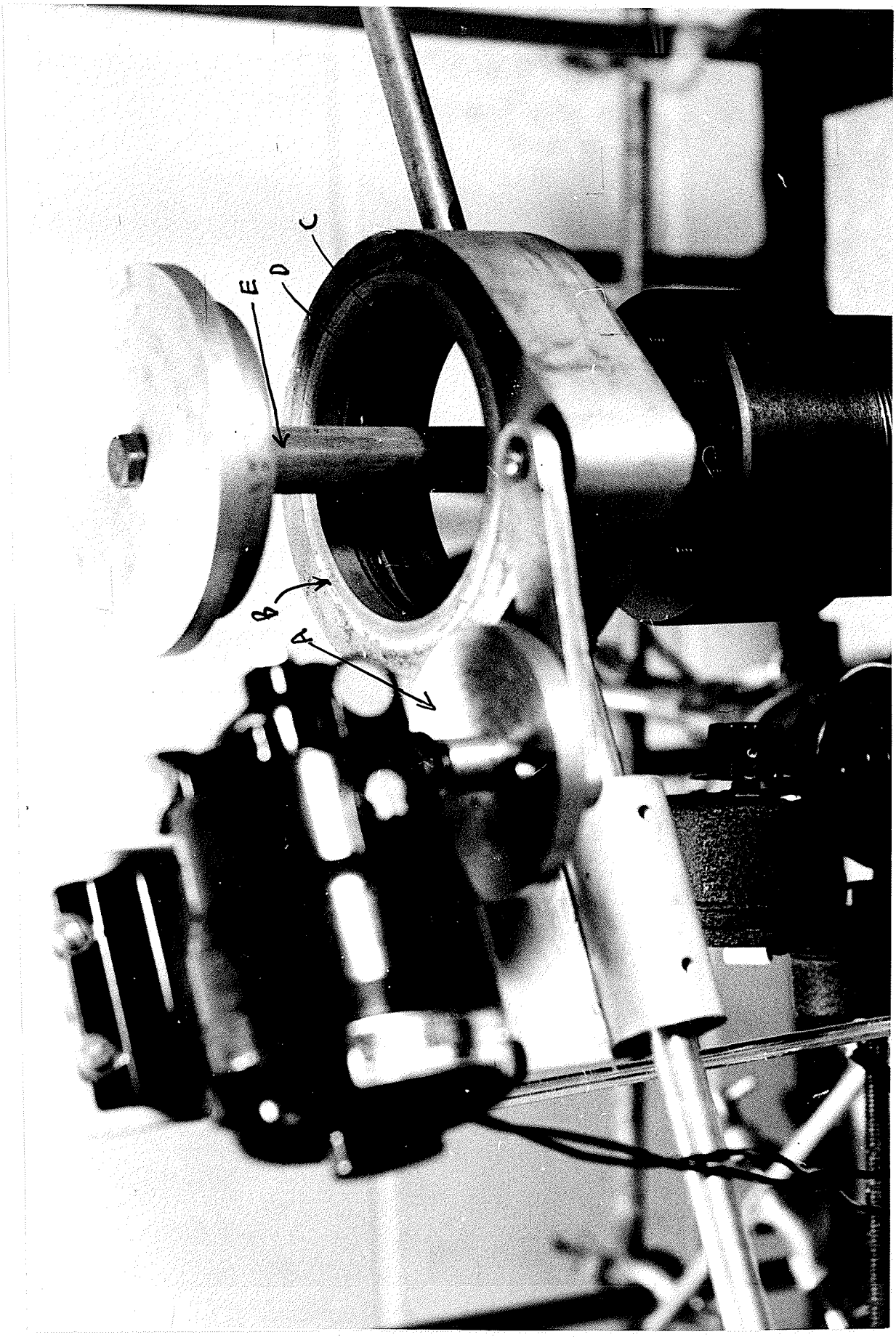
E
D
C
B
A

eccentric cam A which was in turn mounted on another eccentric annular disk B. The disk B consisted of a thrust bearing C mounted inside an aluminium collar which had an annular aluminium cover D resting on the thrust bearing and overhanging the outside of the collar. The metal extension E of the metal container protruding upwards was screwed on to an aluminium disk F which fitted and rested on the annular aluminium aluminium disk B of the shaker. The whole apparatus was kept immersed in the thermostat and shaken for twelve hours to allow equilibration.

The bomb was then removed from the bath and immediately chilled using a mixture of ice and water. The cap was taken off and the glass bomb removed and chilled in cold water. The vapor condensed on the walls of the bomb and collected over the ring seal. The seal on the stem of the bomb was broken and the liquid and vapor phases were withdrawn from the lower and uppercompartments respectively using separate syringes. The two phases were then analysed using an Abbe refractometer maintained at 25.00^{o}C.

V. Measurement of Vapor Pressure

I used a closed manometer, whose operation is based on the compression of a known volume of air, to determine the vapor pressure of the three binary systems over the whole concentration range. The apparatus is shown in Figure VIII. The section of the manometer containing the bulb A was made of thick 3 mm diameter capillary tube and the rest of the apparatus was 1 mm diameter capillary.

The tube C, around 80 cms long, was initially calibrated every 1 cm along its entire length. The calibration was carried out at

FIGURE VIII. Mercury-Air Manometer.

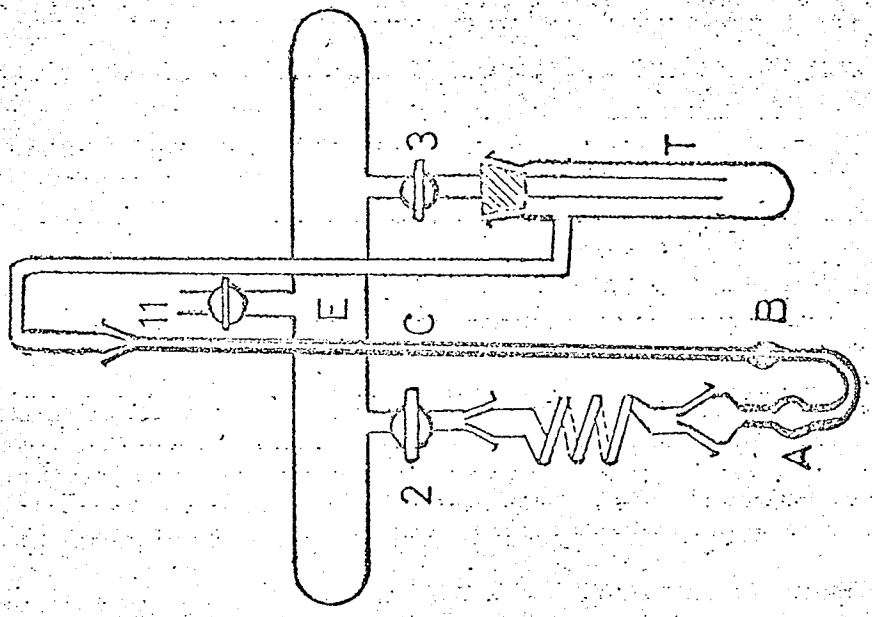
3
T
11
E
C
B
2
A

25.00°C using pure distilled mercury. Bulb A and about 12 cms of 3 mm interval diameter capillary on each side of it were then calibrated so that the volume of vapor and the volume of liquid could be measured. The two tubes were then joined taking care to avoid much distortion in the glass.

Pure mercury was added to the manometer in such a way that bulb A was filled. The apparatus was then attached at both ends to the vacuum pump and the mercury was warmed slowly so that all entrapped air could be removed. The manometer was tapped lightly to help the degassing process.

A sample of known composition was then vacuum distilled on top of the mercury in bulb A by the process described earlier. The mercury and the sample were then frozen using liquid nitrogen and evacuated. The process of freezing-pumping and thawing was continued until all residual air had been expelled. The top of the 3 mm tube was sealed off while the sample was still frozen. The whole manometer was then disconnected from the pump and allowed to warm up when the mercury would push the liquid up to the end of the tube. The end of C was then sealed off and the atmospheric pressure was read. The volume of air in C under atmospheric pressure and at a temperature of 25°C (tube C was enclosed in a glass mantle which was kept at 25.00°C) was obtained using a cathethometer accurate to 0.05 cm.

The apparatus was then placed in the high temperature bath making sure that the 3 mm tube was completely immersed. The thermostat containing silicone fluid 550 was initially kept at 100°C and its temperature was raised to about 5 degree intervals after each reading. The

salt bath kept initially at 200°C was used for the temperature range 200°C to 280°C. The volume of vapor, volume of liquid and volume of air in C were read using a cathethometer. Van der Waals' equation was used to calculate the pressure from the compressed volume of air. The correct vapor pressure was obtained by adding to the calculated pressure, the hydrostatic pressure of the mercury column. It has been shown (80) that the van der Waals' equation is quite satisfactory to calculate the vapor pressure.

Thirty minutes were allowed for establishment of equilibrium--I could not allow more time because the samples decomposed on heating. Two sets of experiments were carried out. The temperature was raised from 100°C to 190°C in one set and using a completely separate filling the temperature was raised from 200°C to 280°C for the other set. It was assumed throughout this work that the composition of the liquid did not change appreciably as the temperature was raised. The vapor phase was always much smaller than the liquid phase.

CHAPTER IV

EXPERIMENTAL RESULTS

I. Critical Temperature

I. (A) Pure Liquids

The temperature at which the meniscus disappears (that is, the mean of the temperatures at which the meniscus disappears and reappears) has been obtained for each pure liquid. They are given below in Table III. The uncertainty of the measurements is $\pm 0.1^{o}C$.

TABLE III

Critical Temperature of the Pure Liquids

Substance	Critical Temperature (^{o}C)
Acetone	235.0
Carbon Tetrachloride	283.2
Benzene	288.0
Chloroform	263.2

I (B) The System Acetone-Chloroform

The gas liquid critical temperatures for this binary system have been determined over the whole concentration range. The results are given in Table IV.

Figure IX represents the variation of the critical temperature with composition in mole per cent. It was observed that chloroform and mixtures having relatively high chloroform content developed a yellowish color on prolonged heating. For this reason the tubes containing these mixtures were introduced in the bath when the temperature was only a few

TABLE IV

Gas Liquid Critical Temperatures of the System Acetone-Chloroform

Composition of the Mixture		Experimental Critical Temperature (^{o}C)
Mole % Acetone	Mole % Chloroform	
100	0	235.0
95.98	4.02	236.50
86.50	13.50	239.70
76.94	23.06	243.05
70.60	29.40	245.00
60.57	39.43	248.15
53.00	47.00	249.75
39.85	60.15	254.15
22.50	77.50	257.50
7.71	92.29	261.05
0	100	263.20

FIGURE IX. Gas-Liquid Critical Temperatures of the Acetone-Chloroform System as a Function of Mole percent Chloroform.

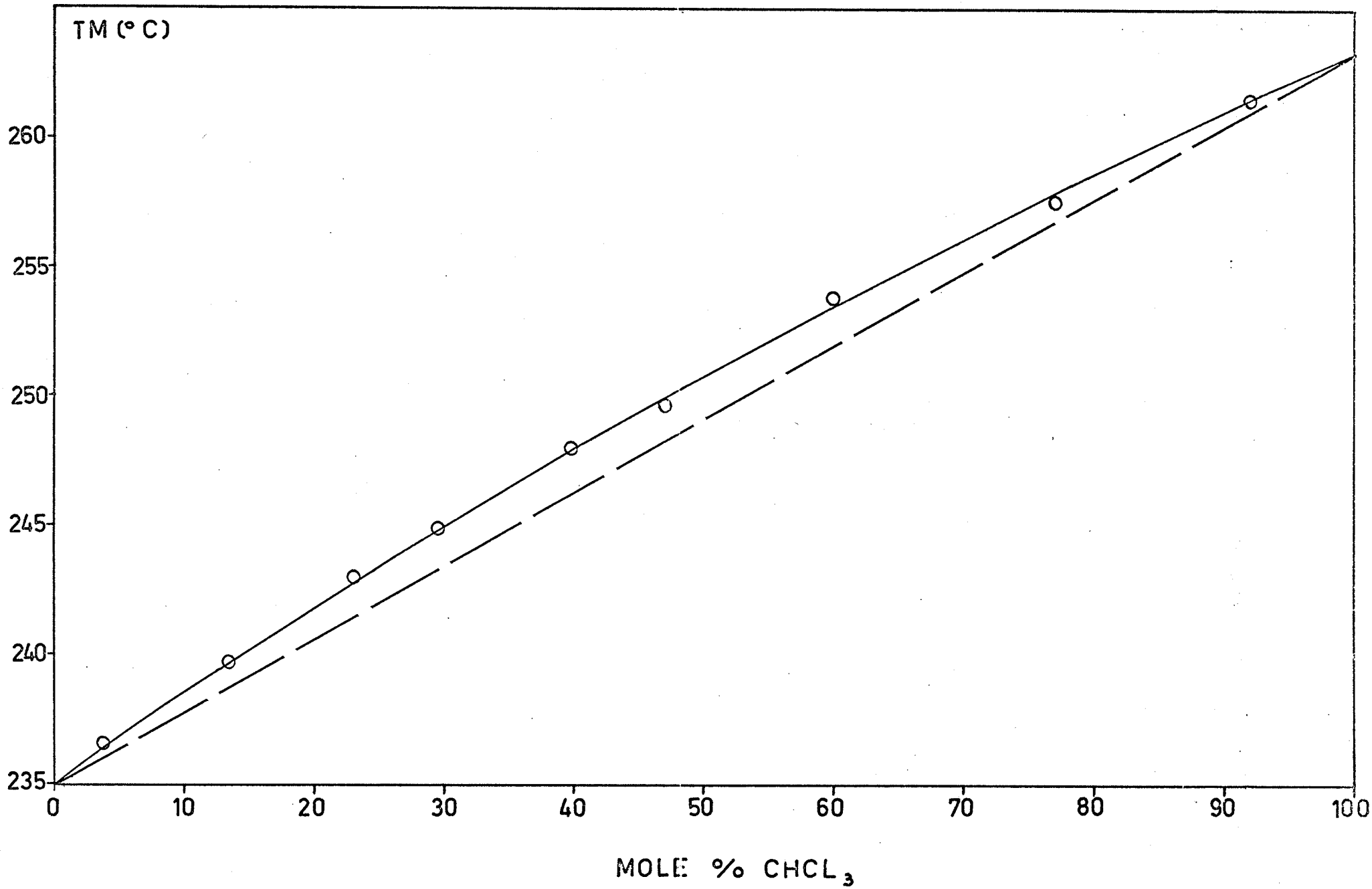
TM (° C)
260
255
250
245
240
235
0
10
20
30
40
50
60
70
80
90
100
MOLE % CHCL3

degrees from the critical point.

I (C) The System Acetone-Carbon Tetrachloride

The gas liquid critical temperatures of this binary system are given in Table V. The data are plotted in Figure X.

TABLE V

Gas Liquid Critical Temperatures of the System Acetone-Carbon Tetrachloride

Composition of the Mixture		Experimental Critical
Mole % Acetone	Mole % CCl_4	Temperature (^oC)
0	100	283.20
6.50	93.50	279.50
12.50	87.50	276.40
20.90	79.10	271.70
27.60	72.40	268.40
39.50	60.50	262.50
52.90	47.10	255.60
64.50	35.50	249.90
78.20	21.80	243.55
95.25	4.75	236.65
100	0	235.0

I (D) The System Benzene-Carbon Tetrachloride

The gas liquid critical temperatures of this binary system have been obtained for the whole concentration range. The results are given in Table VI, and Figure XI represents the variation of the critical points with composition.

FIGURE X. Gas-Liquid Critical Temperatures of the Acetone-Carbon Tetrachloride System as a Function of Mole percent Acetone.

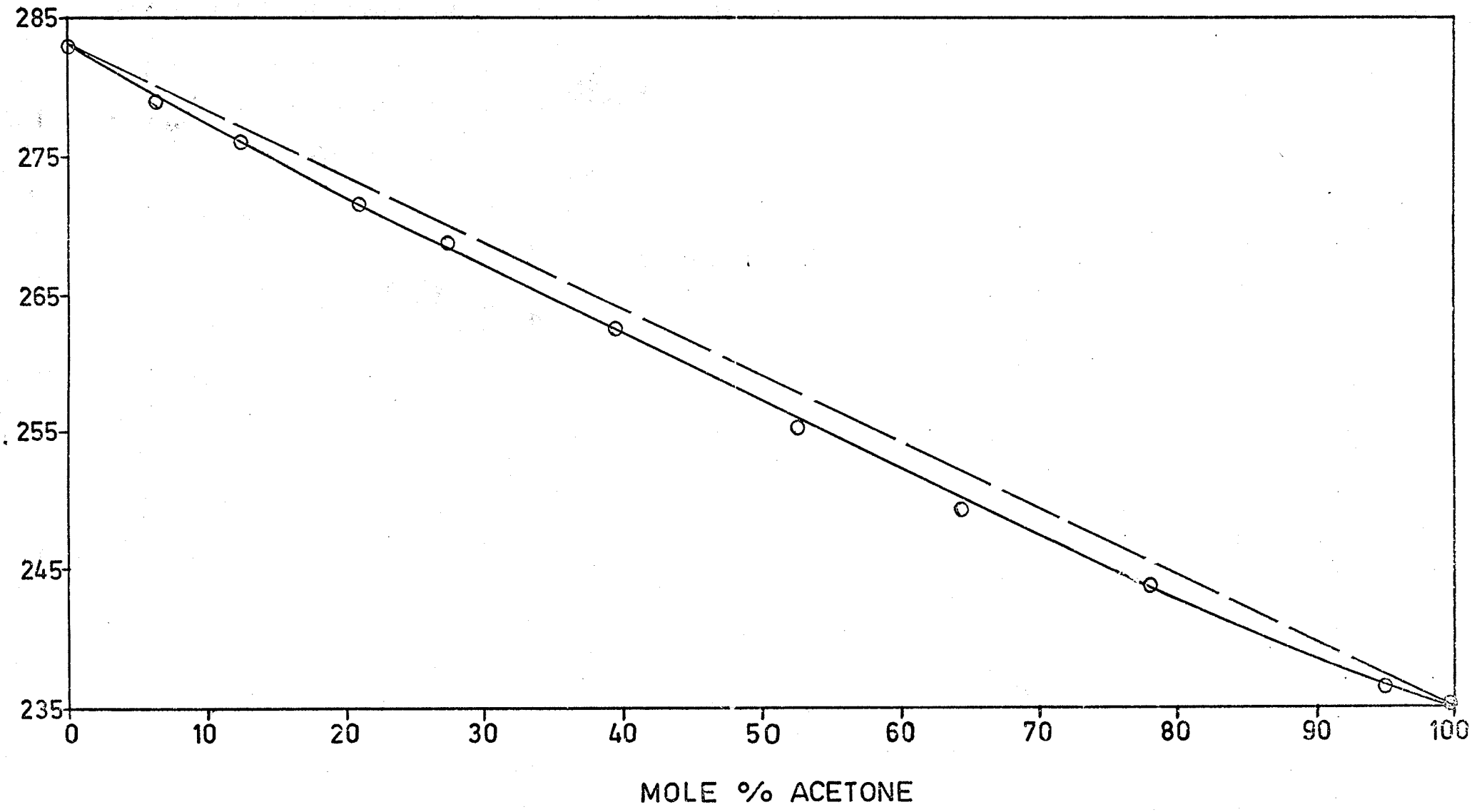
285
275
265
255
245
235
0
10
20
30
40
50
60
70
80
90
100
MOLE % ACETONE

TABLE VI

Gas Liquid Critical Temperatures of the System Benzene-Carbon Tetrachloride

Composition of the Mixture		Experimental Critical Temperature (^{o}C)
Mole % CCl_4	Mole % C_6H_6	
0	100	288.0
5.90	94.10	287.4
16.25	83.75	286.9
26.40	73.60	286.5
38.22	61.78	285.7
47.33	52.67	285.3
56.00	44.00	285.0
76.50	23.50	283.9
90.42	9.58	283.5
100	0	283.2

FIGURE XI. Gas-Liquid Critical Temperatures of the Benzene-Carbon Tetrachloride System as a Function of Mole percent Carbon Tetrachloride.

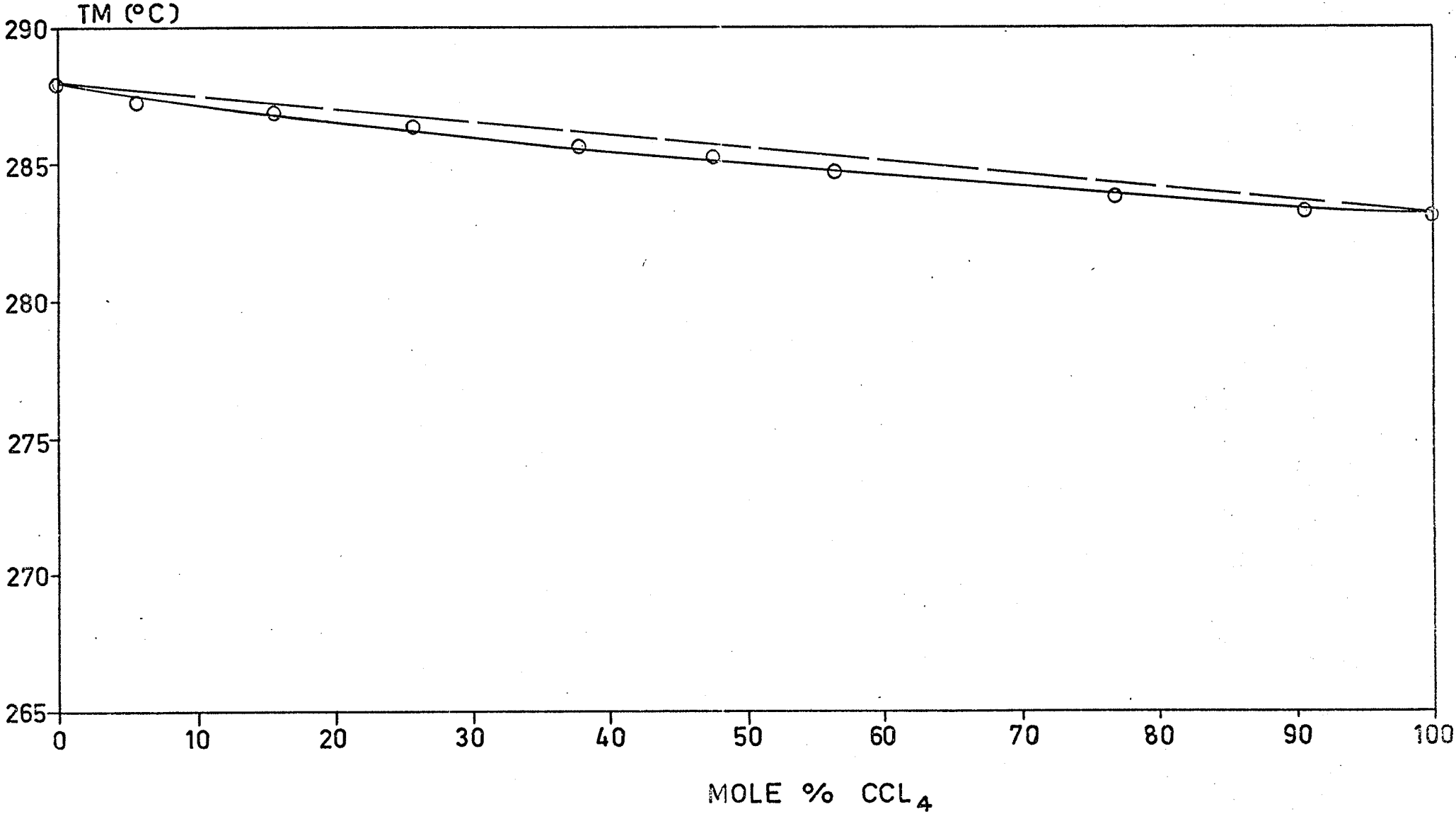
TM (°C)
290
285
280
275
270
265
0
10
20
30
40
50
60
70
80
90
100
MOLE % CCL4

II. Vapor Liquid Equilibrium Compositions

II (A) The System Acetone-Chloroform

The vapor liquid equilibrium compositions of the binary system Acetone-Chloroform have been determined at 100^{o}, 150^{o}, 160^{o}, 170^{o} and 180^{o}C. As mentioned earlier this binary system could not be studied at higher temperatures because of decomposition. The results are given in Table VII, and the data are plotted in Figures XII, XIII, XIV, XV and XVI.

TABLE VII

Experimental Vapor Liquid Equilibrium Compositions of the System Acetone-Chloroform at Different Isotherms

Mole % Acetone in Liquid	Mole % Acetone in Vapor
T = 100°C	
15.5	13.4
21.2	17.8
29.6	26.8
35.7	35.4
46.2	51.5
52.7	61.5
54.8	63.9
63.8	74.2
72.5	83.5
86.99	93.22
T = 150°C	
2.0	1.0
9.4	6.1
16.6	13.4
25.0	22.6
31.1	29.8
38.5	39.5
42.5	45.4
51.5	56.0
60.5	65.0
70.0	75.5
77.5	84.0
85.5	89.5
T = 160°C	
7.0	6.4
19.2	17.6
23.2	21.0
29.8	31.5
31.8	33.0
38.4	41.4
40.8	44.9
46.0	53.4
67.4	75.8
79.2	85.8
T = 170°C	
9.2	7.2
15.0	14.8
18.9	17.0
23.5	23.5
28.1	29.1
31.9	34.0
36.3	39.0
37.8	40.8
45.4	51.0
50.6	57.0
59.6	66.2
70.6	76.8
T = 180°C	
4.6	3.6
9.4	7.9
14.4	13.3
21.6	23.0
29.3	32.4
39.8	44.4
46.4	52.9
53.0	60.0
60.7	68.4
68.0	75.2
78.1	84.8
87.4	92.1

FIGURE XII. Vapor-Liquid Equilibrium Composition Curve of the System Acetone-Chloroform at 100°C.

FIG. XII : THE VAPOUR-LIQUID EQUILIBRIUM COMPOSITION CURVE OF THE SYSTEM ACETONE-CHLOROFORM AT 100° C.

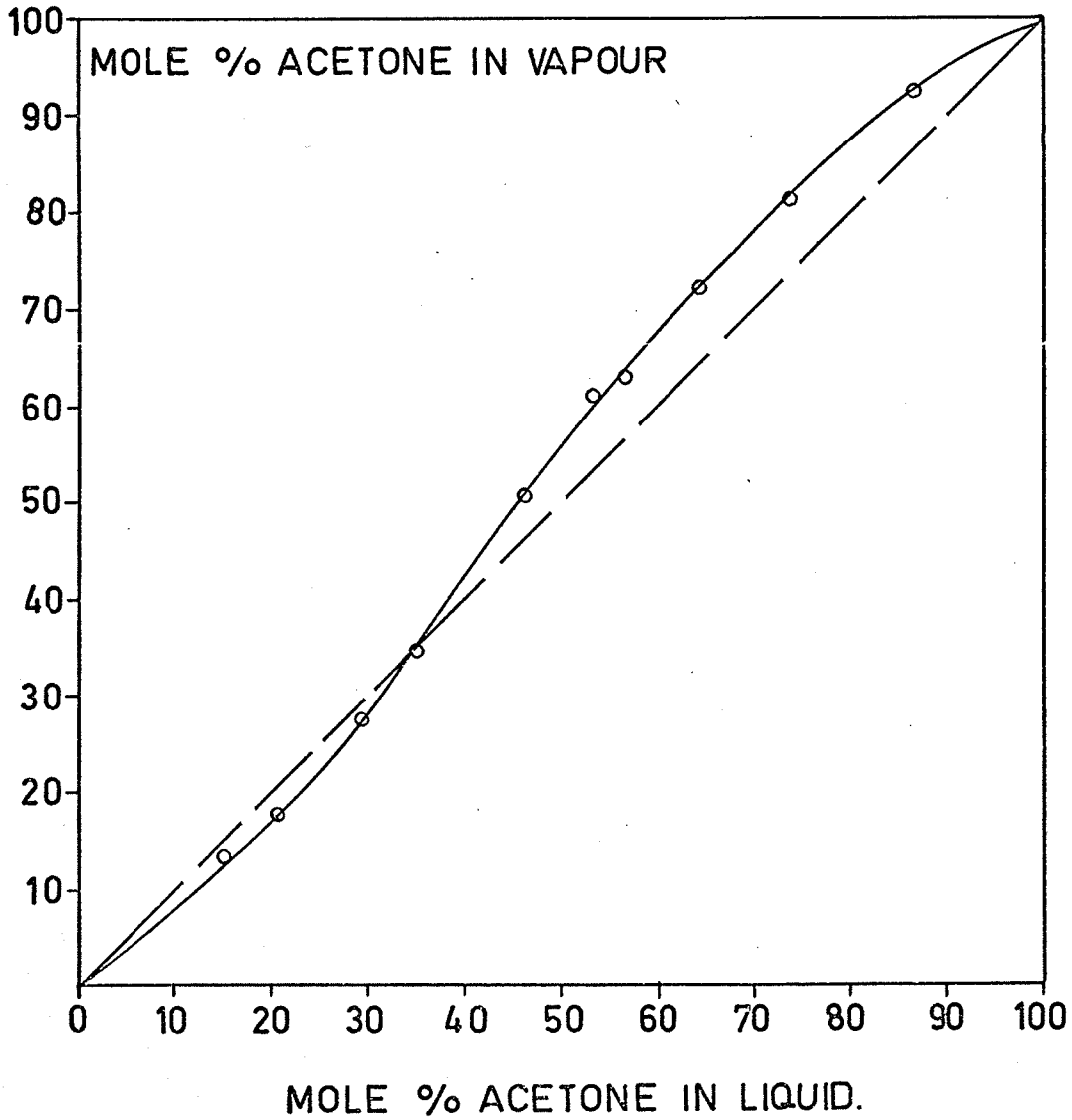

FIGURE XIII. Vapor-Liquid Equilibrium Composition Curve of the System Acetone-Chloroform at 150°C.

FIG. XIII : THE VAPOUR-LIQUID EQUILIBRIUM COMPOSITION CURVE OF THE SYSTEM ACETONE-CHLOROFORM AT 150° C.

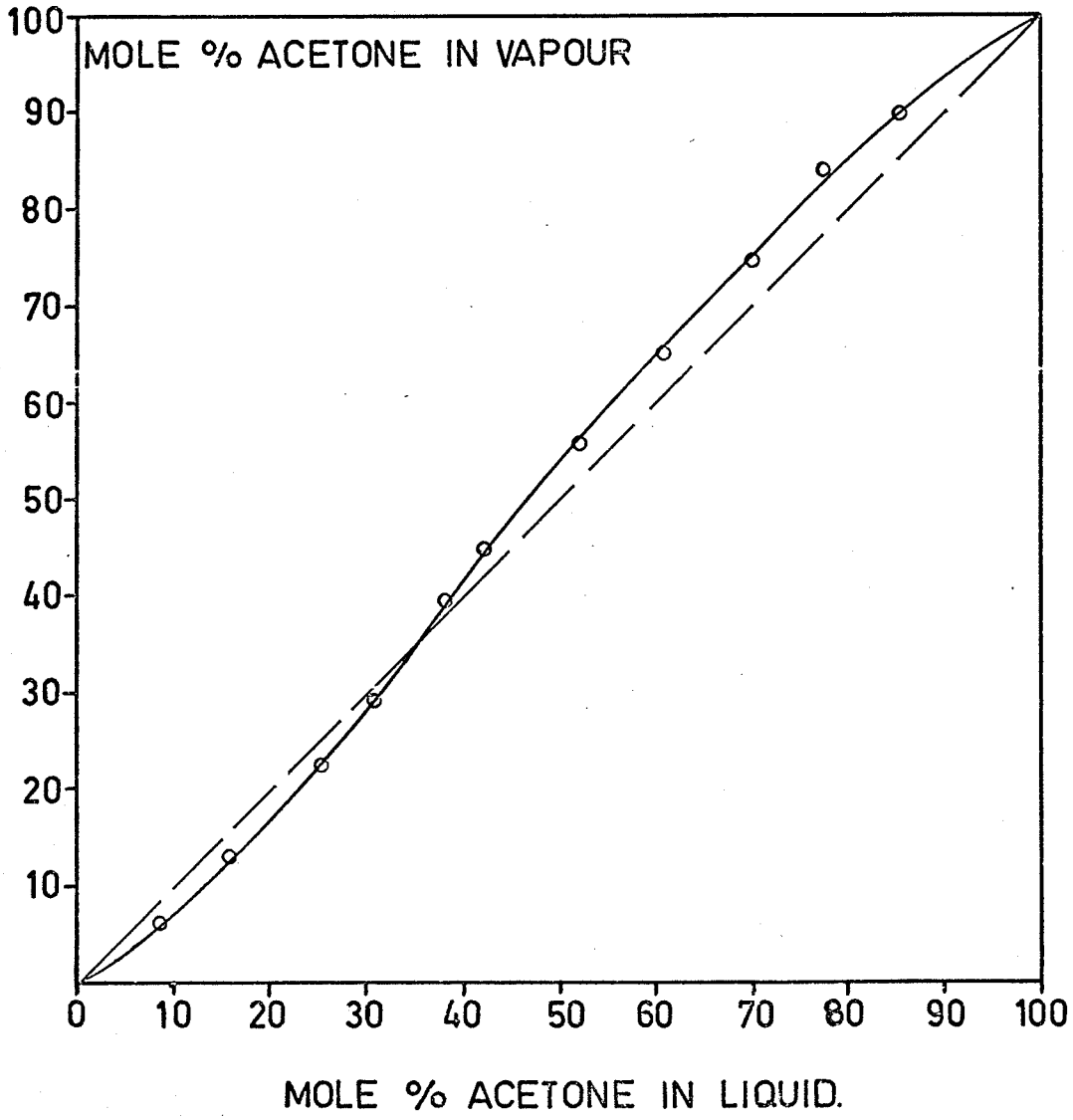

FIGURE XIV. Vapor-Liquid Equilibrium Composition Curve of the System Acetone-Chloroform at 160^{o}C.

FIG. XIV : THE VAPOUR-LIQUID EQUILIBRIUM COMPOSITION CURVE OF THE SYSTEM ACETONE-CHLOROFORM AT 160° C.

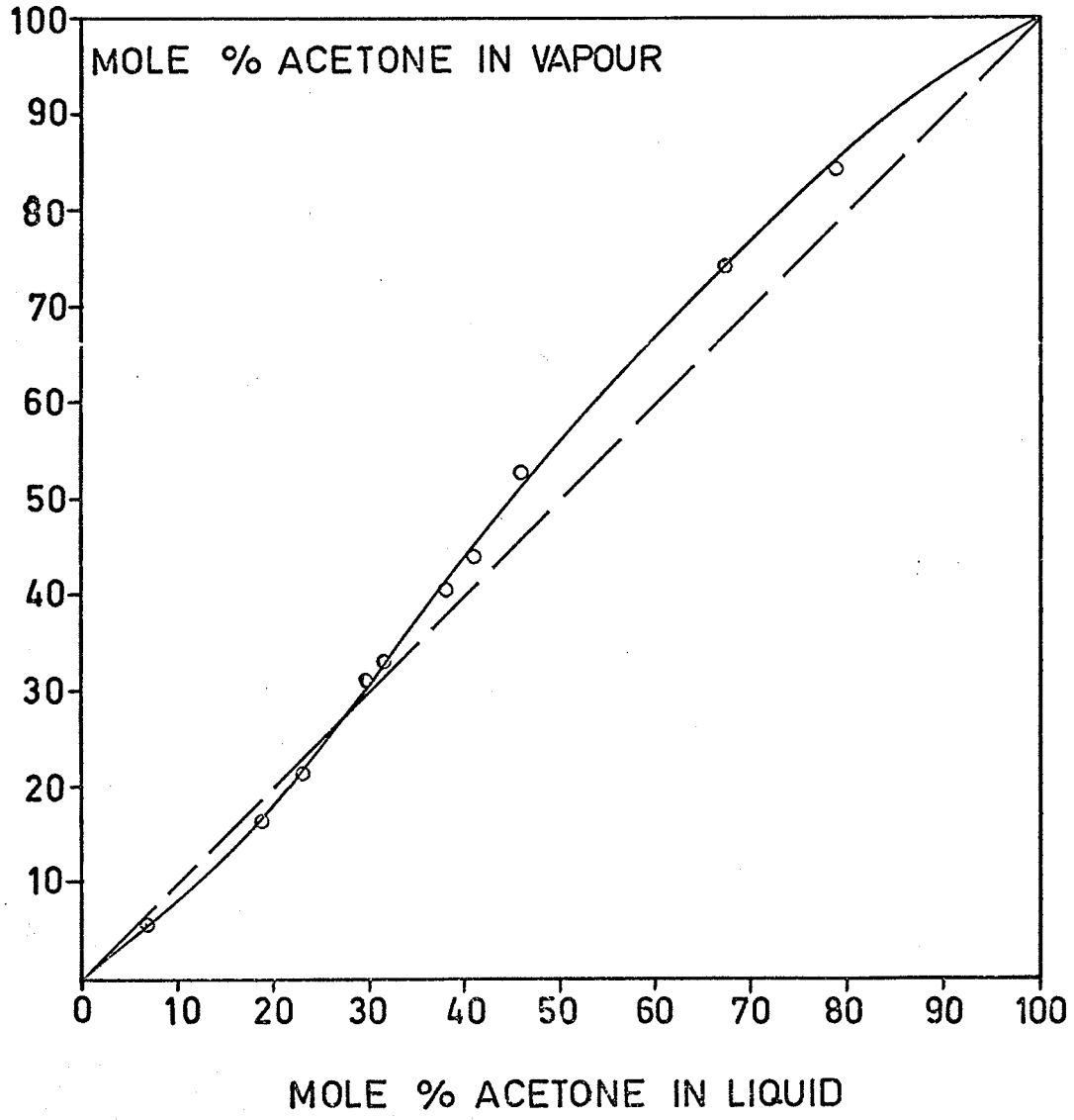

FIGURE XV. Vapor-Liquid Equilibrium Composition Curve of the System Acetone-Chloroform at 170°C.

FIG. XV : THE VAPOUR-LIQUID EQUILIBRIUM COMPOSITION CURVE OF THE SYSTEM ACETONE-CHLOROFORM AT 170° C.

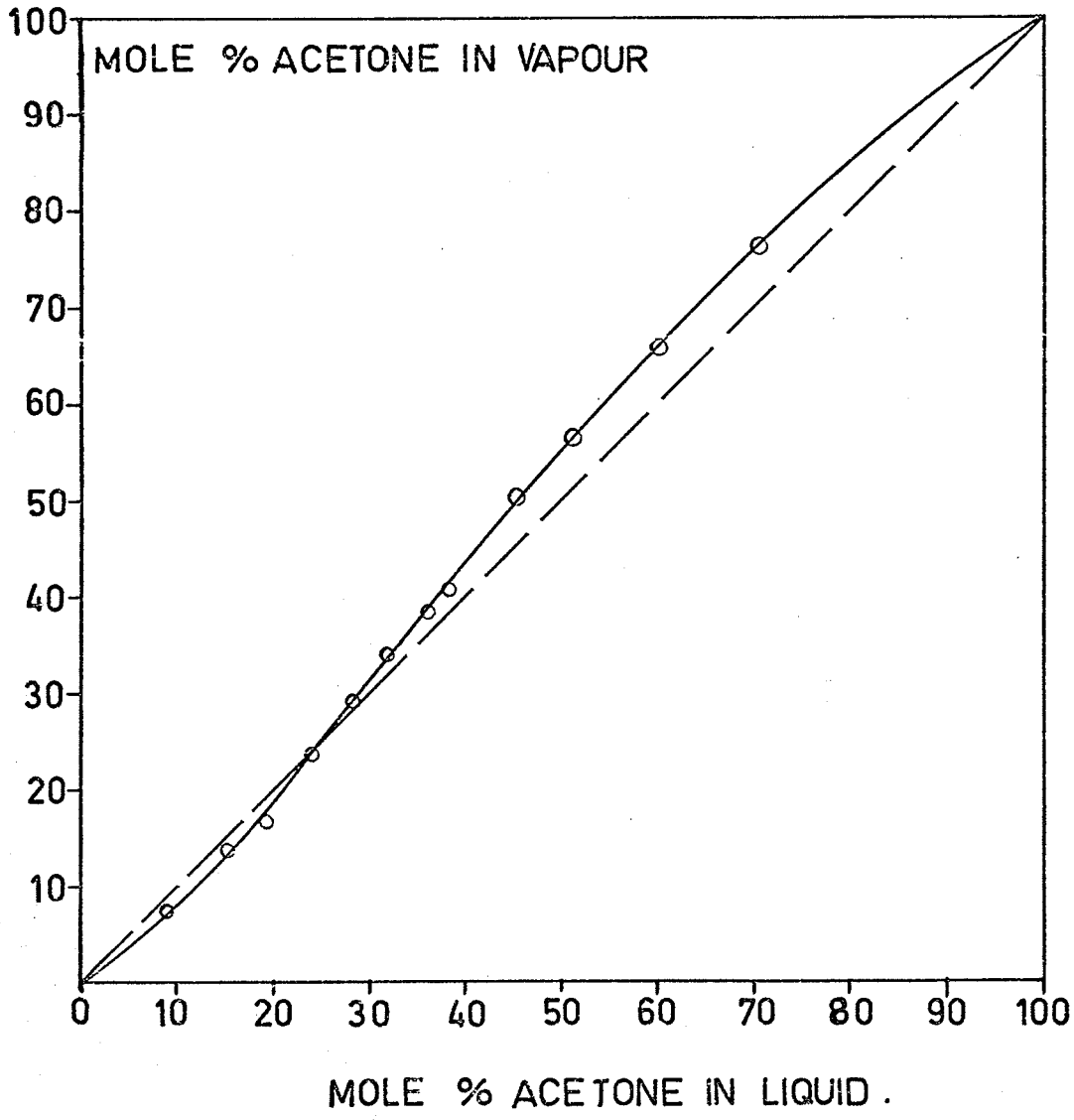

FIGURE XVI. Vapor-Liquid Equilibrium Composition Curve of the System Acetone-Chloroform at 180°C.

FIG. XVI : THE VAPOUR-LIQUID EQUILIBRIUM COMPOSITION CURVE OF THE SYSTEM ACETONE - CHLOROFORM AT 180° C.

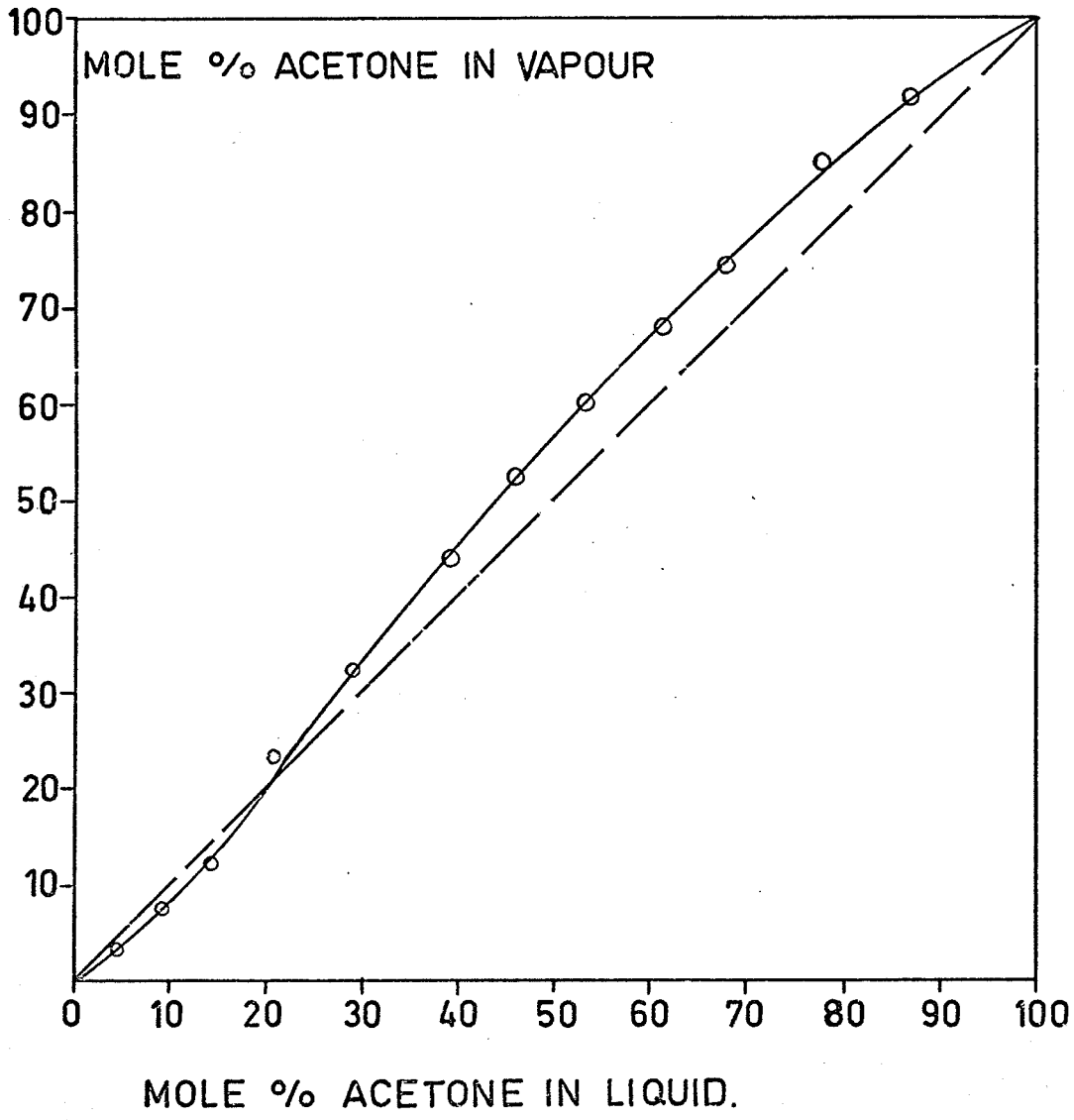

II (B) The System Acetone-Carbon Tetrachloride

The vapor liquid equilibrium compositions of this binary system have been determined at 100^{o}, 150^{o}, 200^{o}, 250^{o} and 270^{o}C. The data, shown in Table VIII are plotted in Figures XVII, XVIII, XIX, XX and XXI.

TABLE VIII

Experimental Vapor Liquid Equilibrium Compositions of the System Acetone-Carbon Tetrachloride at Different Isotherms

Mole % Acetone in Liquid	Mole % Acetone in Vapor
T = 100°C	
2.98	5.97
6.22	13.01
13.45	26.22
15.01	29.50
20.92	37.50
24.89	43.02
34.11	55.01
40.72	60.92
46.80	67.54
52.01	72.12
58.20	76.54
72.02	85.93
86.70	93.60
95.01	97.50
T = 150°C	
3.27	5.87
6.22	11.52
15.01	26.62
20.36	33.72
24.89	37.24
34.11	47.62
40.12	57.02
46.80	58.11
52.01	63.13
58.20	69.26
66.10	78.24
72.02	80.62
86.70	90.68
96.42	98.24
T = 200°C	
6.22	9.00
7.21	10.12
15.01	21.00
24.89	27.21
29.9	36.6
34.11	38.42
46.80	52.16
58.20	64.44
72.02	76.70
77.5	83.0
86.70	90.42
94.0	96.2
T = 250°C	
4.6	7.1
9.8	12.9
21.6	26.6
30.3	36.6
40.1	44.0
46.2	49.9
T = 270°C	
6.3	9.2
12.6	17.2
19.2	22.4

FIGURE XVII. Vapor-Liquid Equilibrium Composition Curve of the System Acetone-Carbon Tetrachloride at 100°C.

FIG. XVII : THE VAPOUR-LIQUID EQUILIBRIUM COMPOSITION CURVE OF THE SYSTEM ACETONE-CARBON TETRACHLORIDE AT 100° C.

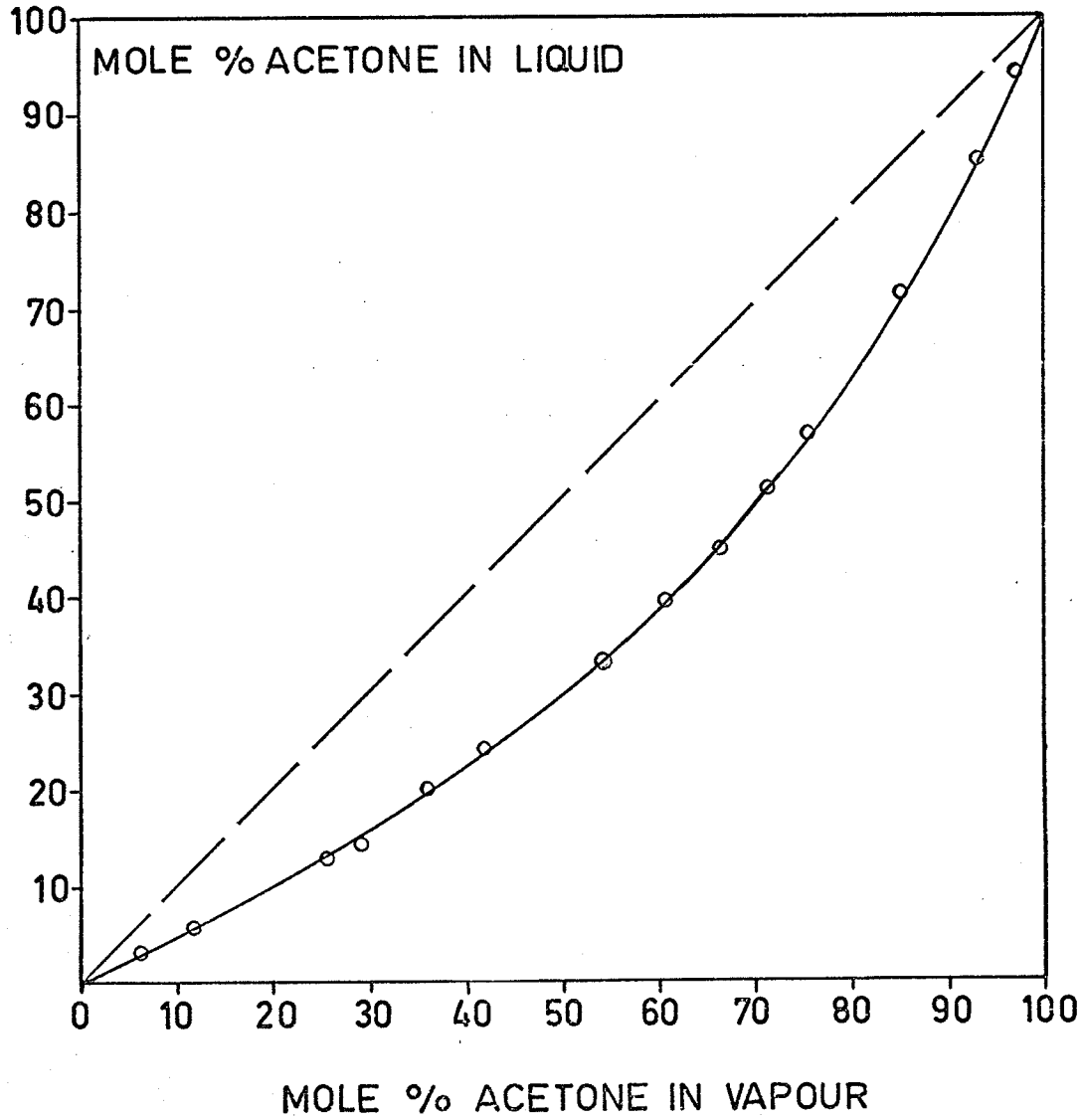

FIGURE XVIII. Vapor-Liquid Equilibrium Composition Curve of the System Acetone-Carbon Tetrachloride at 150°C.

FIG. XVIII : THE VAPOUR-LIQUID EQUILIBRIUM COMPOSITION CURVE OF THE SYSTEM ACETONE-CARBON TETRACHLORIDE AT 150° C.

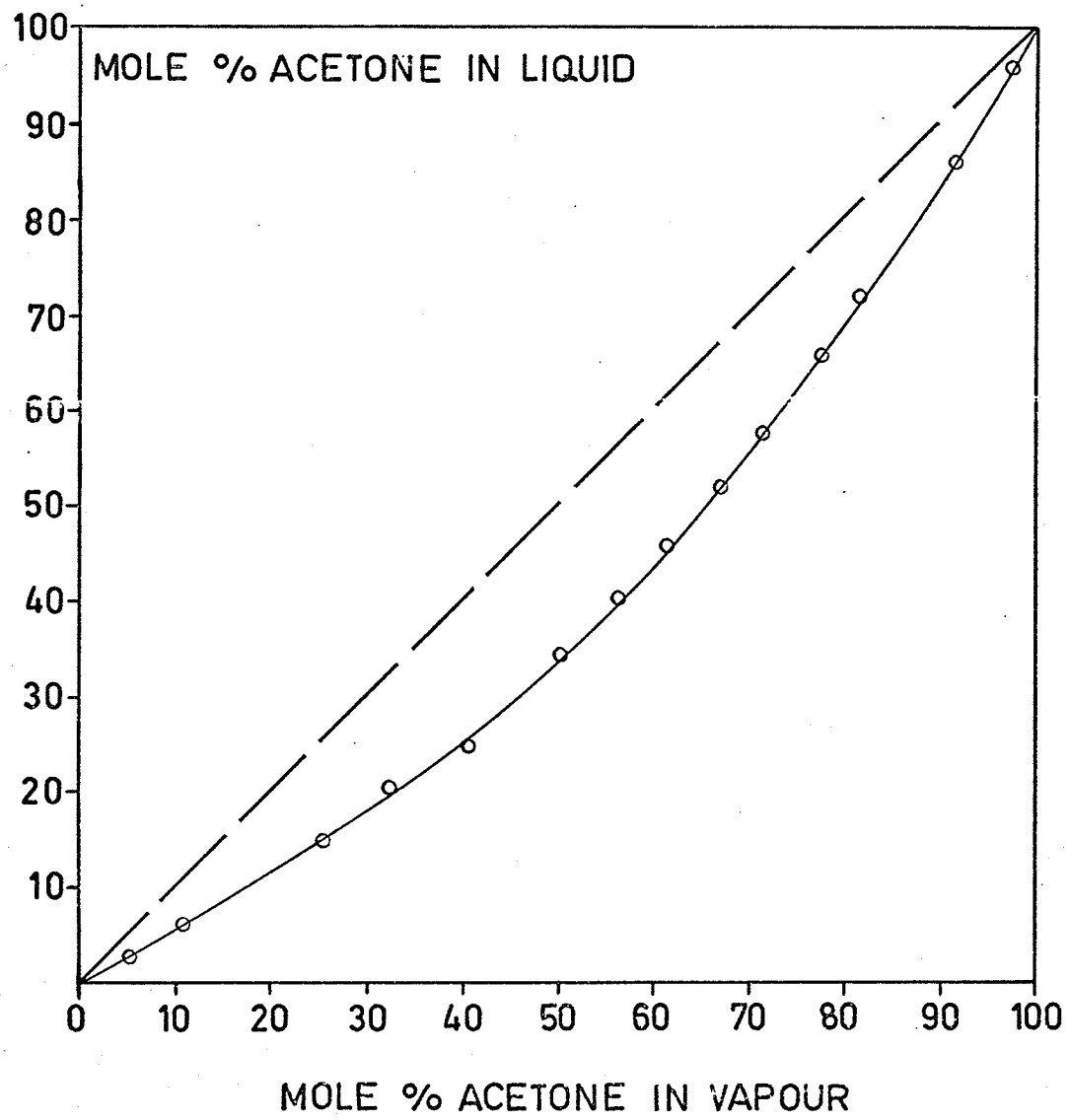

FIGURE XIX. Vapor-Liquid Equilibrium Composition Curve of the System Acetone-Carbon Tetrachloride at 200^{o}C.

FIG. XIX: THE VAPOUR-LIQUID EQUILIBRIUM COMPOSITION CURVE OF THE SYSTEM ACETONE–CARBON TETRACHLORIDE AT 200° C.

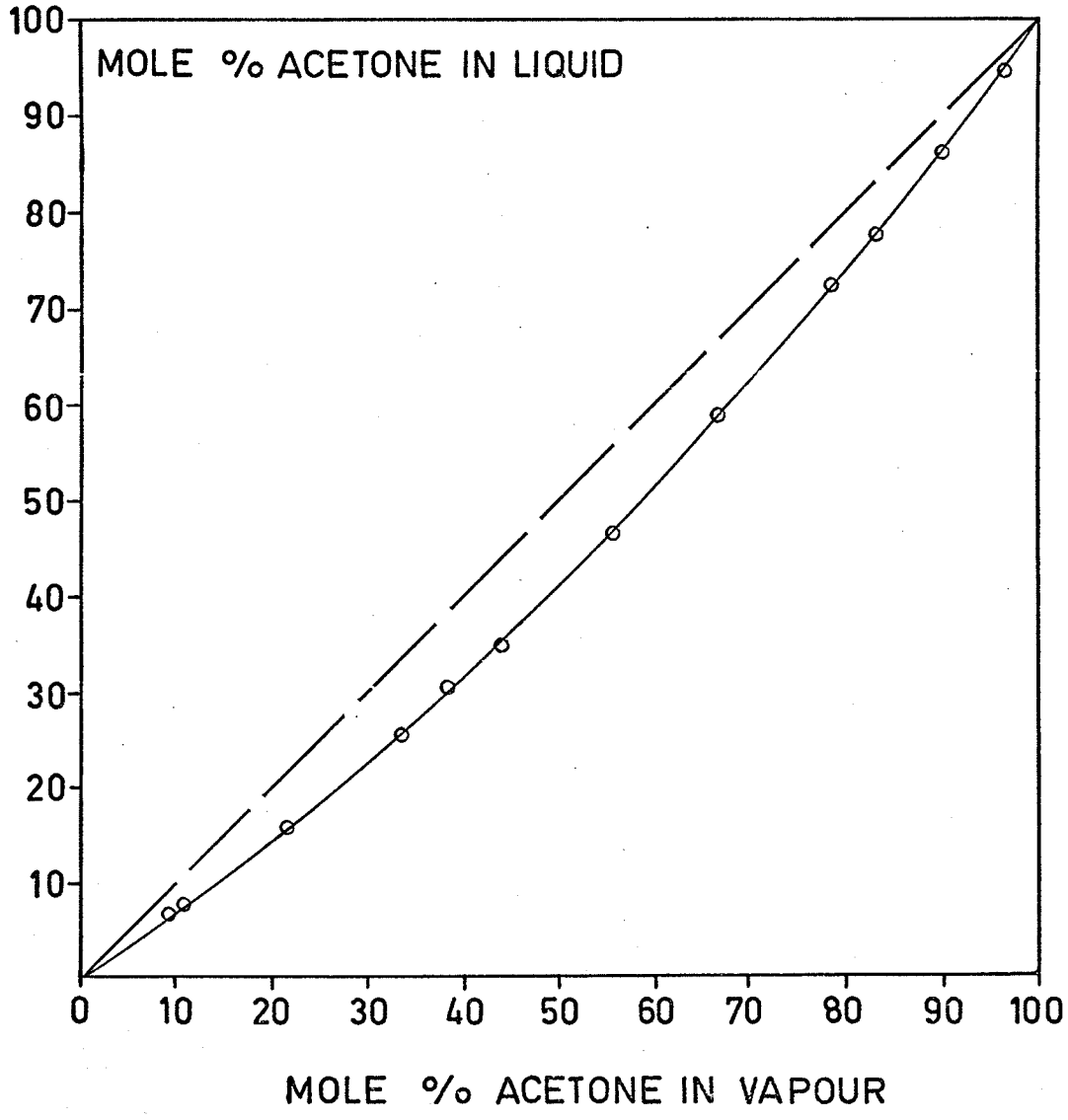

FIGURE XX. Vapor-Liquid Equilibrium Composition Curve of the System Acetone-Carbon Tetrachloride at 250°C.

FIG. XX : THE VAPOUR LIQUID EQUILIBRIUM COMPOSITION CURVE OF THE SYSTEM ACETONE-CARBON TETRACHLORIDE AT 25O° C.

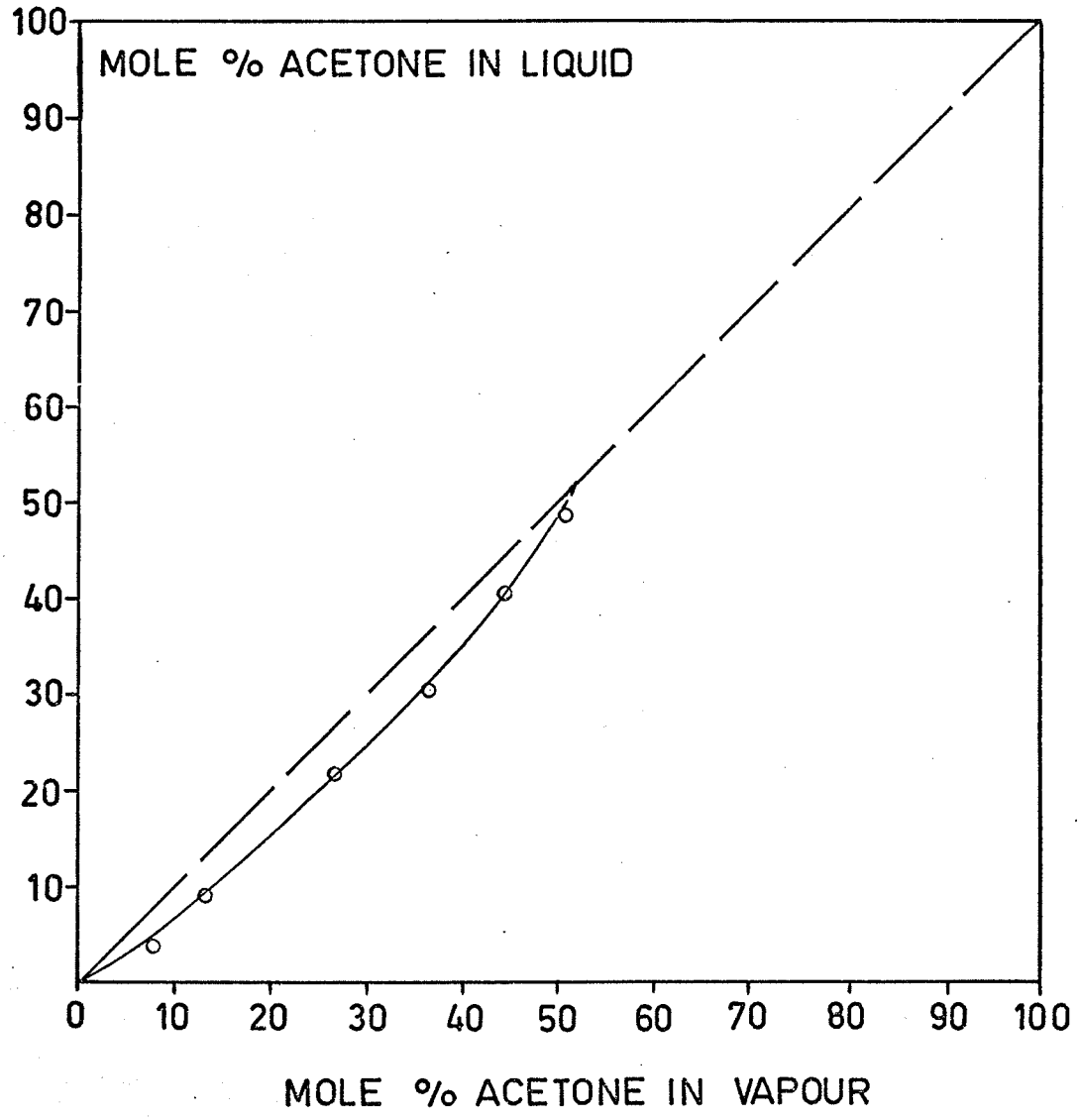

FIGURE XXI. Vapor-Liquid Equilibrium Composition Curve of the System Acetone-Carbon Tetrachloride at 270°C.

FIG. XXI : THE VAPOUR LIQUID EQUILIBRIUM COMPOSITION CURVE OF THE SYSTEM ACETONE - CARBON TETRACHLORIDE AT 27O° C.

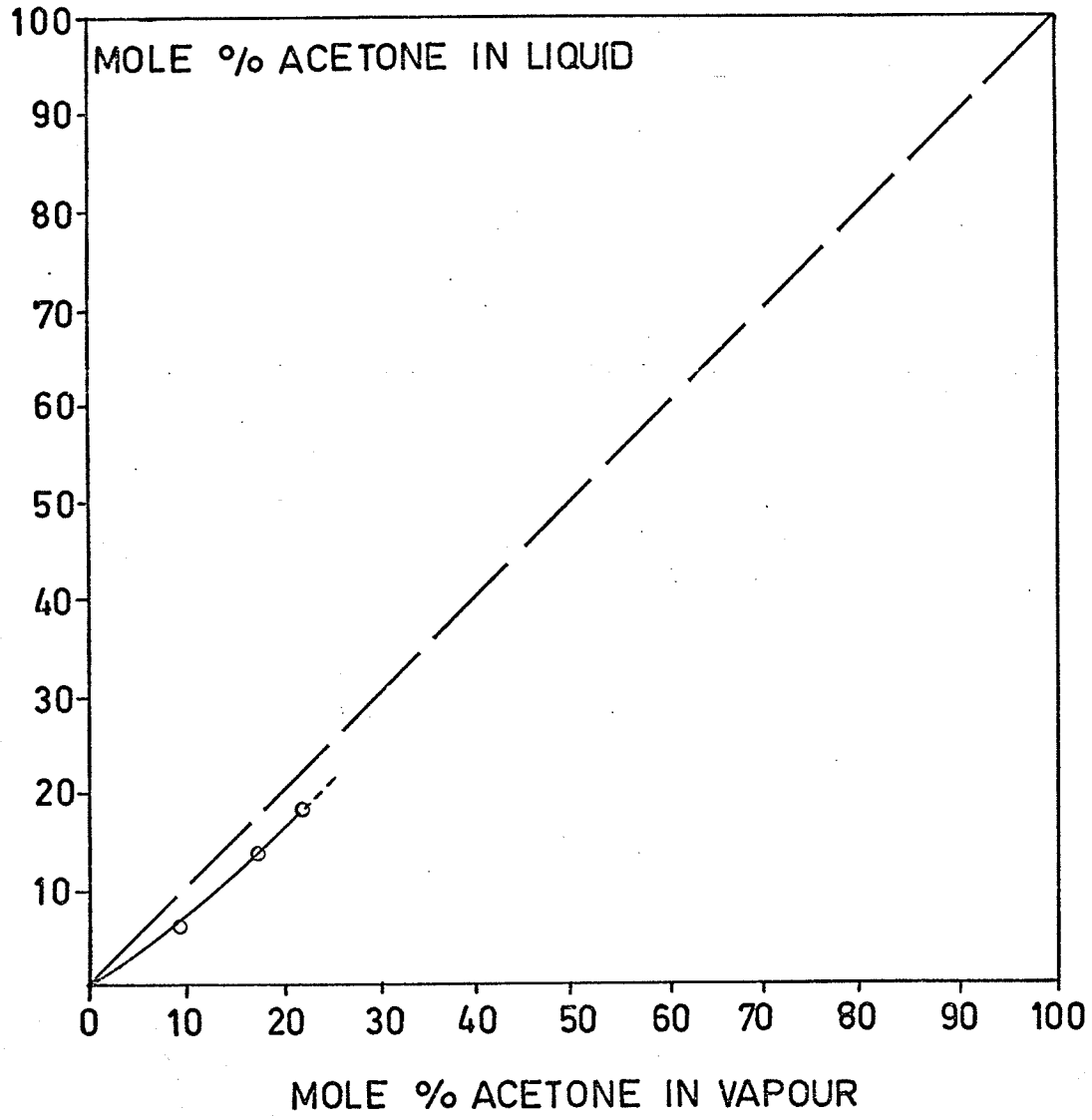

II (C) The System Benzene-Carbon Tetrachloride

The vapor liquid equilibrium compositions of the system Benzene-Carbon Tetrachloride have been determined at 100, 108, 150, 200, 250 and 270^{o}C. The experimental results are shown in Table IX and they are plotted in Figures XXII, XXIII, XXIV, XXV, XXVI and XXVII.

TABLE IX

Experimental Vapor Liquid Equilibrium Compositions of the System Benzene-Carbon Tetrachloride at Different Isotherms

Mole % Carbon Tetrachloride in Liquid	Mole % Carbon Tetrachloride in Vapor
T = 100°C	
8.2	9.5
22.2	24.4
40.5	41.8
43.5	44.2
46.2	47.9
49.6	51.6
61.2	62.6
78.3	80.0
83.9	85.8
87.8	90.2
94.9	97.1
T = 108°C	
18.7	20.0
21.2	22.2
24.4	25.2
34.0	36.3
46.4	47.4
63.8	64.3
70.2	70.9
76.8	77.6
80.5	81.2
85.8	86.3
87.8	88.6
93.7	94.5
96.6	97.7
T = 150°C	
9.6	10.8
14.8	16.0
25.6	26.4
39.3	41.5
46.6	47.9
55.8	56.5
59.6	60.9
66.8	68.6
73.4	74.6
91.8	92.8
95.4	95.9
T = 200°C	
11.0	12.0
17.5	19.5
41.2	42.2
50.8	52.0
51.0	52.0
57.8	59.4
72.6	74.1
81.8	84.2
82.2	84.6
92.8	94.2
96.1	97.3
T = 250°C	
11.8	12.5
26.2	27.1
29.0	29.4
44.0	44.2
50.4	51.6
71.7	72.8
73.6	74.4
80.5	81.3
88.1	90.2
94.0	94.6
96.5	96.6
T = 270°C	
6.2	7.0
18.8	19.6
31.8	32.6
53.6	54.5
64.6	65.7
80.0	82.0
87.3	88.4
91.8	92.4
95.0	95.4

FIGURE XXII. Vapor-Liquid Equilibrium Composition Curve of the System Benzene-Carbon Tetrachloride at 100°C.

FIG. XXII: THE VAPOUR - LIQUID EQUILIBRIUM COMPOSITION CURVE OF THE SYSTEM BENZENE - CARBON TETRACHLORIDE AT 100° C.

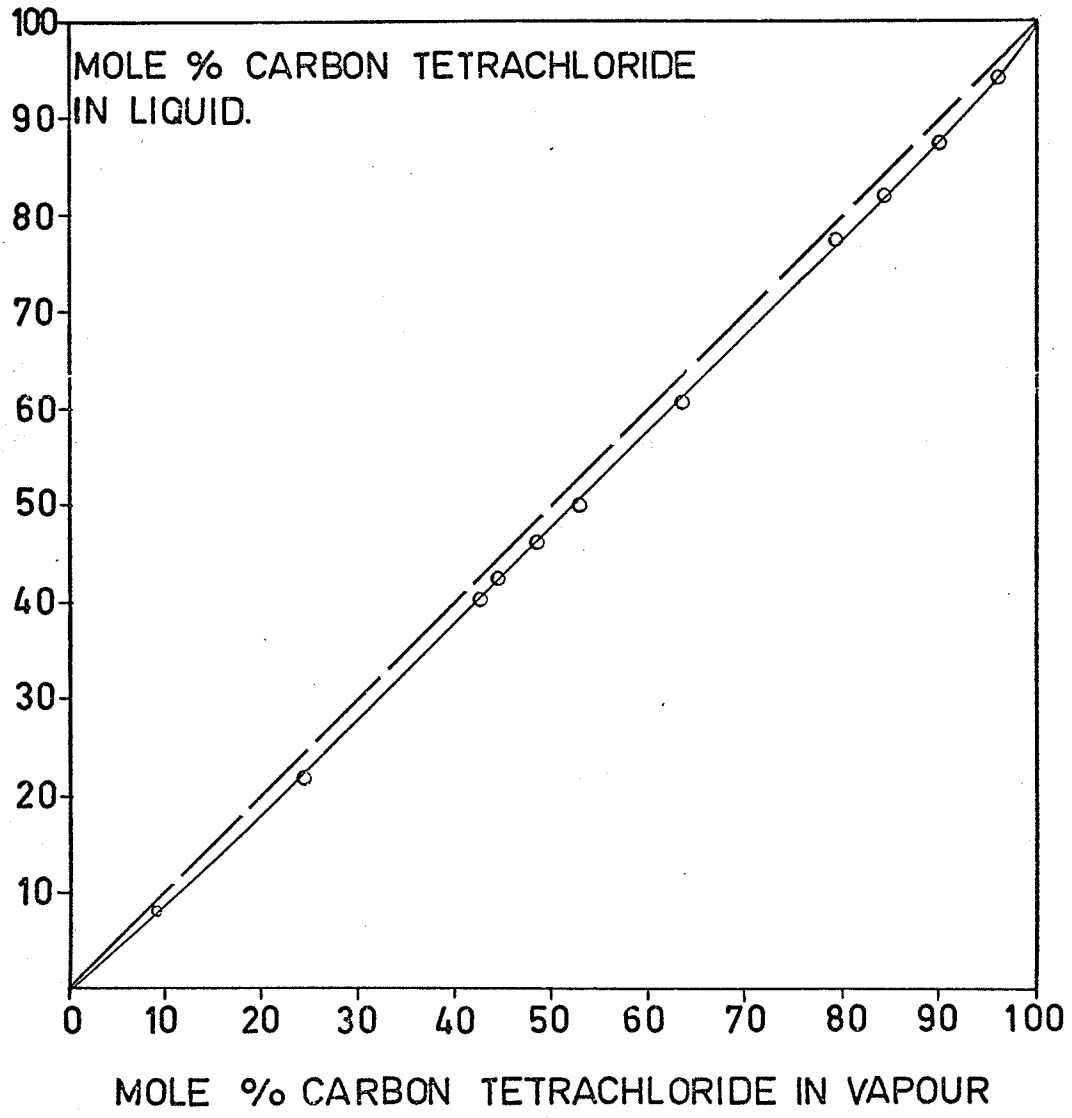

FIGURE XXIII. Vapor-Liquid Equilibrium Composition Curve of the System Benzene-Carbon Tetrachloride at 108°C.

FIG. XXIII: THE VAPOUR-LIQUID EQUILIBRIUM COMPOSITION CURVE OF THE SYSTEM BENZENE-CARBON TETRACHLORIDE AT 108° C.

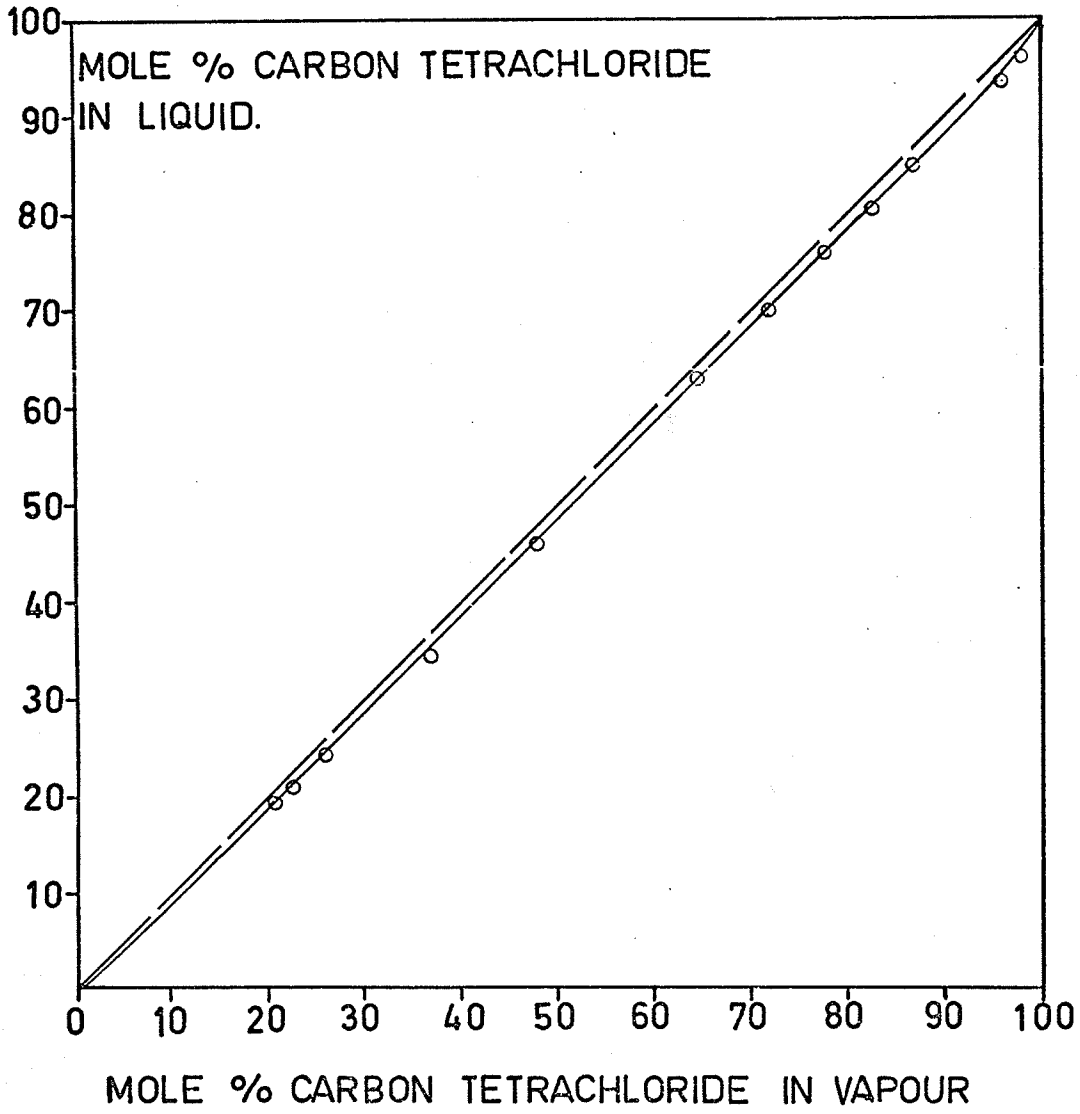

FIGURE XXIV. Vapor-Liquid Equilibrium Composition Curve of the System Benzene-Carbon Tetrachloride at 150°C.

FIG. XXIV: THE VAPOUR - LIQUID EQUILIBRIUM COMPOSITION CURVE OF THE SYSTEM BENZENE - CARBON TETRACHLORIDE AT 150° C.

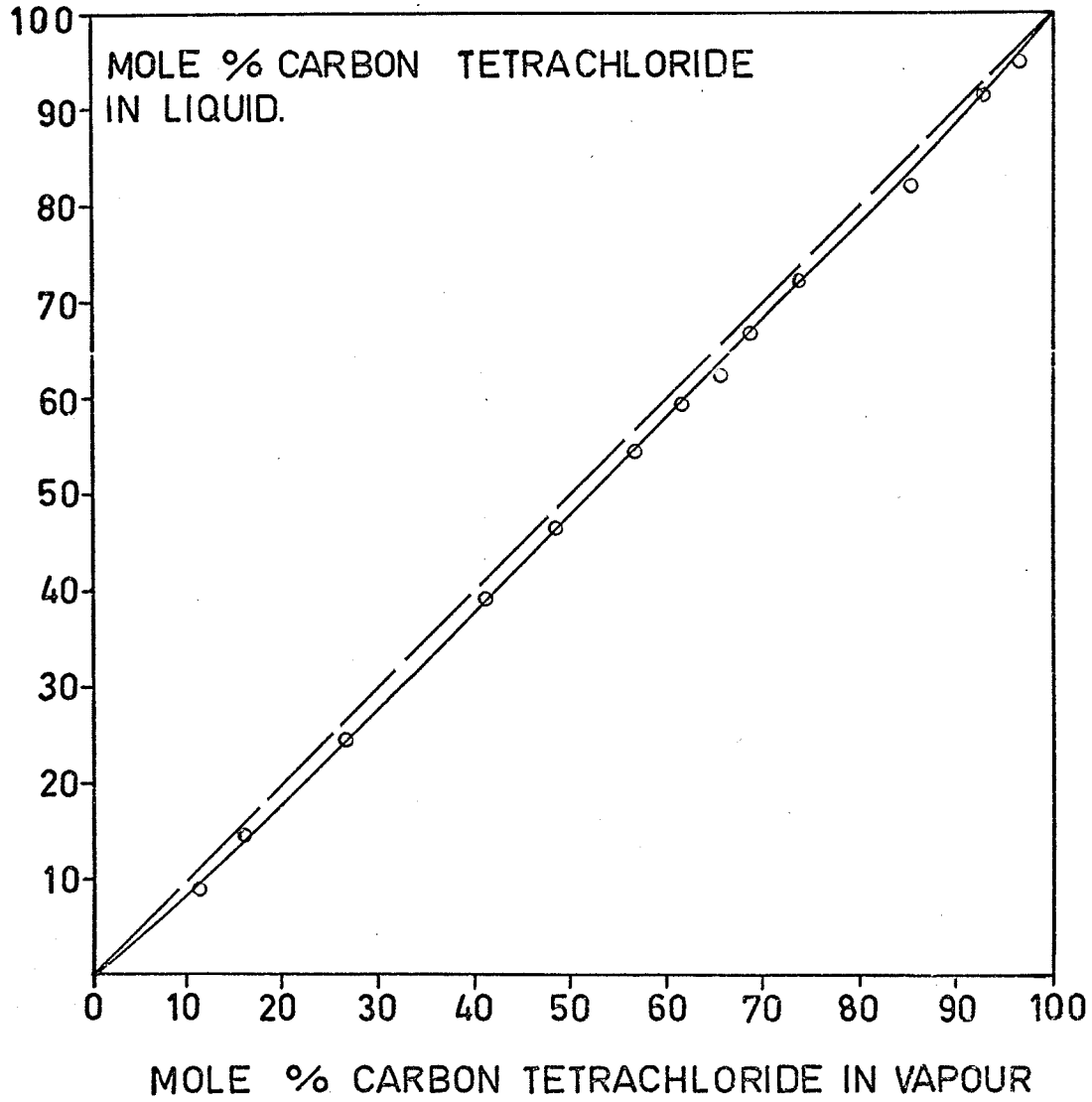

FIGURE XXV. Vapor-Liquid Equilibrium Composition Curve of the System Benzene-Carbon Tetrachloride at 200°C.

FIG. XXV: THE VAPOUR - LIQUID EQUILIBRIUM COMPOSITION CURVE OF THE SYSTEM BENZENE - CARBON TETRACHLORIDE AT 200° C

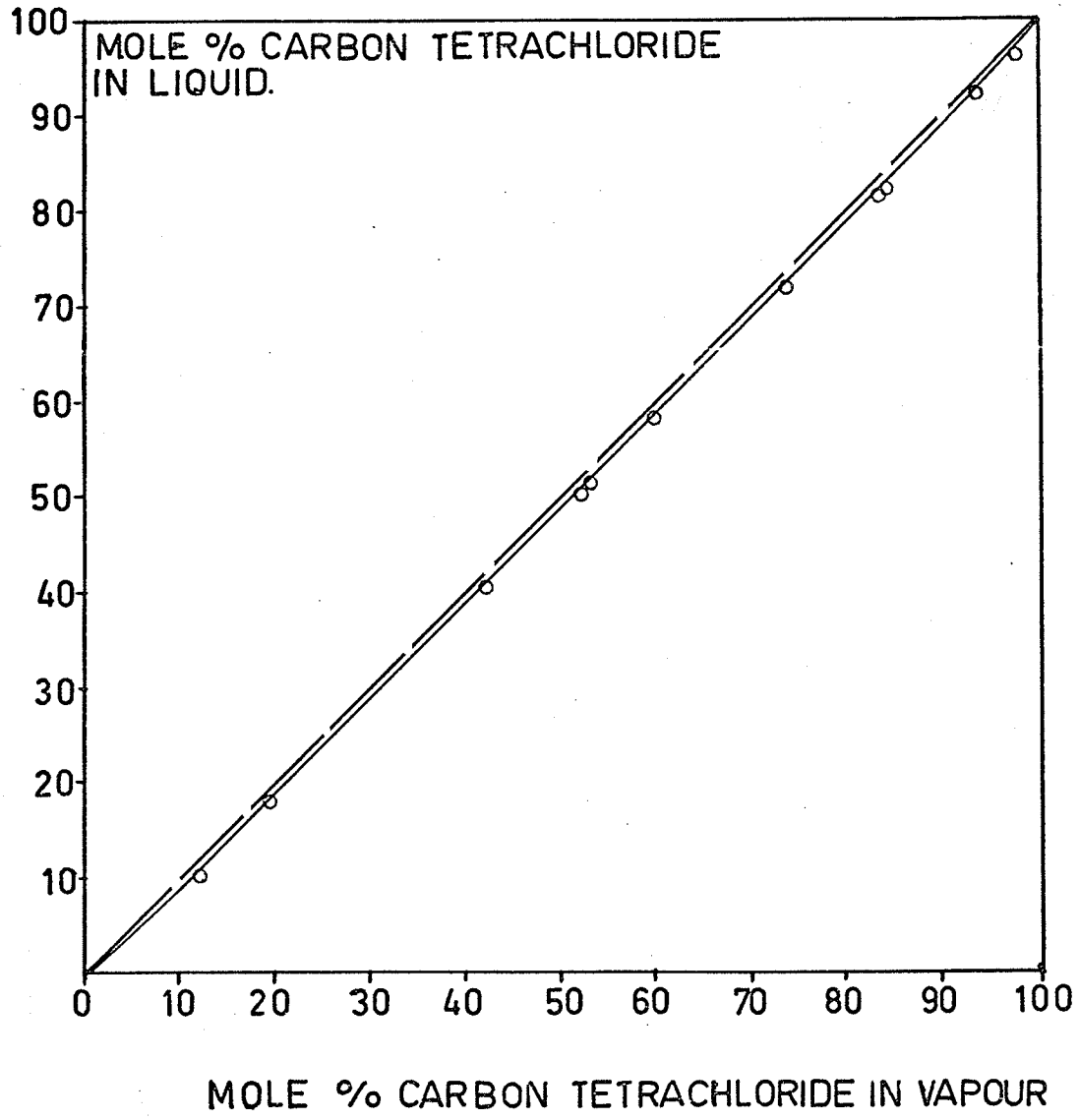

FIGURE XXVI. Vapor-Liquid Equilibrium Composition Curve of the System Benzene-Carbon Tetrachloride at 250°C.

FIG. XXVI: THE VAPOUR-LIQUID EQUILIBRIUM COMPOSITION CURVE OF THE SYSTEM BENZENE - CARBON TETRACHLORIDE AT 250° C.

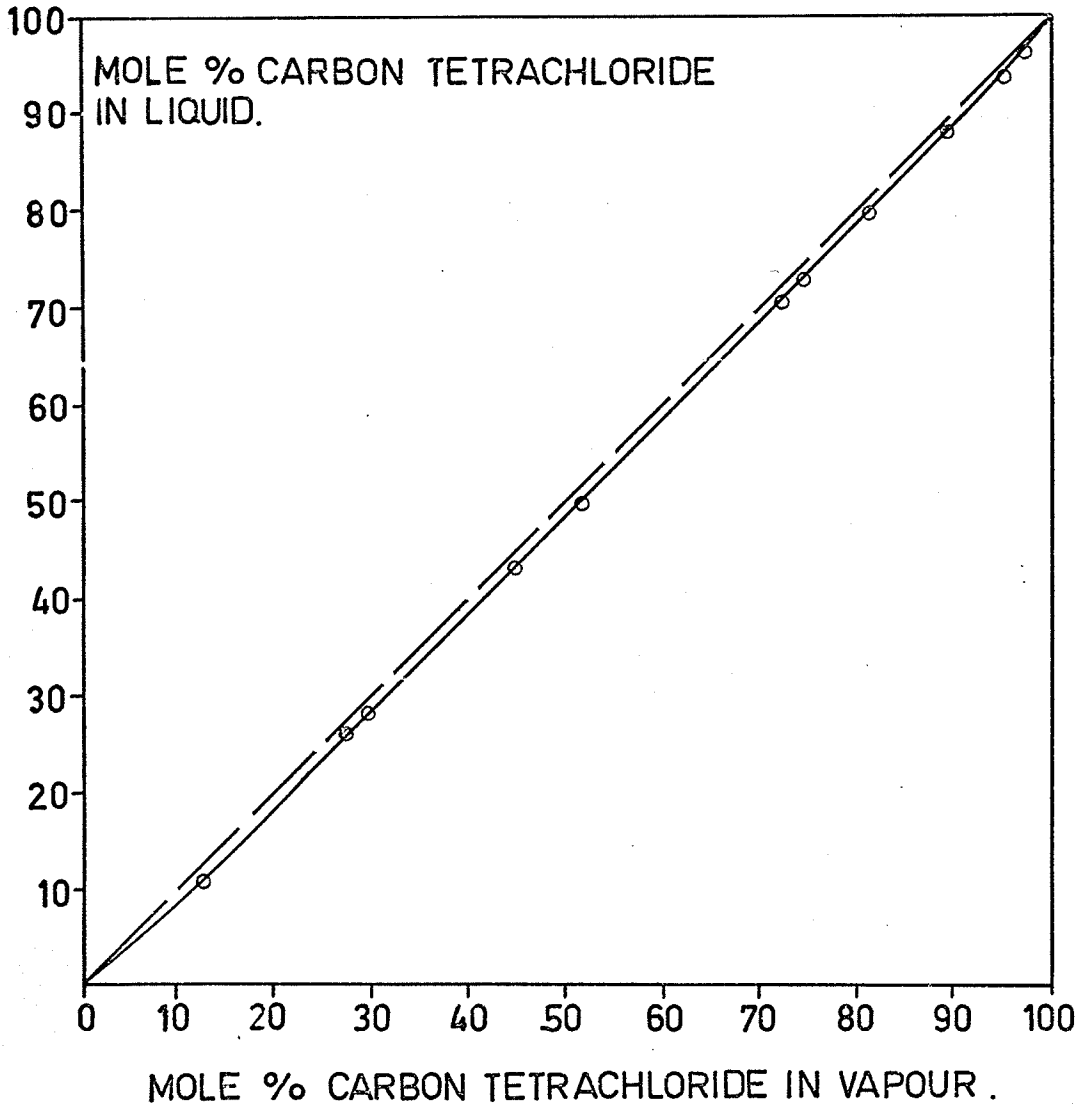

FIGURE XXVII. Vapor-Liquid Equilibrium Composition Curve of the System Benzene-Carbon Tetrachloride at 270°C.

FIG. XXVII: THE VAPOUR-LIQUID EQUILIBRIUM COMPOSITION CURVE OF THE SYSTEM BENZENE-CARBON TETRACHLORIDE AT 270° C.

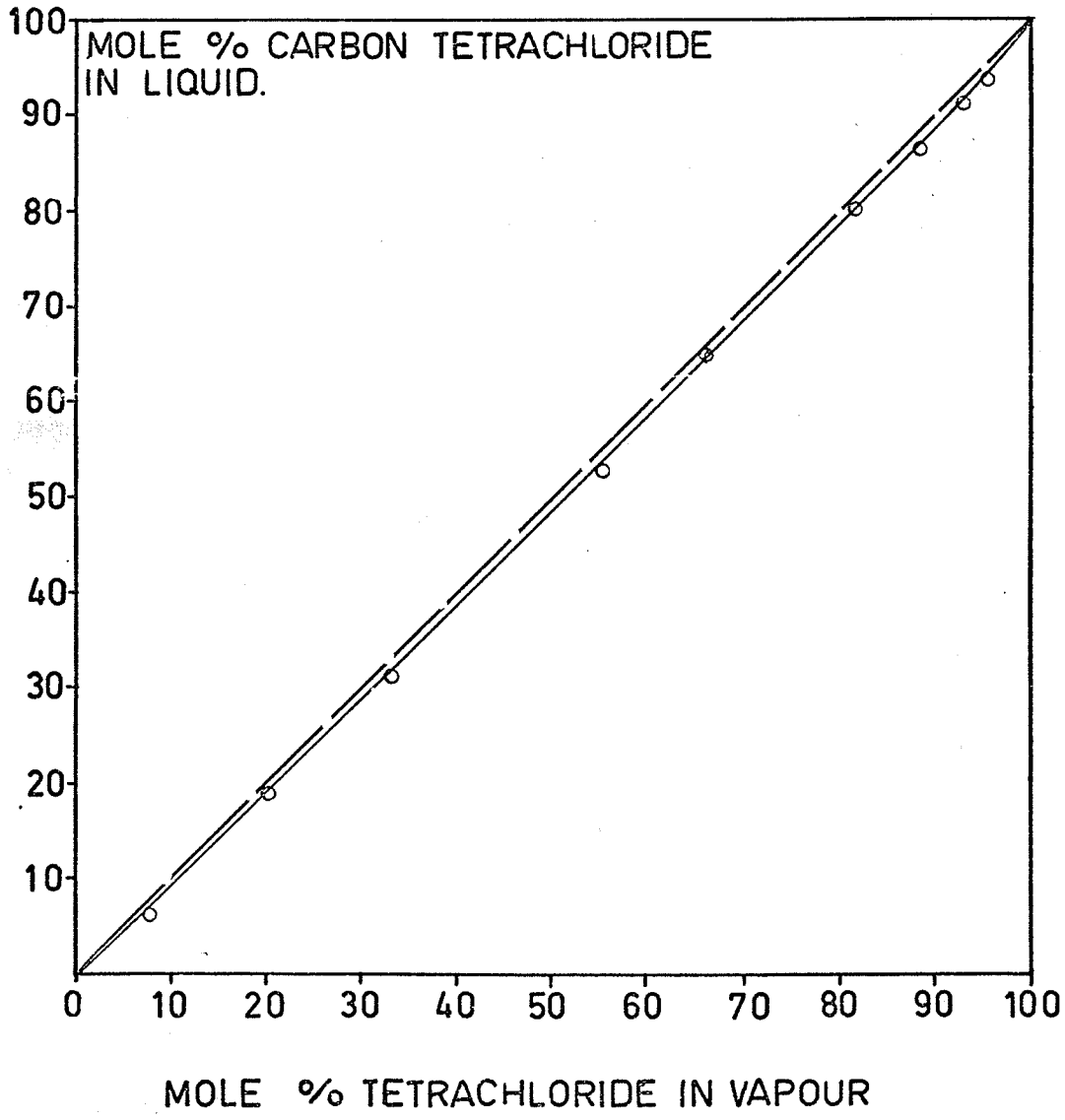

III. Vapor Pressures

III (A) The System Acetone-Chloroform

The saturation vapor pressure of the system acetone-Chloroform was determined over the whole concentration range from 100°C to 180°C. The results are summarised in Table X, and Figure XXVIII illustrates the constant composition plots of the relation between pressure and temperature for a few mixtures.

TABLE X

Experimental Saturation Pressure of the System Acetone-Chloroform

Temp.(°C)	Saturation Pressure(Atm)	Temp.(°C)	Saturation Pressure(Atm)
Mole % Acetone in mixture = 7.50		Mole % Acetone in mixture = 23.54	
100.0	3.20	100.0	3.18
105.5	3.42	101.5	3.27
108.0	3.98	108.2	4.01
110.8	4.14	110.6	4.10
112.5	4.30	115.2	4.94
119.0	5.12	121.0	5.12
121.1	5.19	122.8	5.36
124.5	5.96	130.8	6.38
130.6	6.40	131.6	6.56
132.0	6.62	139.0	7.72
137.0	6.96	141.2	7.83
142.0	7.85	143.5	8.17
144.5	8.13	152.6	9.32
151.2	9.35	155.6	10.26
153.0	9.61	161.8	11.40
160.2	11.42	163.7	12.20
161.0	11.58	170.6	13.79
164.5	12.26	171.6	14.01
172.2	13.76	179.1	16.21
176.5	15.36	180.8	16.46
181.4	16.70		
Mole % Acetone in mixture = 12.52		Mole % Acetone in mixutre = 31.32	
100.0	3.19	100.0	3.18
104.5	3.86	104.2	3.91
111.2	4.12	110.2	4.08
112.2	4.30	110.8	4.20
118.0	5.01	116.5	4.56
120.6	5.14	121.3	5.10
126.8	5.98	122.8	5.67
130.3	6.39	132.0	6.34
131.0	6.52	136.4	7.01
138.5	7.56	141.10	7.82
141.0	7.84	142.0	8.01
142.3	8.07	150.5	9.25
150.4	9.34	156.0	10.21
153.6	9.86	159.2	11.12
162.0	11.41	162.0	11.36
166.2	12.52	163.8	12.26
171.4	13.70	171.6	13.94
178.0	16.00	176.4	16.22
181.5	16.66	180.6	17.10

TABLE X (Cont'd)

Experimental Saturation Pressure of the System Acetone-Chloroform

Temp.(°C)	Saturation Pressure(Atm)	Temp.(°C)	Saturation Pressure (Atm)
Mole % Acetone in mixture = 41.56		Mole % Acetone in mixture = 62.43	
100.0	3.22	100.0	3.31
101.2	3.46	101.2	3.39
109.4	4.01	108.7	3.96
110.8	4.12	111.0	4.23
116.5	4.86	112.5	4.48
121.2	5.16	120.6	5.34
128.0	6.20	126.4	6.02
131.0	6.42	131.2	6.70
132.8	6.82	138.6	7.98
140.0	7.92	141.1	8.28
143.5	8.16	142.5	8.51
150.7	9.50	151.0	10.12
159.0	11.52	156.2	11.01
160.8	11.64	160.8	12.28
164.4	12.28	166.4	13.62
171.2	14.23	172.0	14.86
172.3	14.57	178.8	17.87
180.0	17.35	180.0	18.14
Mole % Acetone in mixture = 54.04		Mole % Acetone in mixture = 80.01	
100.0	3.26	100.0	3.46
106.2	3.86	104.2	3.87
110.9	4.19	111.6	4.46
111.8	4.42	118.8	5.30
122.6	5.25	120.8	5.60
128.2	6.32	129.2	6.86
130.6	6.55	132.0	7.21
132.0	6.72	136.4	8.01
139.8	8.09	141.2	8.72
140.0	8.11	148.4	10.01
146.2	9.02	150.6	10.72
150.8	9.86	152.6	11.21
158.8	11.72	160.0	12.96
160.2	12.00	165.4	13.26
169.8	14.52	170.1	15.56
171.0	14.60	171.8	16.12
172.2	14.82	180.0	18.94
180.6	17.76		

TABLE X (Cont'd)

Experimental Saturation Pressure of the System Acetone-Chloroform

Temp.(°C)	Saturation Pressure(Atm)
Mole % Acetone in mixture = 92.94	
100.0	3.60
102.5	3.86
111.0	4.62
116.2	5.02
120.0	5.86
122.8	6.26
130.8	7.42
137.7	8.56
141.2	9.16
152.0	11.42
154.4	12.12
163.0	13.78
176.0	17.20
180.0	19.60

FIGURE XXVIII. Lines of Constant Composition on a P-T Diagram for the System Acetone-Chloroform. (The mixtures were not plotted for clarity's sake.)

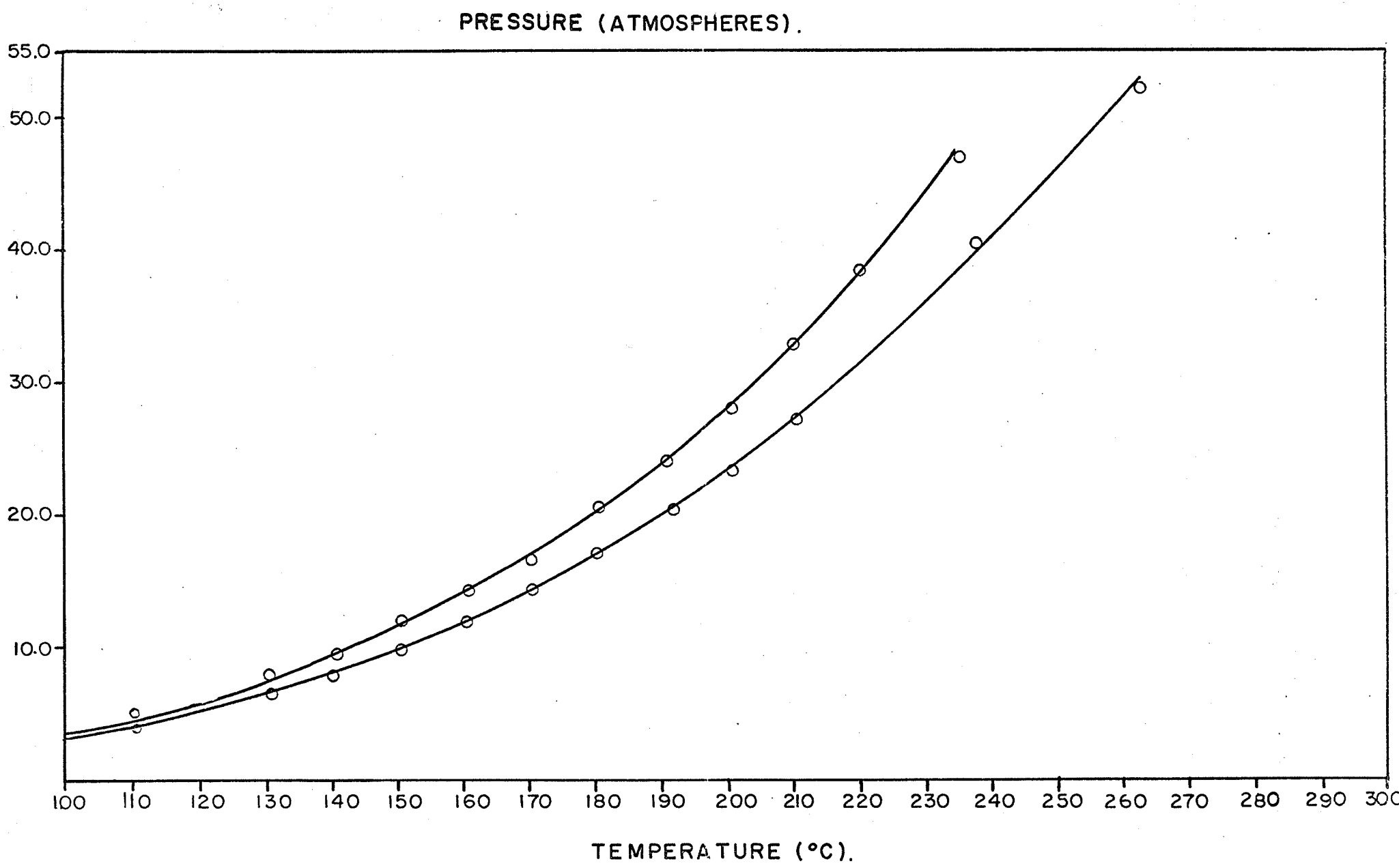
PRESSURE (ATMOSPHERES).
55.0
50.0
40.0
30.0
20.0
10.0
100
110
120
130
140
150
160
170
180
190
200
210
220
230
240
250
260
270
280
290
300
TEMPERATURE (°C).

III (B) The System Acetone-Carbon Tetrachloride

The saturation vapor pressure of the system Acetone-Carbon Tetrachloride was determined over the whole concentration range from $100^{o}C$ to $270^{o}C$. Table XI gives the experimental data obtained for vapor pressure measurements of nine mixtures of the binary mixture. Figure XXIX shows the constant composition plots of the relation between pressure and temperature at the bubble points of the acetone-carbon tetrachloride system.

TABLE XI

Experimental Saturation Pressure of the System

Acetone-Carbon Tetrachloride

Temp.(°C)	Saturation Pressure(Atm)
Mole % Acetone in mixture = 6.22	
100.0	1.98
105.2	2.21
110.8	2.50
112.4	2.73
121.0	3.40
126.2	3.82
130.6	4.38
134.4	4.62
140.9	5.46
142.2	5.62
151.2	6.70
156.0	7.30
160.0	7.62
164.6	8.76
171.0	9.47
178.0	10.90
180.7	11.48
186.2	12.46
190.0	13.25
192.8	13.82
201.0	15.70
209.10	17.76
210.0	18.02
216.4	19.72
221.2	21.60
230.0	24.01
240.0	27.56
250.0	31.42
260.0	35.47
270.0	40.51
Mole % Acetone in mixture = 15.01	
100.0	2.25
104.2	2.56
111.4	3.30
118.2	3.52
120.6	3.86
125.3	4.28
132.0	4.90
133.2	5.02
140.9	5.98
141.3	6.21
154.0	7.43
161.1	8.77
166.2	9.36
172.0	10.22
176.4	11.01
184.0	12.74
186.0	12.98
191.9	14.33
199.0	16.66
204.0	16.96
208.6	18.22
212.0	19.70
218.6	21.56
221.4	22.82
230.0	25.54
240.0	29.42
250.0	33.44
260.0	37.56
270.0	42.25
Mole % Acetone in mixture = 24.89	
100.0	2.65
104.2	2.92
114.0	3.76
118.7	4.12
121.2	4.49
126.8	4.82
132.6	5.60
138.9	6.46
140.8	6.73
142.1	6.92
151.0	8.77
154.3	8.96
160.0	9.30
166.0	10.02
170.9	10.95
175.2	11.62
181.4	12.98
196.0	16.82
198.8	17.16
201.4	17.69
208.2	18.86
210.7	20.34
218.1	23.02
221.0	23.41
230.0	26.64

TABLE XI (Cont'd)

Experimental Saturation Pressure of the System

Acetone-Carbon Tetrachloride

Temp.(°C)	Saturation Pressure(Atm)
Mole % Acetone in mixture = 24.89 (Cont'd)	
240.0	30.47
250.0	34.43
260.0	38.69
270.0	43.52
Mole % Acetone in mixture = 34.11	
100.0	2.79
104.2	3.07
111.6	3.70
118.4	4.11
120.9	4.46
121.3	4.62
132.6	5.66
136.4	6.10
140.0	6.47
142.7	8.01
152.0	9.48
166.0	10.06
171.0	11.37
175.6	12.36
181.7	13.60
192.8	15.96
198.9	17.82
202.5	19.09
210.0	20.97
214.8	22.36
221.6	25.22
230.0	27.52
240.0	31.47
250.0	35.44
260.0	39.71
Mole % Acetone in mixture = 46.80	
100.0	2.98
106.4	3.46
110.0	3.72
118.8	4.67
121.6	4.99
126.2	5.27
132.4	5.89
140.6	7.18
142.4	7.86
151.7	10.02
156.1	10.67
161.0	11.06
162.6	11.56
170.0	11.72
178.4	13.86
181.2	14.67
186.8	15.87
190.8	16.34
192.1	17.01
202.0	18.96
211.6	22.06
217.3	24.66
220.0	25.52
230.0	29.00
240.0	33.17
250.0	37.22
260.0	42.01
Mole % Acetone in mixture = 52.01	
100.0	3.16
108.5	3.87
111.6	4.65
119.8	5.18
121.7	5.41
126.2	5.86
136.3	6.97
140.0	7.60
142.8	8.40
152.0	10.38
154.2	10.62
160.9	10.96
162.3	11.36
171.60	13.08
175.7	14.16
181.0	15.68
190.6	17.68
196.7	18.87
201.0	20.60
206.8	22.88
210.0	23.67
211.7	24.01
221.0	27.02
230.0	30.92
240.0	35.07
250.0	39.48
260.0	44.01

TABLE XI (Cont'd)

Experimental Saturation Pressure of the System

Acetone-Carbon Tetrachloride

Temp.(°C)	Saturation Pressure(Atm)
Mole % Acetone in mixture = 58.20	
100.0	3.20
106.4	3.87
111.2	4.69
118.9	5.32
120.8	5.76
126.4	6.56
131.6	7.80
138.9	8.01
140.2	8.65
143.8	9.26
151.6	10.72
160.0	12.05
166.4	13.26
170.6	14.67
178.9	16.86
182.2	17.71
190.7	20.72
192.8	21.38
201.4	23.86
209.6	26.38
210.0	26.52
212.4	27.06
220.0	30.61
230.0	35.00
240.0	39.98
250.0	45.90
Mole % Acetone in mixture = 72.02	
100.0	3.29
111.0	4.61
118.2	5.52
122.0	5.92
124.4	6.56
131.6	7.65
142.4	9.04
150.6	10.99
152.8	11.58
160.0	13.16
161.8	13.96
172.2	16.04
181.0	18.92
186.8	19.82
190.6	21.94
201.9	26.56
210.0	29.25
220.0	33.60
230.0	38.02
240.0	43.62

Temp.(°C)	Saturation Pressure(Atm)
Mole % Acetone in mixture = 86.70	
100.0	3.38
102.1	3.66
110.0	4.69
118.9	5.67
121.2	6.06
126.4	6.92
130.0	7.49
132.8	8.06
140.0	9.20
146.6	10.12
151.0	12.06
162.3	14.65
168.8	15.87
170.0	16.35
186.0	21.37
190.0	22.58
200.0	26.60
210.0	30.86
220.0	36.21
230.0	41.81

FIGURE XXIX. Lines of Constant Composition on a P-T Diagram for the System Acetone-Carbon Tetrachloride.

(The compositions are 0, 6.22, 15.01, 24.89, 34.11, 46.80, 52.01, 58.20, 72.02, 86.70 and 100 percent acetone.)

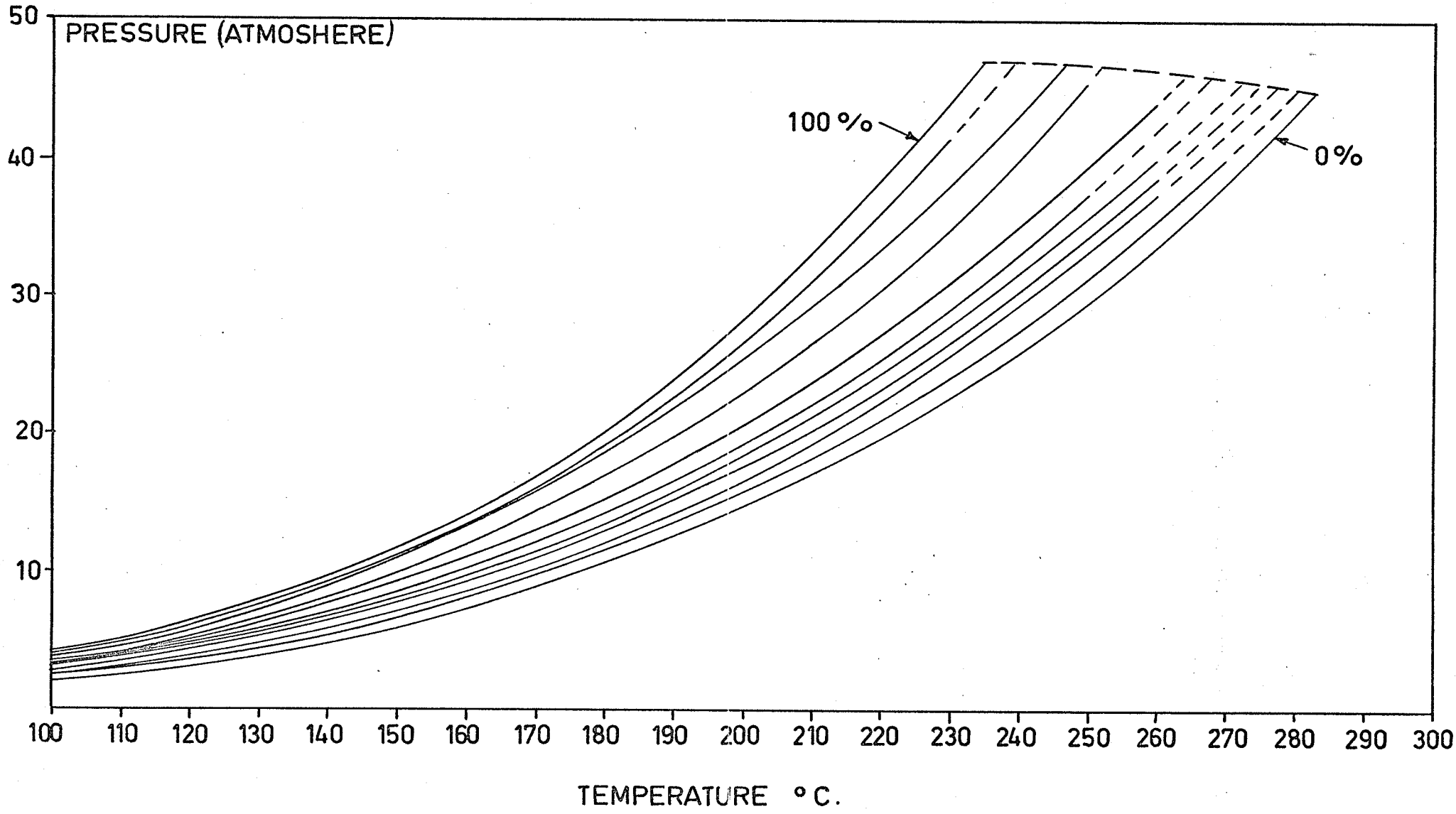
PRESSURE (ATMOSHERE)
50
40
30
20
10
100 %
0 %
100
110
120
130
140
150
160
170
180
190
200
210
220
230
240
250
260
270
280
290
300
TEMPERATURE °C.

III (C) The System Benzene-Carbon Tetrachloride

Table XII gives the experimental data obtained for vapor pressure measurements of ten mixtures of the binary system Benzene-Carbon Tetrachloride from a temperature of 100°C to about 270°C. Figure XXX shows the constant composition plots of the relation between pressure and temperature at the bubble points for a few mixtures.

TABLE XII

Experimental Saturation Pressure of the System

Benzene-Carbon Tetrachloride

Temp.(^{o}C)	Saturation Pressure(Atm)
Mole % Carbon Tetrachloride in mixture = 5.00	
100.0	1.79
106.4	2.01
110.6	2.36
118.2	2.74
121.3	3.07
124.1	3.27
130.8	3.76
132.5	3.94
141.6	4.98
150.7	5.82
158.6	6.53
162.4	7.19
164.0	7.76
170.1	8.44
180.9	10.29
182.3	10.54
190.7	11.98
196.4	13.67
200.2	14.19
210.7	16.53
215.3	17.78
220.8	19.34
230.0	22.17
240.0	25.49
250.0	29.24
260.0	33.39
270.0	38.00
Mole % Carbon Tetrachloride in mixture = 10.34	
100.0	1.82
102.1	1.97
110.7	2.44
118.2	2.87
122.6	3.41
126.2	3.62
130.6	3.86
134.8	4.11
140.4	4.80
146.7	5.26
150.8	5.87
153.1	6.18
161.3	7.31
166.8	8.02
170.6	8.52
181.2	10.41
187.4	11.06
190.7	11.99
193.6	12.62
200.8	14.22
202.4	14.56
210.7	16.67
218.4	18.72
220.8	19.39
230.0	22.20
240.0	25.52
250.0	29.30
260.0	33.42
270.0	38.04
280.0	43.16
Mole % Carbon Tetrachloride in mixture = 16.50	
100.0	1.84
108.2	2.07
110.7	2.48
122.3	3.25
128.4	3.62
131.0	3.90
133.8	4.06
140.6	4.83
143.4	5.01
151.1	5.89
157.8	6.76
160.2	7.16
164.7	7.58
170.6	8.71
178.9	10.01
181.4	10.49
190.7	12.21
198.4	13.86
200.8	14.40

TABLE XII (Cont'd)

Experimental Saturation Pressure of the System

Benzene-Carbon Tetrachloride

Temp.(°C)	Saturation Pressure(Atm)
Mole % Carbon Tetrachloride in mixture = 16.50 (Cont'd)	
202.0	14.84
210.9	16.62
216.4	18.26
220.1	19.34
230.0	22.27
240.0	25.59
250.0	29.39
260.0	33.49
270.0	38.07
Mole % Carbon Tetrachloride in mixture = 24.35	
100.0	1.87
108.1	2.06
110.8	2.51
112.2	2.71
121.6	3.39
126.4	3.52
130.0	3.86
138.4	4.48
140.1	4.80
150.7	5.86
154.2	6.22
160.0	7.11
168.7	8.13
170.4	8.66
171.2	8.82
180.2	10.28
191.0	12.22
198.2	13.88
200.1	14.43
206.2	15.27
210.7	16.83
214.1	17.22
220.4	19.41
230.0	22.32
240.0	25.64
250.0	29.42
260.0	33.51
270.0	38.10

Temp.(°C)	Saturation Pressure(Atm)
Mole % Carbon Tetrachloride in mixture = 32.60	
100.0	1.89
101.9	2.02
110.7	2.47
118.1	3.00
120.6	3.16
123.4	3.32
131.6	3.96
137.8	4.21
140.1	4.84
150.6	5.94
156.4	6.21
160.7	7.21
163.9	7.56
170.2	8.67
178.3	9.87
180.8	10.41
186.4	11.26
190.7	12.25
191.2	12.42
200.1	14.34
205.4	15.02
210.8	16.78
214.7	17.12
220.6	19.47
230.0	22.39
240.0	25.69
250.0	29.44
260.0	33.53
270.0	38.12
Mole % Carbon Tetrachloride in mixture = 38.20	
100.0	1.90
102.6	1.98
110.2	2.46
114.8	2.87
121.4	3.32
127.2	3.63
130.6	3.98
140.0	4.83

TABLE XII (Cont'd)

Experimental Saturation Pressure of the System

Benzene-Carbon Tetrachloride

Temp.(°C)	Saturation Pressure(Atm)
Mole % Carbon Tetrachloride in mixture = 38.20 (Cont'd)	
141.8	4.97
150.3	5.99
156.4	6.83
160.7	7.38
170.0	8.68
172.8	8.96
181.6	10.63
190.7	12.68
193.4	13.12
200.1	14.41
202.3	14.92
210.8	16.82
211.1	17.09
220.6	19.60
230.0	22.41
240.0	25.71
250.0	29.45
260.0	33.54
270.0	38.12
Mole % Carbon Tetrachloride in mixture = 52.00	
100.0	1.90
101.9	2.01
110.6	2.48
113.7	2.63
120.2	3.24
126.8	3.56
131.1	4.03
140.0	4.85
142.8	4.97
150.2	5.99
155.6	6.13
160.7	7.32
162.3	7.56
170.6	8.80
171.4	8.96
181.4	10.66
192.2	12.63
197.8	13.89
200.1	14.44
201.4	14.73
210.7	16.84
220.1	19.64
230.0	22.41
240.0	25.71
250.0	29.46
260.0	33.54
270.0	38.14
Mole % Carbon Tetrachloride in mixture = 62.12	
100.0	1.92
101.8	2.02
110.7	2.48
113.7	2.64
121.1	3.35
128.2	3.72
130.4	4.06
136.2	4.41
140.2	4.89
150.7	6.06
151.3	6.21
160.8	7.34
168.4	8.56
170.6	8.80
176.6	9.28
181.2	10.66
187.8	11.77
190.4	12.28
200.1	14.50
208.4	16.21
210.7	16.84
220.6	19.56
230.0	22.43
240.0	25.72
250.0	29.49
260.0	33.56
270.0	38.16

TABLE XII (Cont'd)

Experimental Saturation Pressure of the System

Benzene-Carbon Tetrachloride

Temp.(°C)	Saturation Pressure(Atm)	Temp.(°C)	Saturation Pressure(ATm)
Mole % Carbon Tetrachloride in mixture = 82.00		Mole % Carbon Tetrachloride in mixture = 97.21	
100.0	1.92	100.0	1.92
103.6	2.12	101.2	2.03
110.4	2.49	110.6	2.56
113.8	2.64	118.4	3.01
121.2	3.35	120.4	3.18
128.7	3.78	136.0	4.12
130.6	3.99	141.2	4.99
134.4	4.28	143.1	5.12
140.7	4.98	150.2	6.01
141.1	5.02	160.7	7.38
150.4	6.03	171.2	8.86
156.7	6.76	183.4	10.80
160.1	7.36	190.6	12.44
170.0	8.72	201.6	14.70
173.8	9.02	212.3	16.96
180.7	10.60	220.7	19.66
191.2	12.44	230.0	22.43
196.4	13.06	240.0	25.76
200.6	14.59	250.0	29.49
202.2	14.66	260.0	33.56
210.7	16.86	270.0	38.14
221.4	19.67		
230.0	22.43		
240.0	25.74		
250.0	29.48		
260.0	33.57		
270.0	38.14		

FIGURE XXX. Lines of Constant Composition on a P-T Diagram for the System Benzene-Carbon Tetrachloride.

(The mixtures were not plotted for clarity's sake.)

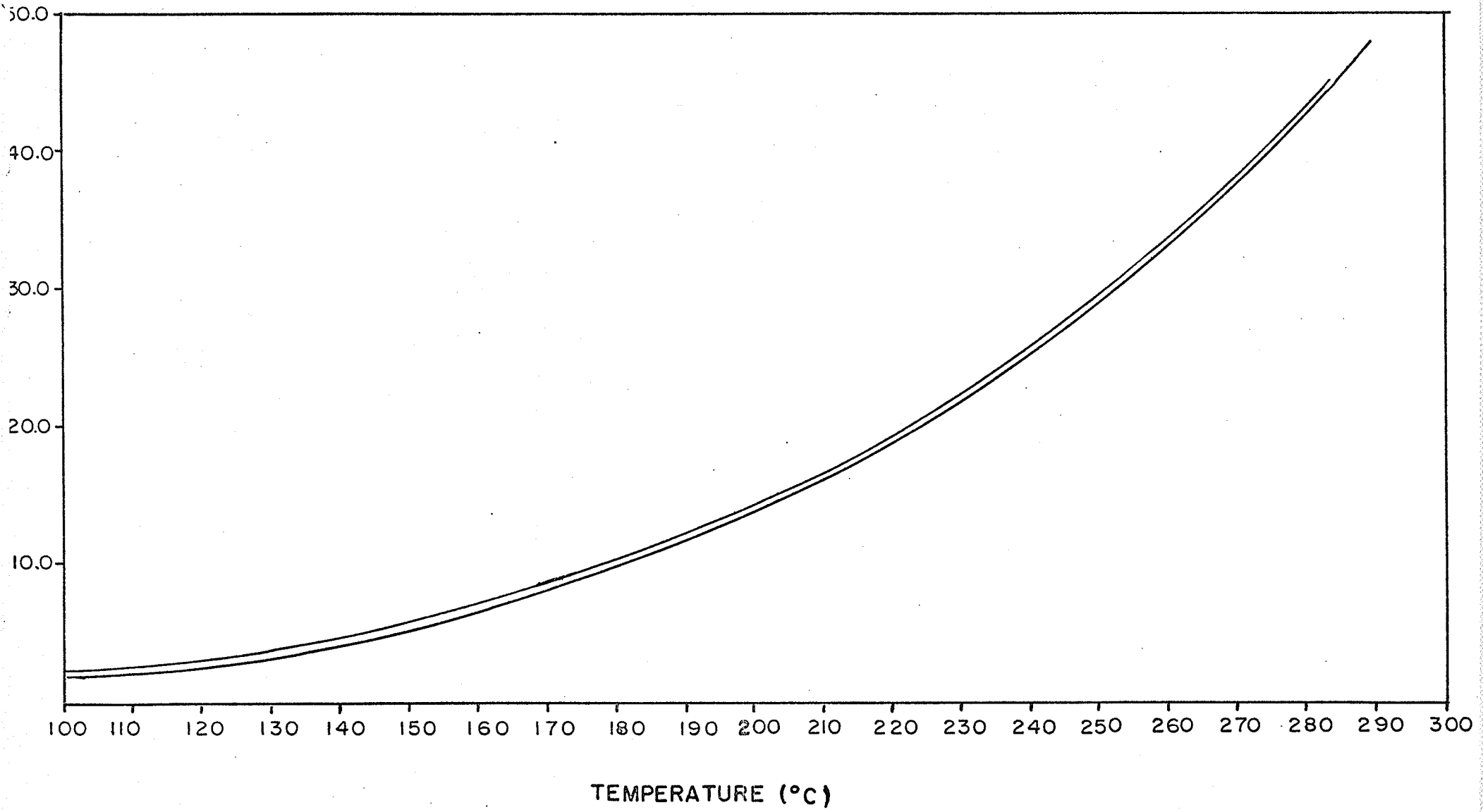
PRESSURE (ATMOSPHERES).
50.0
40.0
30.0
20.0
10.0
100 110 120 130 140 150 160 170 180 190 200 210 220 230 240 250 260 270 280 290 300
TEMPERATURE (°C)

CHAPTER V

TREATMENT OF DATA AND DISCUSSION OF RESULTS

V (A). Thermodynamic Analysis

Thermodynamic analysis is a tool for interpreting phase equilibrium data; such interpretation is necessary for interpolating or extrapolating data to new conditions and for correlating phase behaviour in terms of physiochemical parameters. Thermodynamic reduction and correlation of vapor $\rightleftharpoons$ liquid equilibrium data are common at low pressures, but despite a large supply of equilibrium data at high pressures, little attempt has been made to reduce such data with thermodynamically significant functions.

In high pressure phase equilibria it is not possible to make the simplifying assumptions commonly made at low pressures, and, as a result, thermodynamic analysis has only rarely been applied to high pressure systems. In such systems, both phases, vapor and liquid, exhibit large deviations from ideal behaviour.

I chose the method suggested by Chueh and Prausnitz (50) for the treatment of my experimental data. Vapor phase non-idealities are expressed as fugacity coefficients (ϕ_i) and the liquid phase non-idealities are given by activity coefficients (γ_i). The Redlich-Kwong equation, modified by the introduction of binary interaction constants, to increase its accuracy for mixtures, has been used for vapor phase properties. The van Laar equation, modified to allow for the rapid change of liquid molar volume which occurs in the critical

region, has been used to represent the effect of composition on liquid phase properties. The parameters which I have determined are: (1)Henry's constant $H_{2(1)}^{(Po)}$, (2) binary interaction constant $\alpha_{22(1)}$ which represents the self-interaction constant of molecules 2 in the environment of molecules 1 and is defined by equation 54 or (α_{12} which represents the interaction constant of molecules 1 and 2 is defined by the equation $\frac{G^E}{RT(x_1V_{c_1} + x_2V_{c_2})} = \alpha_{12}\,\Phi_1\,\Phi_2$), and (3)dilation constant $\eta_{2(1)}$. For a given binary system, the above parameters depend only on temperature. Therefore, isothermal experimental data are required. From the large scale plot of P versus T for various fixed liquid compositions (Figures XXVIII to XXX) and from large scale plots of vapor⇌liquid equilibria compositions (Figures XII to XXVII), P-x-y data were read for each isotherm. The programs used are those written by Chueh and Prausnitz (50) and the analysis was carried out using an IBM 360/65 electronic computer.

At system temperatures appreciably lower than the critical temperature of the light component (component 2), the dilation constant η, obtained from data reduction becomes so small that it can be effectively equated to zero. Under these conditions, the constant-pressure activity coefficient of both components can be correlated with only one parameter, α. Empirically, Chueh and Prausnitz found that this occurs at T_{R_2} smaller than 0.93. Therefore, systems for which T_{R_1} and T_{R_2} are smaller than 0.93 are correlated with $\eta = 0$ and only one parameter, α. Systems for which T_{R_1} and T_{R_2} are greater than 0.93 are correlated with a two-parameter model.

Hence, the present discussion will be divided into two parts, (A) and (B).

(A) Data reduction for binary mixtures of condensable components (both T_{R_1} and T_{R_2} less than 0.93) using the symmetric convention of normalization for activity coefficients. A one-parameter model for

the excess Gibbs energy with $\eta_{2(1)} = 0$ is used.

(B) Data reduction for binary mixtures wherein component 2 is at a reduced temperature $T_{R_2} \geqslant 0.93$ has been carried out using a two parameter model for the excess Gibbs energy and the unsymmetric convention for normalization of activity coefficients.

V (A) (1) Analysis of the Binary Systems where T_{R_1} and $T_{R_2} < 0.93$

As mentioned before, the constant-pressure activity coefficients for binary systems for which both T_{R_1} and T_{R_2} fall below 0.93 are analysed with a one-parameter model ($\eta_{2(1)} = 0$), using the symmetric convention of normalization.

A main program, SYMFIT, and three subroutines, VOLPAR, PHIMIX and CUBEQN are used for the data reduction. The program SYMFIT fits binary vapor $\rightleftharpoons$ liquid equilibrium data to a symmetric one term van Laar equation. The subroutine VOLPAR calculates partial molar volumes in the liquid mixture using equation (76). This quantity is required to take into account the effect of pressure on liquid phase activity coefficients, that is, the Poynting correction. The subroutine PHIMIX, through equation (37) calculates the fugacity coefficient of a component in the vapor mixture using the revised Redlich-Kwong equation. The molar volume V of the gas mixture, required in equation (37) is obtained by solving equation (24) and taking the largest real root of V. This is carried out by the subroutine CUBEQN.

As an example, the input data of the binary system Carbon Tetrachloride (1) - Acetone (2) for the program SYMFIT are given

below in the order they appear on the cards.

First card

The first card contains the title "CCl_4(1) - Acetone (2) at 100^o, 150^o, 200^o, SYMFIT."

Second Card

This card contains the following properties of component 1 (CCl_4 in this case):- (1)Critical pressure in pounds per square inch absolute. (2)The critical volume in ft^3/lb-mole. (3)The critical temperature in degree Rankine. (4)The acentric factor, ω which was obtained using the equation (81)

$$\omega = - \log P_{R_{T_R = 0.7}} - 1.00 \tag{81}$$

and the vapor pressure of the pure component. (5)The dimensionless constants Ω_a for the vapor, Ω_b for the vapor, Ω_a for the liquid and Ω_b for the liquid, which were obtained by fitting the Redlich-Kwong equation (24) to the volumetric data of the pure saturated vapor and saturated liquid. (6)The molecular weight of component 1 and (7) the name of component 1.

Third Card

This card contains the reference fugacity $f_{pure}^{(Po)}$ of component 1. The reference fugacity of each pure substance at temperature T was obtained by correcting the experimental vapor pressures of the substance at T using fugacity charts. The equation

$$\log \frac{f}{P} = \frac{P_r}{2.303} \left[(0.1445 + 0.073\omega)T_R^{-1} - (0.0330 - 0.46\omega)T_R^{-2} - (0.1385 + 0.50\omega)T_R^{-3} - (0.0121 + 0.097\omega)T_R^{-4} - 0.0073\omega T_R^{-9} \right]$$

was not used because of its inaccuracies at high pressures.

Fourth and Fifth Cards

These two cards contain information on component 2 similar to that on the Second and Third Cards.

Sixth Card

This card contains (1) K_{12} (correction to geometric mean $T_{c_{12}}$ - (equation (36)) for the vapor and for the liquid, (2) the critical binary constants $2\tau_{12}/(T_{c_1} + T_{c_2})$ and (3) the correlating parameter for critical volumes $2\nu_{12}/(V_{c_1} + V_{c_2})$.

K_{12} was obtained from equation (36) and Table V. It was found that K_{12} was slightly dependent on concentration. Hence a mean of a few values of K_{12} at different concentrations was taken. The critical binary constant $2\tau_{12}/T_{c_1} + T_{c_2})$ was obtained from the experimental data of the critical temperatures of the binary mixtures shown in Table V, using equation (79). The correlating parameter for critical volumes, $2\nu_{12}/(V_{c_1} + V_{c_2})$ was obtained by extrapolation from the generalized chart (page 41, reference 50) given in the monograph.

The seventh card contains the temperature of the binary system in degrees Rankine.

The eighth card contains the number of data points for each isotherm and the minimum mole fraction for a data point to be weighted (0.005 was chosen in this study).

The cards which follow contain, on each card, the liquid mole fraction of component 2, the vapor mole fraction of component 2, and the total pressure in pounds per square inch absolute.

The partial molar volumes $\bar{V}_1^L$ and $\bar{V}_2^L$ and the fugacity coefficients ϕ_1 and ϕ_2 are calculated for each data point using the subroutines

VOLPAR and PHIMIX. The constant pressure activity coefficients γ_1 and γ_2 are then calculated using equations (44) and (45) assuming the liquid partial molar volumes to be incompressible.

As shown in Table XIII to Table XVIII the computer prints out, for each round of fitting, the binary interaction parameter α_{12}, the number of experimental points used for γ_1 and γ_2, the calculated and experimental activity coefficients for each point, and the average deviation in γ_1 and γ_2. The standard state fugacities, liquid-phase partial molar volumes, the Poynting corrections and vapor phase fugacity coefficients are also obtained for each point. The program SYMFIT has a provision for testing the thermodynamic consistency of the experimental data (see section V (A) (3)).

V (A) (2) Analysis of the Binary Systems where T_{R_1} and $T_{R_2} \geq 0.93$

Binary systems for which the reduced temperature of the lighter component exceeds 0.93 are analysed with the two-parameter dilated van Laar model using the unsymmetric convention for normalization. The standard-state fugacity for component 2($T_{R_2} > 0.93$) is Henry's constant of 2 in 1, $H_{2(1)}^{(PO)}$ and must be determined before data reduction is carried out. Henry's constant is determined by a main program HENRYS and subroutines VOLPAR, PHIMIX and CUBEQN.

The input data for program HENRYS are only slightly different from those of program SYMFIT. The first two cards are identical but the third card now contains the properties of component 2 and the fourth card contains the coefficients for the reduced liquid fugacity of component 1. The coefficients for the reduced liquid fugacity of

component 2 are not required for this program. The fifth card contains K_{12} for the vapor, K_{12} for the liquid, $2\tau_{12}/(T_{c_1} + T_{c_2})$ and $2\nu_{12}/V_{c_1} + V_{c_2})$. The sixth card contains the temperature of the binary system in degrees Rankine and the saturation pressure of component 1 at that temperature. The composition cards follow, one card for each composition, containing liquid mole fraction of component 2, vapor mole fraction of component 2 and the total pressure in pounds per square inch absolute.

The program calculates $f_2^{(P)}/x_2$ for each point, and, by plotting $\ln f_2^{(P)}/x_2$ versus x_2 and extrapolating to $x_2 = 0$, Henry's constant $H_{2(1)}^{(P_1^S)}$ is obtained. Henry's constant is corrected to zero pressure in the fitting program. The program HENRYS also gives output of x_2, y_2, P, $\bar{V}_1^L$, $\bar{V}_2^L$, ϕ_1 and ϕ_2 which are used in the FITTING program to evaluate the self-interaction constant, $\alpha_{22(1)}$, and the dilation constant $\eta_{2(1)}$ in the dilated van Laar model. This fitting program has a provision for testing the thermodynamic consistency of the experimental data (see section V (A) (3)).

V (A) (3) Thermodynamic Consistency Test of the Vapor ⇌ Liquid Equilibrium Data

Vapor ⇌ liquid equilibrium data are said to be thermodynamically consistent when they satisfy the Gibbs-Duhem equation. When the data satisfy this equation, it is likely, but by no means certain, that they are correct; however, if they do not satisfy this equation, it is certain that they are incorrect.

Thermodynamic consistency tests for binary vapor⇌liquid equilibria at low pressures have been described by many authors; a good review is given in the monograph by Van Ness (100).

Extension of these methods to isothermal high pressure equilibria presents two difficulties: (1) it is necessary to have experimental data for the density of the liquid mixture along the saturation line and (2) since the ideal gas law is not valid, it is necessary to calculate vapor phase fugacity coefficients either from volumetric data for the vapor mixture or else from an equation of state.

Adler et al (101) have presented a method for testing the thermodynamic consistency of binary liquid ⇌ vapor equilibrium data when one component is above its critical temperature. They used the Lewis fugacity rule to calculate vapor phase fugacities but errors in this approximation are often very large and it is not possible to come to any significant conclusions concerning the thermodynamic consistency of experimental equilibrium data when this approximation is used as an essential part of the consistency test.

Chueh et al (102) have described a consistency test which is an extension to isothermal high-pressure data of the integral (area) test given by Redlich and Kister (103) and by Herington (104) for isothermal low pressure data. The Gibbs-Duhem equation for a binary system at constant temperature is written as:

$$x_1 d \ln f_1 + x_2 d \ln f_2 = \frac{V^L}{RT} dp \qquad (83)$$

Using the identity

$$x_1 d \ln x_1 + x_2 d \ln x_2 = 0 \qquad (84)$$

equation (83) can be rearranged to give equation (85)

$$\ln \left(\frac{f_2/x_2}{f_1/x_1} \right) dx_2 + \frac{V^L}{RT} dp = d \left[\ln \frac{f_1}{x_1} + x_2 \ln \left(\frac{f_2/x_2}{f_1/f_2} \right) \right] \qquad (85)$$

Introducing fugacity coefficients ϕ and K factors ($K_i = \frac{y_i}{x_i}$) into equation (85) we obtain

$$\left(\ln \frac{\phi_2}{\phi_1} + \ln \frac{K_2}{K_1}\right) dx_2 + \frac{V^L}{RT} dp =$$

$$d\left(\ln K_1 + \ln \phi_1 P + x_2\left(\ln \frac{\phi_2}{\phi_1} + \ln \frac{K_2}{K_1}\right)\right) \qquad (86)$$

where subscript 2 refers to the light component.

Equation (86) is integrated from $x_2 = 0$ to some arbitrary upper limit x_2 with the following boundary conditions:

when $x_2 = 0$, $\phi_1 = \phi_1^s$, $p = p_1^s$ and $K_1 = 1$

The integrated form can be written as

Area I + Area II + Area III =

$$\left(\ln K_1 + \ln \frac{\phi_1 P}{\phi_1^s P_1^s} + x_2\left(\ln \frac{\phi_2}{\phi 1} + \ln \frac{K_2}{K_1}\right)\right) \text{ at } x_2 \qquad (87)$$

$$\text{where Area I} = \int_{x_2=0}^{x_2} \ln \frac{K_2}{K_1} \, dx_2 \qquad (88)$$

$$\text{Area II} = \int_{x_2=0}^{x_2} \ln \frac{\phi_2}{\phi_1} \, dx_2 \qquad (89)$$

$$\text{Area III} = \frac{1}{RT} \int_{x_2=0}^{x_2} V^L dp \qquad (90)$$

The thermodynamic consistency test consists of comparing the sum of the three areas, which are found by graphical integration, with the right hand side of equation (87). The three areas depend upon equilibrium data for the composition range $x_2 = 0$ to equilibrium data at the upper limit $x_2 = x_2$. The comparison indicated by equation (87) should be made for several values of x_2 up to and including the critical

composition.

Chueh and Prausnitz (50) have replaced the data plotting procedure by a regression analysis. In their analysis, which I applied to my experimental data, at the end of the first round of fitting, the average deviations of γ_1 and γ_2 (or γ_2^*) are computed respectively. They are nearly equal in magnitude and generally small if the experimental data are thermodynamically consistent. If the data are thermodynamically consistent, both γ_1 and γ_2 are utilized in the second round of fitting. If the data are inconsistent, the average deviation of γ for one component is generally much larger than that of the other; this happens because the less accurate set of data, say γ_1, scatters much more than the γ_2 or (γ_2^*) data; the least squares fitting, finding it impossible to fit the γ_1 data any better, automatically fits better to the more accurate data for γ_2 (or γ_2^*). If the data are thermodynamically inconsistent, the less reliable set of γ is discarded in the second round of fitting. Chueh and Prausnitz (50) used the criterion that if the average deviations of γ_1 and γ_2 differ by more than 3%, the data will be considered as inconsistent.

V (B) (1) Discussion of Results

V (B) (1) The System Chloroform (1) - Acetone (2)

From Figure IX which gives a plot of T_M, the temperature of the disappearance of the meniscus versus mole percent chloroform in the mixture, it can be seen that the system Chloroform (1) - Acetone (2) exhibits a negative deviation from ideality. This observation has been made previously by many workers, including Swietoslawski (106) and

Chatterjee (85). The deviation from ideality is also apparent in the vapor pressure plots. This negative deviation from Raoult's law has been explained by the fact that a 1:1 hydrogen bonding compound exists in the system and, Campbell and Kartzmark (82) have determined the energy of the hydrogen bond and found it to be a -2.7 kcal per mole. It is very doubtful though if this compound exists under critical conditions.

The existence of an azeotrope has been confirmed from the vapor liquid equilibrium composition curves, Figures XII to XVI and the vapor pressure plots. It was found that the composition of the azeotrope, a negative azeotrope in the terminology of Rowlinson (19), which is 36.2 mole percent acetone at 100°C, shifted towards lower acetone content as the temperature was raised.* The same deduction was made by Rock and Schröder (84) in their study of this system at temperatures ranging from 10°C to 55°C. The above observation also agrees with the well-known fact that an increase of temperature in a negative azeotrope decreases the mole fraction of the component whose vapor pressure increases the more rapidly with temperature. The above system was investigated only up to 180°C because of decomposition on heating but it is known (107) that the azeotrope does not exist up to the critical point, that is, the system chloroform-acetone exhibits limited azeotropic behaviour.

The experimental data, vapor⇌liquid equilibrium compositions and saturation vapor pressure for this binary system have been treated to yield the fugacity coefficients ϕ_1 and ϕ_2 and the activity coefficients γ_1 and γ_2 of the two components in the vapor and liquid mixtures. For this purpose the program SYMFIT and the subroutines VOLPAR, PHIMIX and

(See Table XII A.)

TABLE XII (A)

Dependence of Azeotropic Composition on Temperature in the System $CHCl_3$(1)-Acetone(2)

Temperature (°C)	Azeotropic Composition (Mole Fraction Acetone)
100	0.362
150	0.347
160	0.292
170	0.235
180	0.209

TABLE XIII

THERMODYNAMIC ANALYSIS OF THE SYSTEM $CHCl_3$ (1) - ACETONE (2) AT 150°C

Correction to Geometric mean $K_{12} = 0.010$, $2\tau_{12}/(T_{C_1} + T_{C_2}) = 0.008$, $2\nu_{12}/(V_{C_1} + V_{C_2}) = -0.035$

Temperature = 150.0°C, Reference Fugacity (1) = 9.92 atm., Reference Fugacity (2) = 11.43 atm

x_2	y_2	Vol. fraction of component 2 in the liquid phase	P(atm)	$\bar{V}_1^L$(cc/mole)	$\bar{V}_2^L$(cc/mole)	Poynting Correction for γ_1	Poynting Correction for γ_2	$\gamma_1^{(PO)}$(exp)	$\gamma_2^{(PO)}$(exp)	ϕ_1	ϕ_2
0.125	0.099	0.112	9.34	109.6	103.0	1.029	1.028	0.844	0.555	0.896	0.882
0.235	0.208	0.214	9.32	109.2	102.2	1.029	1.027	0.847	0.619	0.897	0.882
0.313	0.300	0.288	9.25	108.9	101.7	1.029	1.027	0.828	0.666	0.898	0.882
0.416	0.435	0.387	9.50	108.5	101.1	1.030	1.028	0.805	0.742	0.895	0.878
0.540	0.596	0.510	9.86	108.0	100.4	1.031	1.029	0.755	0.807	0.892	0.873
0.624	0.680	0.596	10.12	107.6	100.0	1.031	1.029	0.749	0.814	0.890	0.869
0.800	0.860	0.780	10.72	106.7	98.9	1.033	1.031	0.648	0.842	0.885	0.861
0.929	0.959	0.920	11.22	105.7	98.1	1.034	1.032	0.556	0.939	0.881	0.855

α_{12}, interaction constant of molecules (1) and (2) = -0.00336 mole/cc.

x_2	(exp) $\ln\gamma_1^{(PO)}$	(calc) $\ln\gamma_1^{(PO)}$	(exp) $\ln\gamma_1^{(PO)}$	(calc) $-\ln\gamma_1^{(PO)}$	(exp) $\ln\gamma_2^{(PO)}$	(calc) $\ln\gamma_2^{(PO)}$	(exp) $\ln\gamma_2^{(PO)}$	(calc) $-\ln\gamma_2^{(PO)}$	(calc) $\gamma_1^{(PO)}$	(exp) $\gamma_1^{(PO)}$	(calc) $-\gamma_1^{(PO)}$	(calc) $\gamma_2^{(PO)}$	(exp) $\gamma_2^{(PO)}$	(calc) $-\gamma_2^{(PO)}$
0.125	-0.169	-0.010	-0.159		-0.587	-0.572	-0.015		0.989	-0.145		0.564	-0.008	
0.235	-0.165	-0.037	-0.128		-0.479	-0.448	-0.030		0.963	-0.115		0.638	-0.019	
0.313	-0.187	-0.068	-0.119		-0.406	-0.368	-0.038		0.934	-0.105		0.691	-0.025	
0.416	-0.216	-0.123	-0.093		-0.297	-0.272	-0.025		0.884	-0.078		0.761	-0.018	
0.540	-0.280	-0.213	-0.066		-0.213	-0.174	-0.039		0.807	-0.052		0.840	-0.032	
0.624	-0.289	-0.290	0.001		-0.204	-0.118	-0.086		0.747	0.001		0.888	-0.073	
0.800	-0.433	-0.498	0.064		-0.171	-0.035	-0.136		0.607	0.040		0.965	-0.123	
0.929	-0.586	-0.693	0.106		-0.075	-0.004	-0.070		0.499	0.056		0.995	-0.056	

Average deviation in $\gamma_1^{(PO)}$ = 0.074

Average deviation in $\ln\gamma_1^{(PO)}$ = 0.092

Average deviation in $\gamma_2^{(PO)}$ = 0.047

Average deviation in $\ln\gamma_2^{(PO)}$ = 0.055

TABLE XIII (Cont'd)

THERMODYNAMIC ANALYSIS OF THE SYSTEM $CHCl_3$ (1) - ACETONE (2) at 160°C

Correction to Geometric mean $K_{12} = 0.010$, $2\tau_{12}/(T_{C_1} + T_{C_2}) = 0.008$, $2\nu_{12}/(V_{C_1} + V_{C_2}) = -0.035$

Temperature = 160.0°C, Reference Fugacity (1) = 11.55atm.,Reference Fugacity (2) = 13.66 atm.

x_2	y_2	Vol.fraction of component 2 in the liquid phase	P(atm)	$\bar{V}_1^L$(cc/mole)	$\bar{V}_2^L$(cc/mole)	Poynting Correction for γ_1	Poynting Correction for γ_2	$\gamma_1^{(PO)}$(exp)	$\gamma_2^{(PO)}$(exp)	ϕ_1	ϕ_2
0.235	0.225	0.214	11.40	112.1	104.7	1.036	1.034	0.851	0.668	0.882	0.865
0.313	0.320	0.288	11.36	111.9	104.3	1.036	1.033	0.829	0.711	0.883	0.865
0.416	0.465	0.387	11.64	111.6	103.7	1.037	1.034	0.784	0.792	0.880	0.860
0.540	0.630	0.510	12.00	111.2	103.0	1.038	1.035	0.707	0.846	0.878	0.855
0.800	0.867	0.780	12.96	110.1	101.6	1.041	1.037	0.624	0.835	0.870	0.843
0.929	0.960	0.920	13.58	109.2	100.8	1.042	1.039	0.550	0.926	0.865	0.835

α_{12}, interaction constant of molecules (1) and (2) = -0.0032 mole/cc.

x_2	(exp) $\ln\gamma_1^{(PO)}$	(calc) $\ln\gamma_1^{(PO)}$	(exp) $\ln\gamma_1^{(PO)}$ - (calc) $\ln\gamma_1^{(PO)}$	(exp) $\ln\gamma_2^{(PO)}$	(calc) $\ln\gamma_2^{(PO)}$	(exp) $\ln\gamma_2^{(PO)}$ - (calc) $\ln\gamma_2^{(PO)}$	(calc) $\gamma_1^{(PO)}$	(exp) $\gamma_1^{(PO)}$ - (calc) $\gamma_1^{(PO)}$	(calc) $\gamma_2^{(PO)}$	(exp) $\gamma_2^{(PO)}$ - (calc) $\gamma_2^{(PO)}$
0.235	-0.160	-0.035	-0.125	-0.403	-0.426	0.023	0.964	-0.113	0.652	0.015
0.313	-0.186	-0.064	-0.122	-0.341	-0.350	0.009	0.937	-0.107	0.704	0.006
0.416	-0.243	-0.117	-0.126	-0.233	-0.259	0.026	0.889	-0.105	0.771	0.020
0.540	-0.346	-0.202	-0.143	-0.166	-0.165	-0.000	0.816	-0.109	0.847	-0.000
0.800	-0.471	-0.473	0.002	-0.179	-0.033	-0.146	0.622	0.001	0.967	-0.131
0.929	-0.597	-0.659	0.061	-0.091	-0.004	-0.086	0.517	0.033	0.995	-0.069

Average deviation in $\gamma_1^{(PO)}$ = 0.078

Average deviation in $\gamma_2^{(PO)}$ = 0.040

Average deviation in $\ln\gamma_1^{(PO)}$ = 0.097

Average deviation in $\ln\gamma_2^{(PO)}$ = 0.048

TABLE XIII (Cont'd)

THERMODYNAMIC ANALYSIS OF THE SYSTEM $CHCl_3$ (1) - ACETONE (2) AT 170°C

Correction to Geometric mean $K_{12} = 0.010$, $2\tau_{12}/(T_{C_1} + T_{C_2}) = 0.008$, $2\nu_{12}/(V_{C_1} + V_{C_2}) = -0.035$

Temperature = 170.0°C, Reference Fugacity (1) = 13.30atm., Reference Fugacity (2) = 15.92atm.

x_2	y_2	Vol. fraction of component 2 in the liquid phase	p(atm)	$\bar{V}_1^L$(cc/mole)	$\bar{V}_2^L$(cc/mole)	Poynting Correction for γ_1	Poynting Correction for γ_2	$\gamma_1^{(PO)}$(exp)	$\gamma_2^{(PO)}$(exp)	ϕ_1	ϕ_2
0.125	0.107	0.112	13.70	115.7	108.2	1.044	1.041	0.872	0.600	0.867	0.849
0.235	0.235	0.214	13.79	115.4	107.5	1.044	1.041	0.860	0.704	0.866	0.847
0.313	0.338	0.288	13.94	115.3	107.0	1.045	1.041	0.836	0.766	0.865	0.844
0.416	0.466	0.387	14.23	115.2	106.5	1.046	1.042	0.807	0.807	0.863	0.840
0.540	0.610	0.510	14.60	114.8	105.9	1.047	1.043	0.765	0.829	0.861	0.835
0.624	0.696	0.596	14.86	114.6	105.5	1.048	1.044	0.740	0.829	0.859	0.832
0.800	0.849	0.780	15.56	113.9	104.6	1.050	1.045	0.718	0.817	0.854	0.824
0.929	0.950	0.920	16.20	113.2	104.0	1.051	1.047	0.693	0.911	0.849	0.816

α_{12}, interaction constant of molecules (1) and (2) = -0.0028 mole/cc.

x_2	(exp) $\ln\gamma_1^{(PO)}$	(calc) $\ln\gamma_1^{(PO)}$	(exp) $\ln\gamma_1^{(PO)}$ - (calc) $\ln\gamma_1^{(PO)}$	(exp) $\ln\gamma_2^{(PO)}$	(calc) $\ln\gamma_2^{(PO)}$	(exp) $\ln\gamma_2^{(PO)}$ - (calc) $\ln\gamma_2^{(PO)}$	(calc) $\gamma_1^{(PO)}$	(exp) $\gamma_1^{(PO)}$ - (calc) $\gamma_1^{(PO)}$	(calc) $\gamma_2^{(PO)}$	(exp) $\gamma_2^{(PO)}$ - (calc) $\gamma_2^{(PO)}$
0.125	-0.135	-0.008	-0.127	-0.509	-0.439	-0.070	0.992	-0.119	0.644	-0.044
0.235	-0.150	-0.028	-0.121	-0.350	-0.344	-0.006	0.971	-0.111	0.708	-0.004
0.313	-0.178	-0.052	-0.126	-0.265	-0.282	0.016	0.949	-0.112	0.754	0.012
0.416	-0.213	-0.094	-0.119	-0.214	-0.209	-0.005	0.910	-0.102	0.811	-0.004
0.540	-0.267	-0.163	-0.104	-0.186	-0.133	-0.053	0.849	-0.083	0.875	-0.045
0.624	-0.300	-0.222	-0.077	-0.186	-0.091	-0.095	0.800	-0.059	0.913	-0.083
0.800	-0.330	-0.382	0.051	-0.201	-0.026	-0.175	0.682	0.036	0.973	-0.156
0.929	-0.366	-0.531	0.165	-0.093	-0.003	-0.089	0.587	0.105	0.996	-0.085

Average deviation in $\gamma_1^{(PO)}$ = 0.091 Average deviation in $\gamma_2^{(PO)}$ = 0.054

Average deviation in $\ln\gamma_1^{(PO)}$ = 0.111 Average deviation in $\ln\gamma_2^{(PO)}$ = 0.064

TABLE XIII (Cont'd)

THERMODYNAMIC ANALYSIS OF THE SYSTEM $CHCl_3$ (1) - ACETONE (2) AT 180°C

Correction to geometric mean $K_{12} = 0.010$, $2\tau_{12}/(T_{C_1} + T_{C_2}) = 0.008$, $2\nu_{12}/(V_{C_1} + V_{C_2}) = -0.035$

Temperature = 180.0°C, Reference Fugacity (1) = 15.18 atm., Reference Fugacity (2) = 18.16atm.

x_2	y_2	Vol.fraction of component 2 in the liquid phase	p(atm)	$\bar{V}_1^L$(cc/mole)	$\bar{V}_2^L$(cc/mole)	Poynting Correction for γ_1	Poynting Correction for γ_2	$\gamma_1^{(PO)}$(exp)	$\gamma_2^{(PO)}$(exp)	ϕ_1	ϕ_2
0.075	0.064	0.067	16.70	119.3	111.6	1.055	1.051	0.895	0.618	0.848	0.828
0.125	0.112	0.112	16.66	119.2	111.3	1.054	1.051	0.896	0.647	0.848	0.828
0.235	0.240	0.214	16.46	119.1	110.6	1.054	1.050	0.869	0.730	0.850	0.829
0.313	0.345	0.288	17.10	119.1	110.1	1.056	1.052	0.859	0.810	0.845	0.821
0.416	0.475	0.387	17.35	119.0	109.6	1.057	1.052	0.820	0.847	0.844	0.817
0.540	0.619	0.510	17.74	118.9	109.1	1.058	1.053	0.769	0.864	0.841	0.812
0.624	0.706	0.596	18.14	118.8	108.7	1.059	1.054	0.740	0.866	0.839	0.808
0.800	0.862	0.780	18.94	118.4	108.0	1.062	1.056	0.676	0.850	0.834	0.799
0.929	0.959	0.920	19.60	117.8	107.3	1.064	1.058	0.581	0.933	0.830	0.792

α_{12}, interaction constant of molecules (1) and (2) = -0.0026 mole/cc.

x_2	$\ln\gamma_1^{(PO)}$ (exp)	$\ln\gamma_1^{(PO)}$ (calc)	$\ln\gamma_1^{(PO)}$ (exp) - $\ln\gamma_1^{(PO)}$ (calc)	$\ln\gamma_2^{(PO)}$ (exp)	$\ln\gamma_2^{(PO)}$ (calc)	$\ln\gamma_2^{(PO)}$ (exp) - $\ln\gamma_2^{(PO)}$ (calc)	$\gamma_1^{(PO)}$ (calc)	$\gamma_1^{(PO)}$ (exp) - $\gamma_1^{(PO)}$ (calc)	$\gamma_2^{(PO)}$ (calc)	$\gamma_2^{(PO)}$ (exp) - $\gamma_2^{(PO)}$ (calc)
0.075	-0.110	-0.002	-0.107	-0.480	-0.496	0.015	0.997	-0.101	0.608	0.009
0.125	-0.109	-0.008	-0.101	-0.434	-0.449	0.014	0.991	-0.095	0.638	0.009
0.235	-0.139	-0.029	-0.110	-0.313	-0.351	0.038	0.970	-0.101	0.703	0.027
0.313	-0.151	-0.053	-0.097	-0.210	-0.288	0.078	0.948	-0.088	0.749	0.061
0.416	-0.197	-0.096	-0.101	-0.165	-0.213	0.048	0.908	-0.087	0.807	0.040
0.540	-0.261	-0.167	-0.094	-0.146	-0.136	-0.009	0.845	-0.076	0.872	-0.008
0.624	-0.301	-0.227	-0.073	-0.143	-0.093	-0.050	0.796	-0.056	0.911	-0.045
0.800	-0.391	-0.390	-0.000	-0.162	-0.027	-0.135	0.676	-0.000	0.972	-0.122
0.929	-0.541	-0.543	0.002	-0.081	-0.003	-0.078	0.580	0.001	0.996	-0.062

Average deviation in $\gamma_1^{(PO)}$ = 0.067

Average deviation in $\ln\gamma_1^{(PO)}$ = 0.076

Average deviation in $\gamma_2^{(PO)}$ = 0.043

Average deviation in $\ln\gamma_2^{(PO)}$ = 0.052

CUBEQN were used and the results are tabulated in Table XIII.

The second round of fitting has been omitted since it is identical to the first round of fitting. From Table XIII it is seen that though $\gamma_i \rightarrow 1$ as $x_i \rightarrow 1$ the system Acetone-Chloroform is not ideal at the temperatures investigated in this work. The activity coefficients have been plotted as function of the mole fraction acetone in the liquid phase in Figure XXXI to Figure XXXIC. The deviations between the experimental values of the activity coefficients and the calculated values are rather large but I will have more to say about these facts in Chapter V (C), (General Discussion).

FIGURE XXXI. Activity Coefficients versus Mole Fraction Acetone in Liquid Phase of the System Chloroform-Acetone at 150°C.

(For Figures XXXI to XXXIC the solid line represents the calculated curve.

● represents experimental γ_2 values

represents experimental γ_1 values.

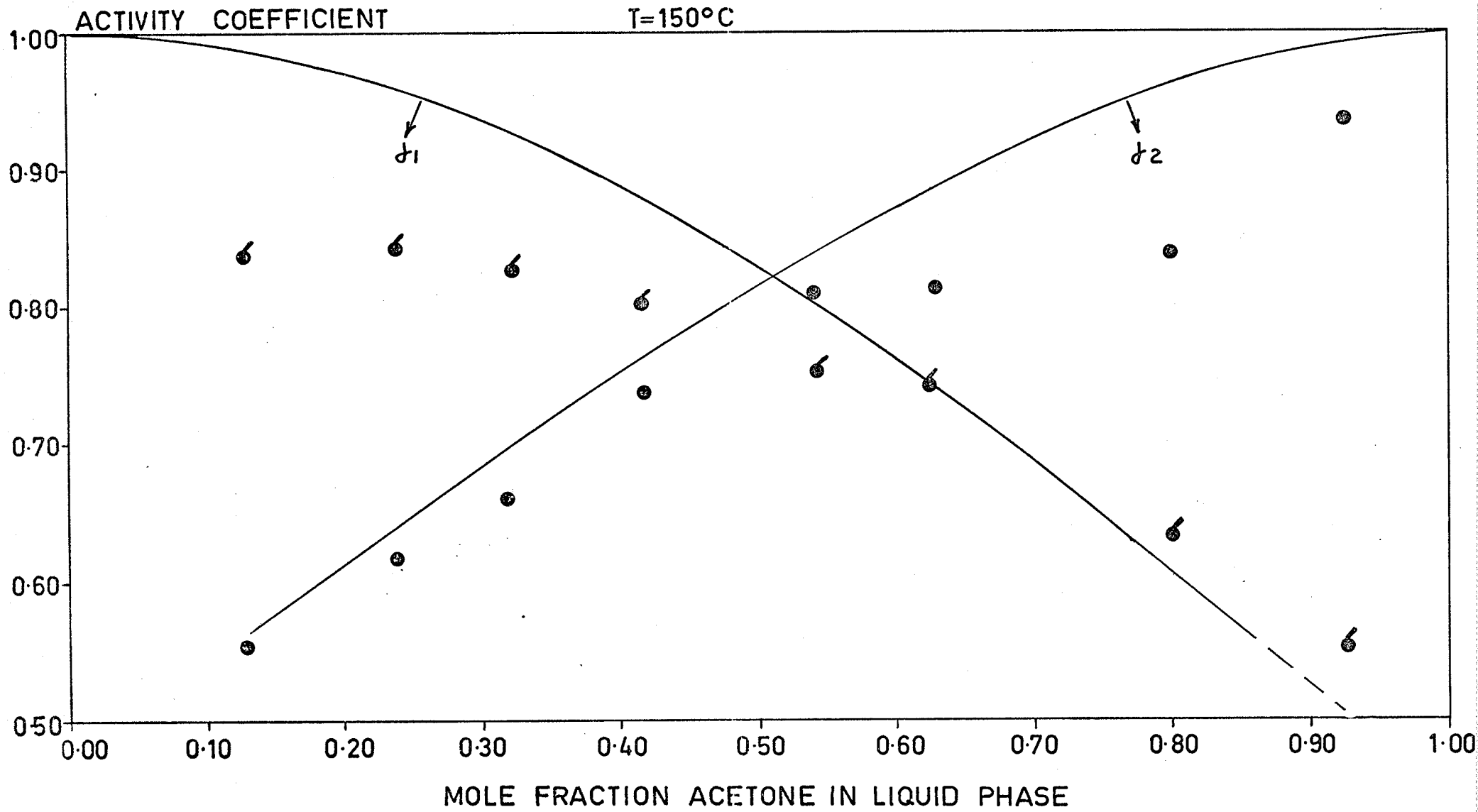
ACTIVITY COEFFICIENT
T=150°C
1·00
0·90
0·80
0·70
0·60
0·50
γ1
γ2
0·00
0·10
0·20
0·30
0·40
0·50
0·60
0·70
0·80
0·90
1·00
MOLE FRACTION ACETONE IN LIQUID PHASE

FIGURE XXXIA. Activity Coefficients versus Mole Fraction Acetone in Liquid Phase of the System Chloroform-Acetone at $160^{o}C$.

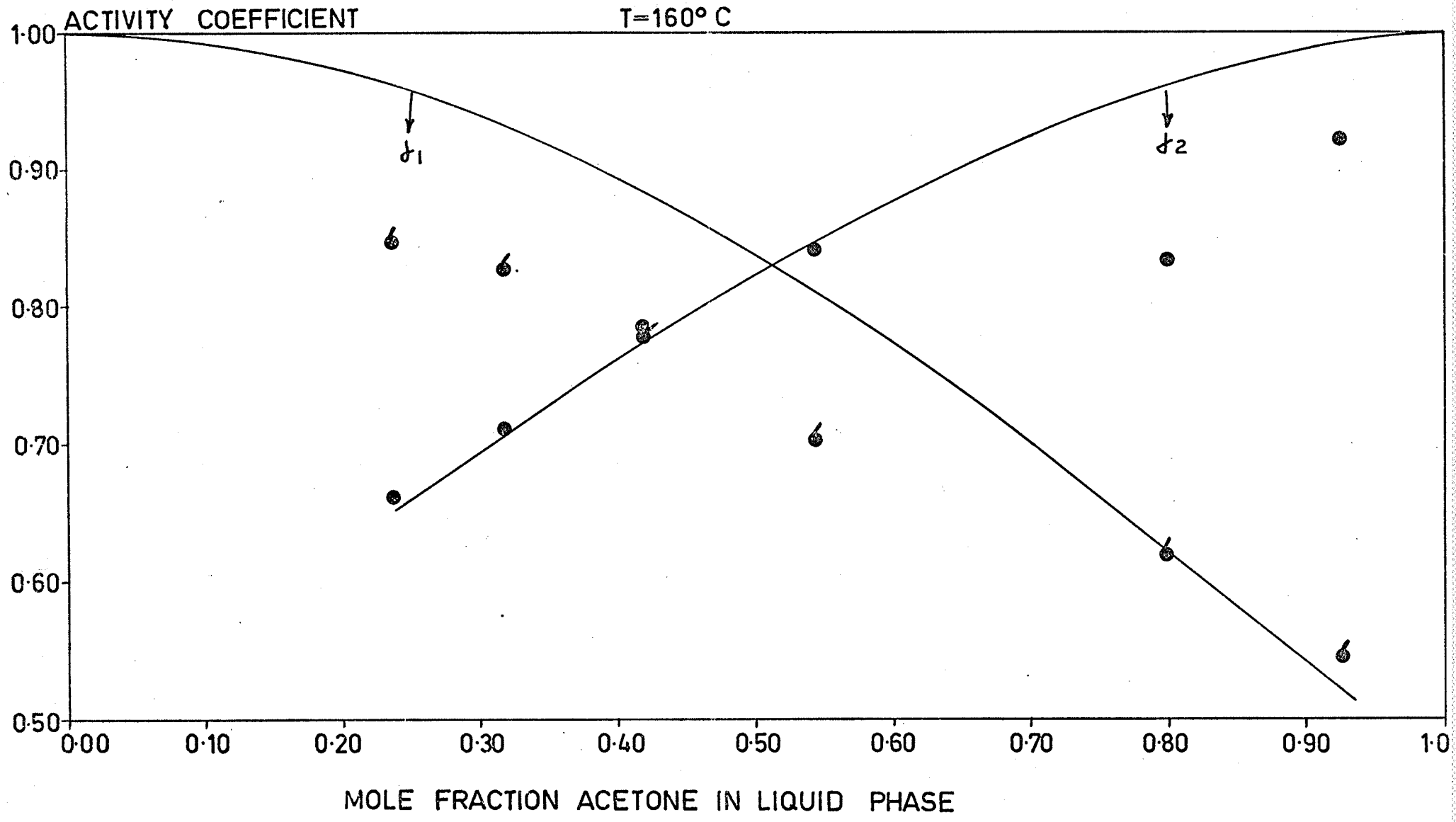
ACTIVITY COEFFICIENT
T=160° C
1·00
0·90
0·80
0·70
0·60
0·50
γ1
γ2
0·00
0·10
0·20
0·30
0·40
0·50
0·60
0·70
0·80
0·90
1·0
MOLE FRACTION ACETONE IN LIQUID PHASE

FIGURE XXXIB. Activity Coefficients versus Mole Fraction Acetone in Liquid Phase of the System Chloroform-Acetone at 170°C.

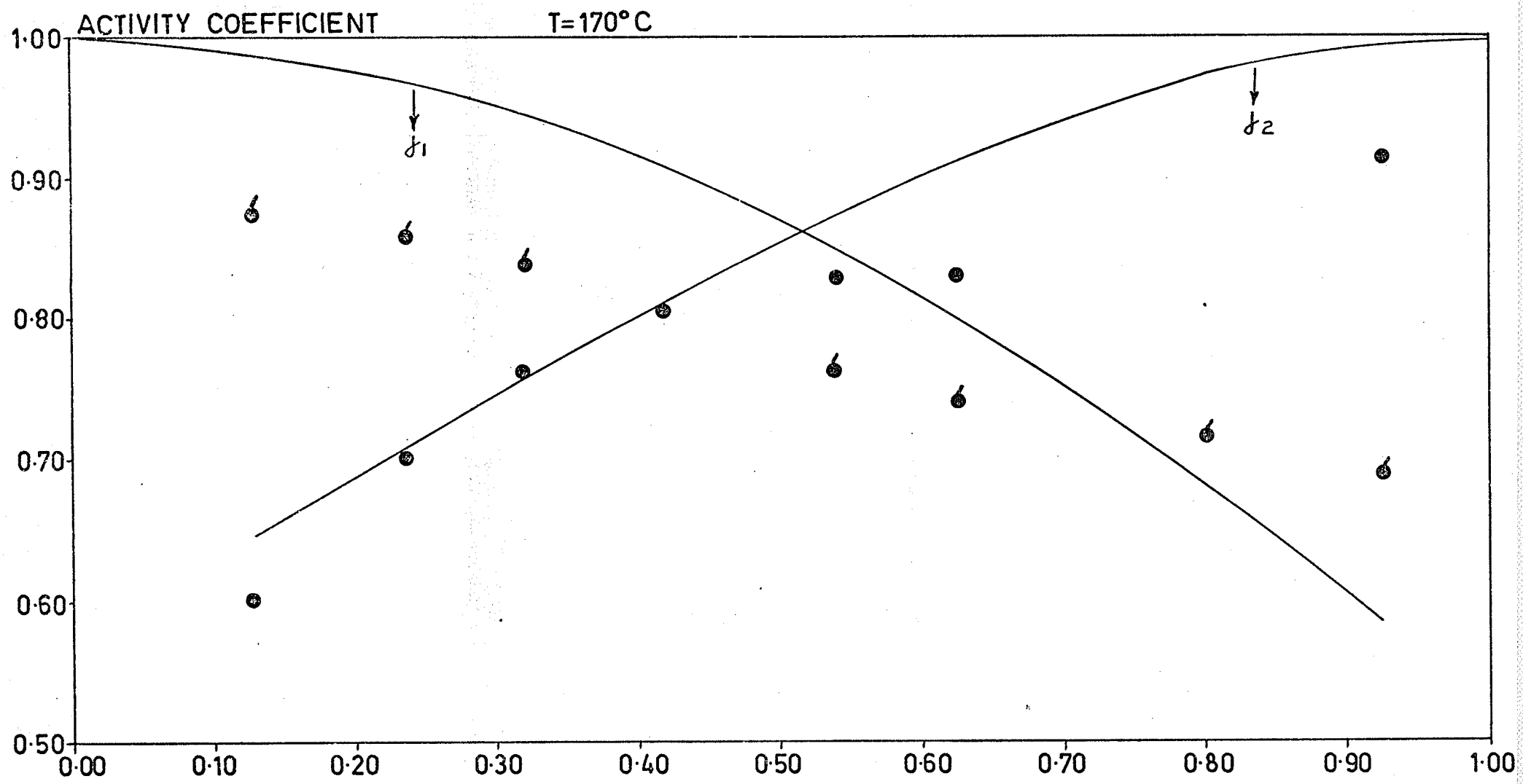
ACTIVITY COEFFICIENT
T=170°C
1·00
0·90
0·80
0·70
0·60
0·50
γ1
γ2
0·00
0·10
0·20
0·30
0·40
0·50
0·60
0·70
0·80
0·90
1·00
MOLE FRACTION ACETONE IN LIQUID PHASE.

FIGURE XXXIC. Activity Coefficients versus Mole Fraction Acetone in Liquid Phase of the System Chloroform-Acetone at 180°C.

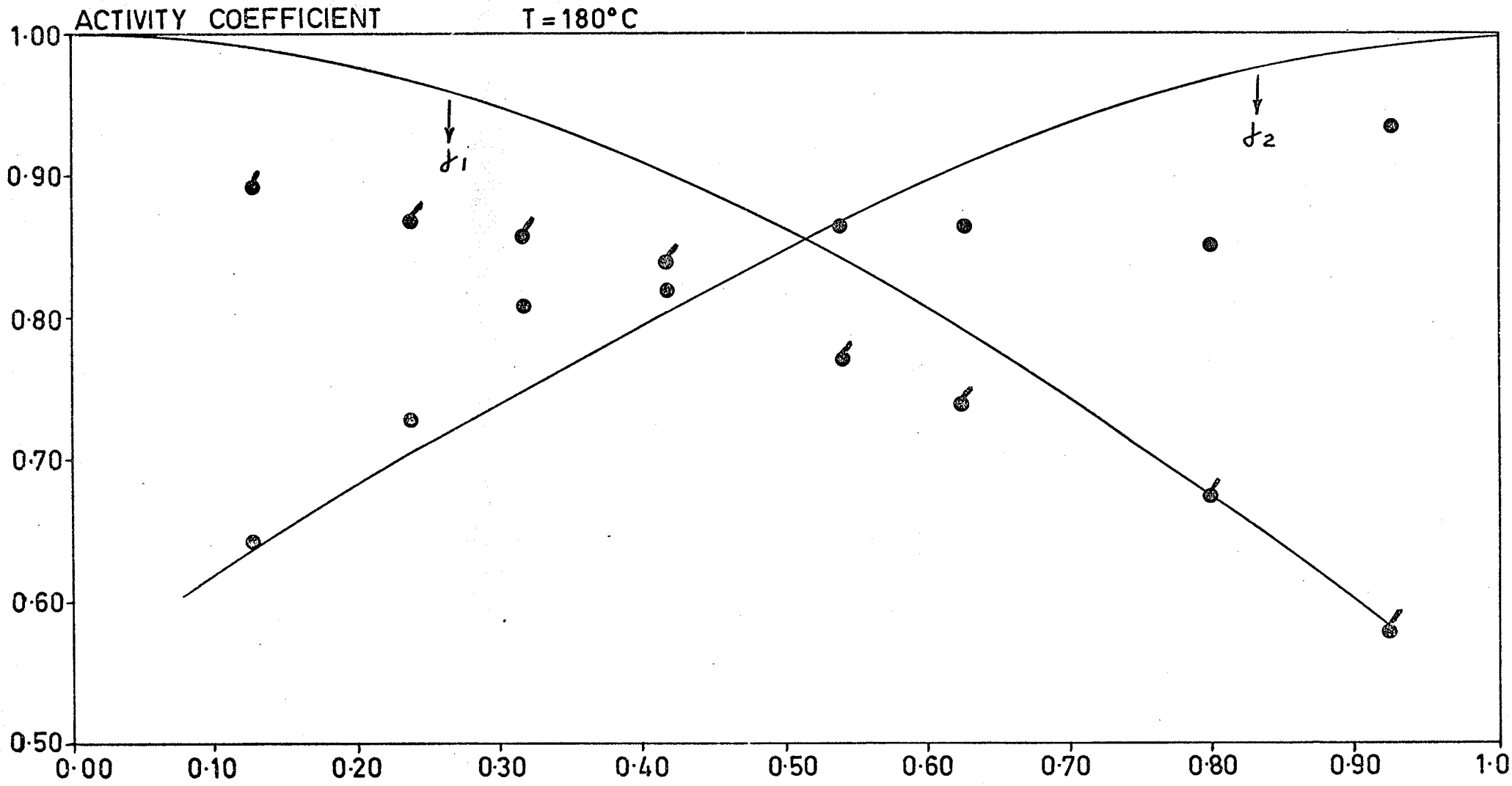
ACTIVITY COEFFICIENT
T = 180°C
1·00
0·90
0·80
0·70
0·60
0·50
γ1
γ2
0·00
0·10
0·20
0·30
0·40
0·50
0·60
0·70
0·80
0·90
1·00
MOLE FRACTION ACETONE IN LIQUID PHASE.

V (B) (2) The System Carbon Tetrachloride (1) - Acetone (2)

The plot of T_M, the temperature of disappearance of the meniscus, versus mole percent acetone (Figure X) for this system shows a slight deviation from ideality, but the vapor pressure plots show no maximum or minimum. The vapor-liquid equilibrium composition curves at the different isotherms, Figures XVII to XXI, do not show the existence of an azeotrope. Brown and Smith (92) who studied the vapor-liquid equilibria of the system Carbon tetrachloride - Acetone at 45°C, claimed the existence of an azeotrope at a mole fraction of acetone of 0.964 and a pressure of 513.2 mm. Hg. In the present research the vapor was found to be always richer in acetone; at no point was the liquid richer in acetone, that is, there was no reversal of composition as there would be in passing through an azeotropic point. I therefore conclude that the system Carbon tetrachloride - Acetone exhibits limited azeotropy.

Thermodynamic analysis for this system was carried out in two parts, as mentioned in section V (A). Data reductions for the isotherms at 150° and 200°C were carried out using a one parameter model for the excess Gibbs energy with $\eta_2(1) = 0$. For this purpose the program SYMFIT and the subroutines VOLPAR, PHIMIX and CUBEQN were used. The results of the thermodynamic analysis are given in Table XIV.

Table XIV shows that $\gamma_i \rightarrow 1$ as $x_i \rightarrow 1$ for the system Carbon tetrachloride - Acetone at the temperatures investigated in this project. Figures XXXII and XXXIIA give the plots of the activity coefficients as a function of the mole fraction acetone in the liquid phase. The differences between the experimental values for the activity

coefficients and the calculated values are small in magnitude, in other words, this system responds better to the solution model of Prausnitz et al (50). This system is nearly ideal at 150°C - the activity coefficients are very nearly equal to one, but at 200°C the deviations from ideality are larger. The deviations are positive at 150°C and negative at 200°C.

TABLE XIV

THERMODYNAMIC ANALYSIS OF THE SYSTEM CCl_4 (1) - ACETONE (2) AT 150°C

Correction to Geometric mean $K_{12} = 0.01$, $2\tau_{12}/(T_{C_1} + T_{C_2}) = -0.033$, $2\nu_{12}/(V_{C_1} + V_{C_2}) = -0.124$

Temperature = 150.0°C, Reference Fugacity (1) = 6.07 atm., Reference Fugacity (2) = 10.14 atm.

x_2	y_2	Vol. fraction of component 2 in the liquid phase	p(atm)	$\bar{V}_1^L$(cc/mole)	$\bar{V}_2^L$(cc/mole)	Poynting Correction for γ_1	Poynting Correction for γ_2	$\gamma_1^{(PO)}$(exp)	$\gamma_2^{(PO)}$(exp)	ϕ_1	ϕ_2
0.249	0.372	0.206	8.67	121.0	98.4	1.030	1.024	0.99	1.11	0.872	0.892
0.341	0.476	0.288	9.28	121.3	97.9	1.033	1.026	1.01	1.09	0.865	0.883
0.468	0.581	0.407	9.92	122.0	97.3	1.035	1.028	1.06	1.03	0.857	0.874
0.520	0.631	0.458	10.28	122.4	97.1	1.036	1.029	1.07	1.03	0.853	0.869
0.582	0.692	0.521	10.42	122.9	96.9	1.037	1.029	1.03	1.02	0.852	0.866
0.720	0.806	0.668	10.94	124.6	96.7	1.040	1.031	1.01	1.00	0.847	0.859
0.867	0.906	0.836	11.26	127.0	96.9	1.042	1.031	1.06	0.96	0.846	0.854

α_{12}, interaction constant of molecules (1) and (2) = -0.0087 mole/cc.

x_2	(exp) $\ln\gamma_1^{(PO)}$	(calc) $\ln\gamma_1^{(PO)}$	(exp) $\ln\gamma_1^{(PO)}$ - (calc) $\ln\gamma_1^{(PO)}$	(exp) $\ln\gamma_2^{(PO)}$	(calc) $\ln\gamma_2^{(PO)}$	(exp) $\ln\gamma_2^{(PO)}$ - (calc) $\ln\gamma_2^{(PO)}$	(calc) $\gamma_1^{(PO)}$	(exp) $\gamma_1^{(PO)}$ - (calc) $\gamma_1^{(PO)}$	(calc) $\gamma_2^{(PO)}$	(exp) $\gamma_2^{(PO)}$ - (calc) $\gamma_2^{(PO)}$
0.249	-0.009	0.008	-0.017	0.104	0.086	0.018	1.00	-0.01	1.09	0.02
0.341	0.009	0.009	-0.000	0.086	0.067	0.018	1.00	0.01	1.06	0.03
0.468	0.058	0.010	0.048	0.029	0.029	-0.000	1.00	0.06	1.03	0.00
0.520	0.067	0.009	0.057	0.039	0.029	0.009	1.01	0.05	1.02	0.01
0.582	0.039	0.019	0.019	0.029	0.019	0.009	1.01	0.02	1.02	0.00
0.720	0.019	0.029	-0.009	0.009	0.009	0.000	1.02	-0.01	1.00	0.00
0.867	0.058	0.029	0.028	-0.039	0.007	-0.047	1.03	0.03	1.00	-0.05

Average deviation in $\gamma_1^{(PO)}$ = 0.026 Average deviation in $\gamma_2^{(PO)}$ = 0.019

Average deviation in $\ln\gamma_1^{(PO)}$ = 0.026 Average deviation in $\ln\gamma_2^{(PO)}$ = 0.014

TABLE XIV(Cont'd)

THERMODYNAMIC ANALYSIS OF THE SYSTEM CCl_4 (1) - ACETONE (2) AT 200°C

Correction to Geometric mean $K_{12} = 0.01$, $2\tau_{12}/(T_{C_1} + T_{C_2}) = -0.033$, $2\nu_{12}/(V_{C_1} + V_{C_2}) = -0.124$

Temperature = 200.0°C, Reference Fugacity (1) = 14.24 atm., Reference Fugacity (2) = 19.60 atm.

x_2	y_2	Vol. fraction of component 2 in the liquid phase	p(atm)	$\bar{V}_1^L$(cc/mole)	$\bar{V}_2^L$(cc/mole)	Poynting Correction for γ_1	Poynting Correction for γ_2	$\gamma_1^{(PO)}$(exp)	$\gamma_2^{(PO)}$(exp)	ϕ_1	ϕ_2
0.249	0.272	0.206	19.20	137.6	115.4	1.070	1.058	0.969	0.841	0.793	0.832
0.341	0.384	0.288	20.35	138.3	114.5	1.075	1.061	0.972	0.901	0.782	0.818
0.468	0.521	0.407	22.46	139.9	113.6	1.084	1.068	0.998	0.951	0.762	0.796
0.520	0.584	0.458	22.65	140.8	113.3	1.085	1.068	0.968	0.963	0.762	0.792
0.582	0.647	0.521	23.26	142.1	113.1	1.088	1.070	0.960	0.968	0.758	0.785
0.867	0.904	0.836	26.60	152.1	112.8	1.109	1.081	0.892	0.983	0.734	0.751

α_{12}, interaction constant of molecules (1) and (2) = -0.00187 mole/cc.

x_2	(exp) $\ln\gamma_1^{(PO)}$	(calc) $\ln\gamma_1^{(PO)}$	(exp) $\ln\gamma_1^{(PO)}$ - (calc) $\ln\gamma_1^{(PO)}$	(exp) $\ln\gamma_2^{(PO)}$	(calc) $\ln\gamma_2^{(PO)}$	(exp) $\ln\gamma_2^{(PO)}$ - (calc) $\ln\gamma_2^{(PO)}$	(calc) $\gamma_1^{(PO)}$	(exp)(calc) $\gamma_1^{(PO)} - \gamma_1^{(PO)}$	(calc) $\gamma_2^{(PO)}$	(exp) $\gamma_2^{(PO)}$ - (calc) $\gamma_2^{(PO)}$
0.249	-0.031	-0.020	-0.011	-0.173	-0.096	-0.086	0.980	-0.011	0.905	-0.056
0.341	-0.028	-0.032	0.004	-0.104	-0.075	-0.028	0.968	0.003	0.926	-0.025
0.468	-0.002	-0.049	0.047	-0.050	-0.046	-0.004	0.952	0.046	0.954	-0.003
0.520	-0.032	-0.064	0.031	-0.037	-0.035	-0.002	0.938	0.029	0.965	-0.001
0.582	-0.040	-0.068	0.027	-0.032	-0.028	-0.004	0.934	0.025	0.972	-0.003
0.867	-0.114	-0.137	0.022	-0.016	-0.009	-0.007	0.872	0.020	0.994	-0.007

Average deviation in $\gamma_1^{(PO)}$ = 0.022 Average deviation in $\gamma_2^{(PO)}$ = 0.015

Average deviation in $\ln\gamma_1^{(PO)}$ = 0.024 Average deviation in $\ln\gamma_2^{(PO)}$ = 0.019

FIGURE XXXII. Activity Coefficients versus Mole Fraction Acetone in Liquid Phase for the System Carbon Tetrachloride-Acetone at 150°C.

(For Figures XXXII and XXXIIA:

the solid line represents the calculated curve.

● represents experimental γ_2 values.

◐ represents experimental γ_1 values.)

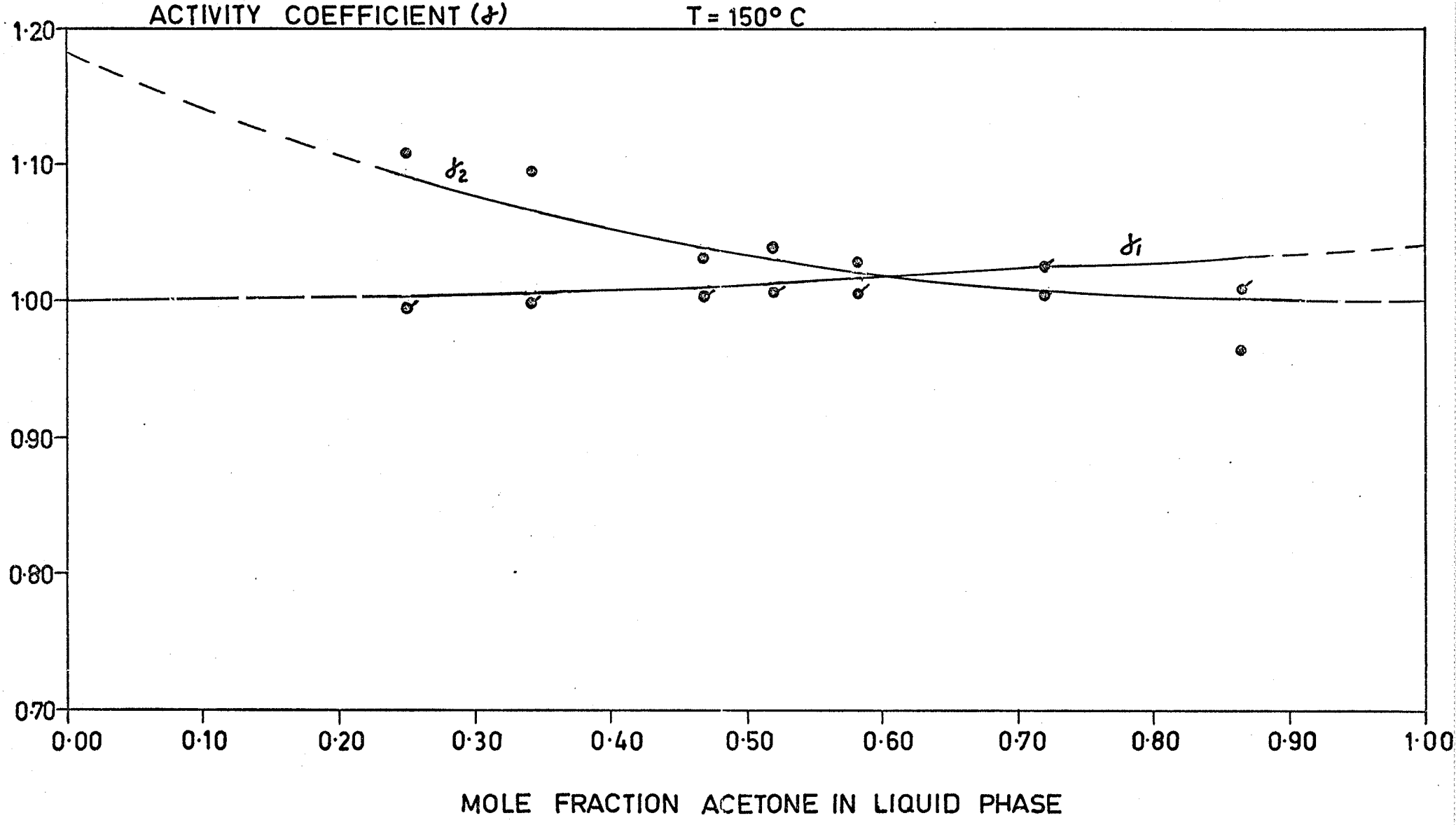
ACTIVITY COEFFICIENT (γ)
T = 150° C
1·20
1·10
1·00
0·90
0·80
0·70
γ2
γ1
0·00
0·10
0·20
0·30
0·40
0·50
0·60
0·70
0·80
0·90
1·00
MOLE FRACTION ACETONE IN LIQUID PHASE

FIGURE XXXIIA. Activity Coefficients versus Mole Fraction Acetone in Liquid Phase for the System Carbon Tetrachloride-Acetone at 200°C.

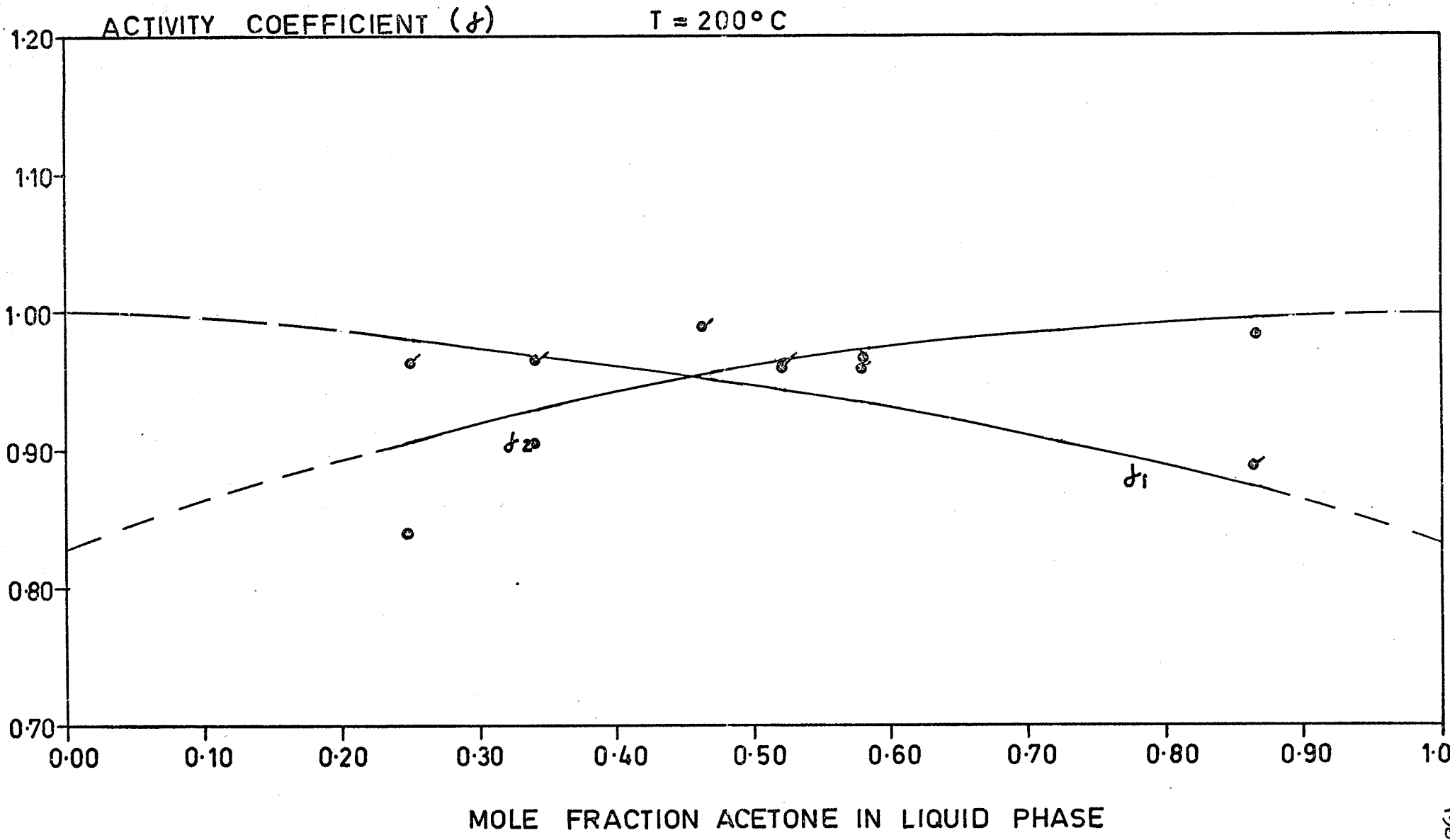
ACTIVITY COEFFICIENT (γ)
T = 200° C
1·20
1·10
1·00
0·90
0·80
0·70
γ2
γ1
0·00
0·10
0·20
0·30
0·40
0·50
0·60
0·70
0·80
0·90
1·00
MOLE FRACTION ACETONE IN LIQUID PHASE

Data reductions for the system at 250° and 270°C were carried out using a two parameter dilated van Laar model for the excess Gibbs energy and the unsymmetric convention of normaliztion for activity coefficients. In this case the program HENRYS and the subroutines VOLPAR, PHIMIX and CUBEQN were used to calculate the standard state fugacity for component 2, $H_{2(1)}^{(PO)}$. As can be seen from Table XV , the program calculates $f_2^{(P)}/x_2$ for each point and, by extrapolating the plot of ln $f_2^{(P)}/x_2$ versus x_2 (Figure XXXIII) to $x_2 = 0$, Henry's constant of 2 in 1, $H_{2(1)}^{(PO)}$ is obtained. The HENRYS program (Table XV) also prints out x_2, y_2, P, $\bar{V}_1^L$, $\bar{V}_2^L$, ϕ_1 and ϕ_2, the saturation pressure of component 1, liquid partial molal volumes of both components at infinite dilution, the reference fugacity of component 1 at zero pressure, molal volumes of the saturated liquid mixture for each concentration and the corrected reduced temperatures of the liquid mixture for each concentration. This information is then used in the program FITTING to evaluate the self-interaction constant, $\alpha_{22(1)}$, and the dilation constant $\eta_2(1)$ in the dilated van Laar model. Table XV gives the results of the analysis.

TABLE XV

THERMODYNAMIC ANALYSIS OF THE SYSTEM CARBON TETRACHLORIDE (1) - ACETONE (2) AT 250°C

Temperature = 250.0°C, Reference Fugacity (1) = 25.75 atm., Saturation Pressure (1) = 29.49 atm.

Liquid Partial Molal Volume (1) at infinite dilution = 172.53 cc/mole, $\bar{V}_2^{\infty}$ = 167.22 cc/mole

T(°C)	$\frac{f_2}{x_2}$(atm)	Saturation Pressure of 1 (atm)	x_2	y_2	P (atm)	Molal Volume of saturated liquid Mix. cc/mole	ϕ_1	ϕ_2	$\bar{V}_1^L$ (cc/mole)	$\bar{V}_2^L$ (cc/mole)	Corrected T_R of Liq. mixture
250.0	32.45	1.933	0.062	0.079	31.42	173.23	0.7455	0.8107	173.58	167.95	0.9756
250.0	32.69	3.953	0.1500	0.185	33.44	175.24	0.7298	0.7925	176.09	170.44	0.9817
250.0	31.82	4.943	0.249	0.295	34.43	180.82	0.7234	0.7802	181.65	178.32	0.9891
250.0			0.341	0.386	35.44	T_R EXCEED 1.0, NO LIQUID PHASE					1.0023
250.0			0.468	0.495	37.22	T_R EXCEED 1.0, NO LIQUID PHASE					1.0117

Henry's constant at the saturation pressure of solvent determined graphically from above data = 32.46 atm.

x_2	y_2	Vol.fraction of component 2 in the liquid phase	p(atm)	$\bar{V}_1^L$(cc/mole)	$\bar{V}_2^L$(cc/mole)	Poynting Correction for γ_1	Poynting Correction for γ_2	$\gamma_1^{(PO)}$(exp)	$\gamma_2^{(PO)}$(exp)	ϕ_1	ϕ_2
0.062	0.079	0.0492	31.42	173.59	167.95	1.1355	1.1309	0.7864	0.9919	0.7455	0.8107
0.150	0.185	0.1214	33.44	176.09	170.44	1.1471	1.1420	0.7921	0.9891	0.7298	0.7925
0.249	0.295	0.2061	34.43	181.65	178.32	1.1569	1.1538	0.7847	0.9533	0.7234	0.7802

$\alpha_{22(1)}$, self-interaction constant of molecules 2 in the environment of molecules 1 = -0.001788 mole/cc.

$\eta_{2(1)}$, dilation constant of solute 2 in solvent 1 = 1.2868.

Henry's constant at zero pressure = 28.98 atmospheres.

TABLE XV (Cont'd)

THERMODYNAMIC ANALYSIS OF THE SYSTEM CARBON TETRACHLORIDE (1) - ACETONE (2) at 250°C

Temperature = 250.0°C, Reference Fugacity (1) = 25.75 atm., Saturation Pressure (1) = 29.49 atm.

Liquid Partial Molal Volume (1) at infinite dilution = 172.53 cc/mole, $\bar{V}_2^{\infty}$ = 167.22 cc/mole

x_2	(exp) $\ln\gamma_1^{(PO)}$	(calc) $\ln\gamma_1^{(PO)}$	(exp) $\ln\gamma_1^{(PO)} - \ln\gamma_1^{(PO)}$	(calc)	(exp) $\ln\gamma_2^{(PO)}$	(calc) $\ln\gamma_2^{(PO)}$	(exp) $\ln\gamma_2^{(PO)} - \ln\gamma_2^{(PO)}$	(calc)	(calc) $\gamma_1^{(PO)}$	(exp) $\gamma_1^{(PO)} - \gamma_1^{(PO)}$	(calc)	(calc) $\gamma_2^{(PO)}$	(exp) $\gamma_2^{(PO)} - \gamma_2^{(PO)}$	(calc)
0.062	-0.2408	-0.1188	-0.1220		-0.0083	-0.0274	0.0191		0.8876	-0.1012		0.9726	+0.0193	
0.150	-0.2332	-0.1370	-0.0962		-0.0111	-0.0202	0.0091		0.8721	-0.1200		0.9801	+0.0090	
0.249	-0.2421	-0.1732	-0.0689		-0.0481	-0.0141	-0.0340		0.8412	-0.0565		0.9856	-0.0323	

Average deviation in $\gamma_1^{(PO)}$ = 0.0926 No. of γ_1 data = 3.0

Average deviation in $\gamma_2^{(PO)}$ = 0.0202 No. of γ_2 data = 3.0

THERMODYNAMIC ANALYSIS OF THE SYSTEM CARBON TETRACHLORIDE (1) - ACETONE (2) AT 270°C

Temperature = 270.0°C, Reference Fugacity (1) = 34.25 atm., Saturation Pressure (1) = 38.16 atm.

Liquid partial molal volume (1) at infinite dilution = 192.24 cc/mole, $\bar{V}_2^{\infty}$ = 184.93 cc/mole

T(°C)	$\frac{f_2}{x_2}$(atm)	Saturation Pressure of 1(atm)	x_2	y_2	P (atm)	Molal Volume of saturated liquid mix. cc/mole	ϕ_1	ϕ_2	$\bar{V}_1^L$ (cc/mole)	$\bar{V}_2^L$ (cc/mole)	Corrected T_R of Liq. mixture
270.0	33.71	4.857	0.062	0.076	40.51	192.97	0.7135	0.7936	193.17	185.82	0.9816
270.0	33.90	5.926	0.150	0.175	42.25	194.02	0.7082	0.7694	194.86	187.18	0.9939
270.0			0.249	0.261	43.52	T_R EXCEED 1.0, NO LIQUID PHASE					0.10015

Henry's constant at the saturation pressure of solvent determined graphically from above data = 33.95 atm.

The above data were not fitted to a least squares fitting, that is, the program FITTING was not used in this case, because I thought that there were not enough data points.

FIGURE XXXIII. Plot of Henry's Constant $H^{ps}_{2(1)}$.

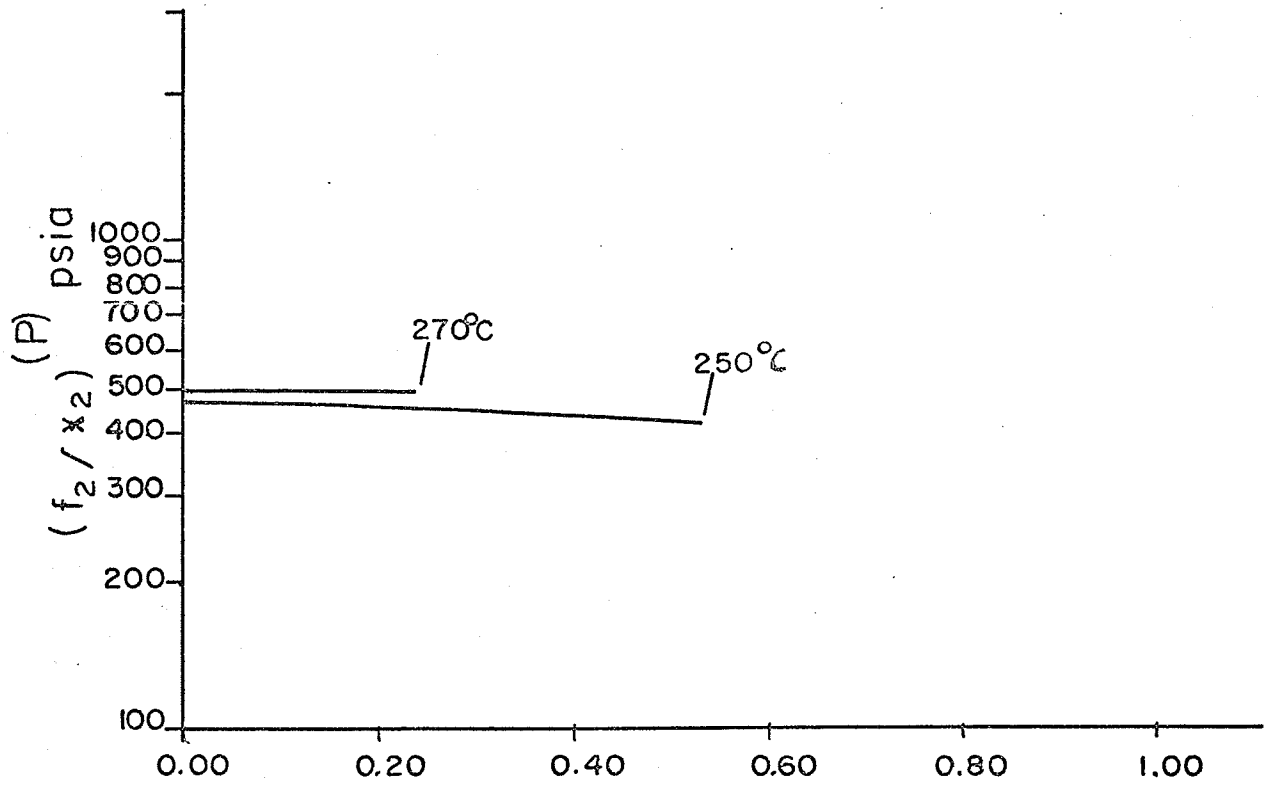
(P) psia
(f_2 / x_2)
1000
900
800
700
600
500
400
300
200
100
270°C
250°C
0.00
0.20
0.40
0.60
0.80
1.00
MOLE FRACTION ACETONE

V (B) (3) The System Benzene (1) - Carbon Tetrachloride (2)

The plot of T_M, the temperature of the disappearance of the meniscus versus composition (Figure XI) for this system deviates very slightly from the straight line joining the critical temperatures of the pure components. The vapor-liquid equilibrium composition curves, Figures XXII to XXVII, do not indicate the existence of an azeotrope- the vapor is always richer in carbon tetrachloride.

Due to the fact that the volatilites of the two pure components, benzene and carbon tetrachloride, are very similar no η, dilation constant is required and the binary system can be treated using a one parameter model for the excess Gibbs energy. Therefore, data reduction for this binary system was carried out using the symmetric convention of normalization for activity coefficients. The program SYMFIT and the subroutines VOLPAR, PHIMIX and CUBEQN were used for this purpose. The thermodynamic analysis of this system at temperatures of 150^{o}, 200^{o}, 250^{o} and 270^{o}C are given in Table XVI.

The deviations of the activity coefficients from one are not great but they are large enough that I cannot conclude that the system Benzene-Carbon tetrachloride is an ideal one. On the other hand, this system consisting of two non-polar components is the ideal one to test the solution model of Prausnitz et al (50). Table XVI shows that the deviations between the experimental values of the activity coefficients and the calculated values are quite small in magnitude which indicates that the solution model of Prausnitz et al (50) is applicable in this case. The activity coefficients have been plotted as a function of the mole fraction carbon tetrachloride in the liquid phase in Figure XXXIV to Figure XXXVII.

TABLE XVI

THERMODYNAMIC ANALYSIS OF THE SYSTEM C_6H_6 (1) - CCl_4 (2) AT 150°C

Correction to Geometric mean $K_{12} = 0.010$, $2\tau_{12}/(T_{C_1} + T_{C_2}) = -0.003$, $2\nu_{12}/(V_{C_1} + V_{C_2}) = -0.040$

Temperature = 150.0°C, Reference Fugacity (1) = 5.10 atm., Reference Fugacity (2) = 6.07 atm.

x_2	y_2	Vol.fraction of component 2 in the liquid phase	p(atm)	$\bar{V}_1^L$(cc/mole)	$\bar{V}_2^L$(cc/mole)	Poynting Correction for γ_1	Poynting Correction for γ_2	$\gamma_1^{(PO)}$(exp)	$\gamma_2^{(PO)}$(exp)	ϕ_1	ϕ_2
0.050	0.052	0.053	5.72	106.9	131.9	1.017	1.022	0.998	0.873	0.907	0.918
0.103	0.105	0.110	5.77	106.4	131.0	1.017	1.022	1.006	0.869	0.907	0.917
0.165	0.170	0.176	5.79	105.9	130.0	1.017	1.021	1.005	0.870	0.906	0.916
0.244	0.250	0.258	5.83	105.3	128.7	1.017	1.021	1.010	0.882	0.906	0.915
0.326	0.342	0.343	5.86	104.7	127.5	1.017	1.021	0.998	0.907	0.905	0.914
0.382	0.401	0.400	5.90	104.4	126.8	1.017	1.021	0.997	0.912	0.905	0.913
0.520	0.594	0.539	5.94	103.7	125.1	1.017	1.021	0.976	0.998	0.905	0.912
0.621	0.661	0.639	5.94	103.3	124.0	1.007	1.021	0.953	0.948	0.917	0.912

α_{12}, interaction constant of molecules (1) and (2) = -0.0022 mole/cc.

x_2	(exp) $\ln\gamma_1^{(PO)}$	(calc) $\ln\gamma_1^{(PO)}$	(exp) $\ln\gamma_1^{(PO)}$ - (calc) $\ln\gamma_1^{(PO)}$	(exp) $\ln\gamma_2^{(PO)}$	(calc) $\ln\gamma_2^{(PO)}$	(exp) $\ln\gamma_2^{(PO)}$ - (calc) $\ln\gamma_2^{(PO)}$	(calc) $\gamma_1^{(PO)}$	(exp) $\gamma_1^{(PO)}$ - (calc) $\gamma_1^{(PO)}$	(calc) $\gamma_2^{(PO)}$	(exp) $\gamma_2^{(PO)}$ - (calc) $\gamma_2^{(PO)}$
0.050	-0.001	-0.003	0.002	-0.135	-0.180	0.044	0.998	0.000	0.835	0.038
0.103	0.009	-0.004	0.013	-0.140	-0.163	0.023	0.996	0.010	0.849	0.020
0.165	0.009	-0.005	0.014	-0.138	-0.143	0.005	0.994	0.010	0.866	0.004
0.244	0.009	-0.011	0.020	-0.125	-0.123	-0.002	0.989	0.020	0.884	0.003
0.326	-0.001	-0.017	0.016	-0.097	-0.097	0.000	0.983	0.015	0.907	-0.000
0.382	-0.003	-0.022	0.019	-0.092	-0.085	-0.006	0.978	0.019	0.918	-0.005
0.520	-0.023	-0.036	0.013	-0.002	-0.055	0.053	0.963	0.013	0.946	0.051
0.621	-0.048	-0.051	0.004	-0.052	-0.035	-0.016	0.950	0.003	0.965	-0.016

Average deviation in $\gamma_1^{(PO)}$ = 0.011 Average deviation in $\gamma_2^{(PO)}$ = 0.017

Average deviation in $\ln\gamma_1^{(PO)}$ = 0.013 Average deviation in $\ln\gamma_2^{(PO)}$ = 0.019

TABLE XVI (Cont'd)

THERMODYNAMIC ANALYSIS OF THE SYSTEM C_6H_6 (1) - CCl_4 (2) AT 200°C

Correction to Geometric mean $K_{12} = 0.010$, $2\tau_{12}/(T_{C_1} + T_{C_2}) = -0.003$, $2\nu_{12}/(V_{C_1} + V_{C_2}) = -0.040$

Temperature = 200.0°C, Reference Fugacity (1) = 11.62 atm., Reference Fugacity (2) = 14.24 atm.

x_2	y_2	Vol. fraction of component 2 in the liquid phase	p(atm)	$\bar{V}_1^L$(cc/mole)	$\bar{V}_2^L$(cc/mole)	Poynting Correction for γ_1	Poynting Correction for γ_2	$\gamma_1^{(PO)}$(exp)	$\gamma_2^{(PO)}$(exp)	ϕ_1	ϕ_2
0.103	0.104	0.110	14.12	118.3	151.8	1.044	1.056	0.973	0.807	0.832	0.852
0.165	0.168	0.176	14.20	117.5	150.3	1.043	1.056	0.971	0.817	0.832	0.850
0.244	0.248	0.258	14.23	116.6	148.5	1.043	1.056	0.971	0.817	0.832	0.849
0.326	0.332	0.343	14.29	115.9	146.8	1.043	1.055	0.972	0.821	0.832	0.848
0.520	0.582	0.539	14.34	114.5	143.2	1.043	1.054	0.858	0.903	0.833	0.845
0.621	0.684	0.639	14.40	114.1	141.6	1.043	1.053	0.825	0.892	0.833	0.844

α_{12}, interaction constant of molecules (1) and (2) = -0.00201 mole/cc.

x_2	(exp) $\ln\gamma_1^{(PO)}$	(calc) $\ln\gamma_1^{(PO)}$	(exp) $-$ (calc) $\ln\gamma_1^{(PO)}$	(exp) $\ln\gamma_2^{(PO)}$	(calc) $\ln\gamma_2^{(PO)}$	(exp) $-$ (calc) $\ln\gamma_2^{(PO)}$	(calc) $\gamma_1^{(PO)}$	(exp) $-$ (calc) $\gamma_1^{(PO)}$	(calc) $\gamma_2^{(PO)}$	(exp) $-$ (calc) $\gamma_2^{(PO)}$
0.103	-0.027	-0.006	-0.021	-0.213	-0.274	0.061	0.993	-0.020	0.760	0.047
0.165	-0.028	-0.015	-0.012	-0.200	-0.240	0.040	0.984	-0.012	0.786	0.031
0.244	-0.028	-0.034	0.006	-0.200	-0.202	0.001	0.966	0.005	0.816	0.000
0.326	-0.028	-0.060	0.031	-0.197	-0.167	-0.030	0.941	0.030	0.845	-0.024
0.520	-0.151	-0.112	-0.039	-0.100	-0.103	0.002	0.894	-0.035	0.902	0.001
0.621	-0.191	-0.155	-0.035	-0.114	-0.067	-0.047	0.856	-0.030	0.935	-0.042

Average deviation in $\gamma_1^{(PO)}$ = 0.022 Average deviation in $\gamma_2^{(PO)}$ = 0.024

Average deviation in ln $\gamma_1^{(PO)}$ = 0.024 Average deviation in ln $\gamma_2^{(PO)}$ = 0.030

TABLE XVI (Cont'd)

THERMODYNAMIC ANALYSIS OF THE SYSTEM C_6H_6 (1) - CCl_4 (2) AT 250°C

Correction to Geometric mean $K_{12} = 0.010$, $2\tau_{12}/(T_{C_1} + T_{C_2}) = -0.003$, $2\nu_{12}/(V_{C_1} + V_{C_2}) = -0.040$

Temperature = 250.0°C, Reference Fugacity (1) = 19.89 atm., Reference Fugacity (2) = 21.23 atm.

x_2	y_2	Vol.Fraction of component 2 in the liquid phase	p(atm)	$\bar{V}_1^L$(cc/mole)	$\bar{V}_2^L$(-c/mole)	Poynting Correction for γ_1	Poynting Correction for γ_2	$\gamma_1^{(PO)}$(exp)	$\gamma_2^{(PO)}$(exp)	ϕ	ϕ
0.103	0.104	0.110	29.30	137.7	193.2	1.098	1.141	0.992	0.944	0.741	0.773
0.165	0.166	0.176	29.40	136.4	190.9	1.097	1.139	0.995	0.942	0.740	0.771
0.244	0.246	0.258	29.42	134.9	188.1	1.096	1.137	0.996	0.943	0.740	0.769
0.326	0.329	0.343	29.44	133.6	185.5	1.096	1.135	0.996	0.945	0.741	0.767
0.382	0.392	0.400	29.45	132.9	183.8	1.095	1.134	0.986	0.961	0.741	0.766
0.520	0.548	0.539	29.46	131.5	180.0	1.094	1.131	0.947	0.987	0.743	0.764
0.621	0.656	0.639	29.49	131.0	177.8	1.094	1.129	0.916	0.990	0.744	0.762
0.820	0.861	0.831	29.49	131.1	174.3	1.094	1.127	0.783	0.985	0.748	0.761

α_{12}, interaction constant of molecules (1) and (2) = -0.00135 mole/cc.

x_2	(exp) $\ln\gamma_1^{(PO)}$	(calc) $\ln\gamma_1^{(PO)}$	(exp) $\ln\gamma_1^{(PO)}$ - $\ln\gamma_1^{(PO)}$	(calc)	(exp) $\ln\gamma_2^{(PO)}$	(calc) $\ln\gamma_2^{(PO)}$	(exp) $\ln\gamma_2^{(PO)}$ - $\ln\gamma_2^{(PO)}$	(calc)	(calc) $\gamma_1^{(PO)}$	(exp) $\gamma_1^{(PO)}$ - $\gamma_1^{(PO)}$	(calc)	(calc) $\gamma_2^{(PO)}$	(exp) $\gamma_2^{(PO)}$ - $\gamma_2^{(PO)}$	(calc)
0.103	-0.007	-0.004	-0.002		-0.056	-0.087	0.031		0.995	-0.002		0.916	0.028	
0.165	-0.004	-0.011	0.006		-0.058	-0.077	0.018		0.989	0.006		0.925	0.017	
0.244	-0.003	-0.024	0.020		-0.058	-0.057	-0.001		0.976	0.020		0.943	-0.000	
0.326	-0.003	-0.042	0.038		-0.055	-0.045	-0.010		0.958	0.038		0.956	-0.010	
0.382	-0.013	-0.057	0.043		-0.038	-0.034	-0.004		0.944	0.042		0.966	-0.004	
0.520	-0.053	-0.104	0.050		-0.013	-0.020	0.007		0.901	0.046		0.980	0.007	
0.621	-0.087	-0.146	0.058		-0.010	-0.009	-0.001		0.863	0.052		0.991	-0.000	
0.820	-0.244	-0.247	0.003		-0.015	-0.005	-0.010		0.780	0.002		0.995	-0.010	

Average deviation in $\gamma_1^{(PO)}$ = 0.028 Average deviation in $\gamma_2^{(PO)}$ = 0.010

Average deviation in $\ln\gamma_1^{(PO)}$ = 0.031 Average deviation in $\ln\gamma_2^{(PO)}$ = 0.010

TABLE XVI (Cont'd)

THERMODYNAMIC ANALYSIS OF THE SYSTEM C_6H_6 (1) - CCl_4 (2) AT 270°C

Correction to Geometric mean $K_{12} = 0.010$, $2\tau_{12}/(T_{C_1} + T_{C_2}) = -0.003$, $2\nu_{12}/(V_{C_1} + V_{C_2}) = -0.040$

Temperature = 270.0°C, Reference Fugacity (1) = 23.96 atm., Reference Fugacity (2) = 25.94 atm.

x_2	y_2	Vol. fraction of component 2 in the liquid phase	p(atm)	$\bar{V}_1^L$(cc/mole)	$\bar{V}_2^L$(cc/mole)	Poynting Correction for γ_1	Poynting Correction for γ_2	$\gamma_1^{(PO)}$(exp)	$\gamma_2^{(PO)}$(exp)	ϕ_1	ϕ_2
0.103	0.104	0.110	38.04	152.6	240.6	1.139	1.228	0.971	0.891	0.698	0.739
0.165	0.166	0.176	38.07	150.5	239.4	1.137	1.227	0.974	0.886	0.698	0.736
0.244	0.245	0.258	38.10	147.9	238.5	1.134	1.226	0.977	0.882	0.698	0.734
0.326	0.328	0.343	38.12	145.2	236.9	1.132	1.226	0.979	0.882	0.699	0.731
0.382	0.390	0.400	38.13	143.2	238.9	1.130	1.226	0.972	0.893	0.700	0.730
0.520	0.538	0.539	38.14	137.0	244.0	1.124	1.232	0.956	0.897	0.702	0.727
0.621	0.647	0.639	38.16	124.6	260.3	1.112	1.249	0.938	0.890	0.704	0.725
0.820	0.867	0.831	38.17	124.6	260.3	1.112	1.249	0.749	0.901	0.709	0.724

α_{12}, interaction constant of molecules (1) and (2) = -0.00124 mole/cc.

x_2	(exp) $\ln\gamma_1^{(PO)}$	(calc) $\ln\gamma_1^{(PO)}$	(exp) $\ln\gamma_1^{(PO)}$	(calc) $\ln\gamma_1^{(PO)}$	(exp) $\ln\gamma_2^{(PO)}$	(calc) $\ln\gamma_2^{(PO)}$	(exp) $\ln\gamma_2^{(PO)}$	(calc) $\ln\gamma_2^{(PO)}$	(calc) $\gamma_1^{(PO)}$	(exp) $\gamma_1^{(PO)}$	(calc) $\gamma_1^{(PO)}$	(calc) $\gamma_2^{(PO)}$	(exp) $\gamma_2^{(PO)}$	(calc) $\gamma_2^{(PO)}$
0.103	-0.028	-0.003	-0.024	-0.115	-0.171	0.056	0.996	-0.024	0.842	0.059				
0.165	-0.026	-0.009	-0.016	-0.119	-0.148	0.028	0.990	-0.016	0.862	0.024				
0.244	-0.022	-0.021	-0.001	-0.124	-0.119	-0.004	0.978	-0.001	0.887	-0.004				
0.326	-0.020	-0.037	0.016	-0.124	-0.096	-0.027	0.963	0.016	0.908	-0.026				
0.382	-0.028	-0.051	0.023	-0.113	-0.082	-0.030	0.950	0.022	0.920	-0.027				
0.520	-0.044	-0.092	0.048	-0.107	-0.053	-0.054	0.911	0.045	0.948	-0.050				
0.621	-0.063	-0.130	0.066	-0.116	-0.035	-0.081	0.878	0.060	0.965	-0.075				
0.820	-0.288	-0.231	-0.056	-0.103	-0.011	-0.092	0.793	-0.043	0.989	-0.088				

Average deviation in $\gamma_1^{(PO)}$ = 0.028 Average deviation in $\gamma_2^{(PO)}$ = 0.044

Average deviation in $\ln\gamma_1^{(PO)}$ = 0.035 Average deviation in $\ln\gamma_2^{(PO)}$ = 0.046

FIGURE XXXIV. Activity Coefficients versus Mole Fraction Carbon Tetrachloride in Liquid Phase for the System Benzene-Carbon Tetrachloride at 150°C.

(For Figures XXXIV to XXXVII:

the solid line represents the calculated curve.

● represents experimental γ_2 values.

● represents experimental γ_1 values.)

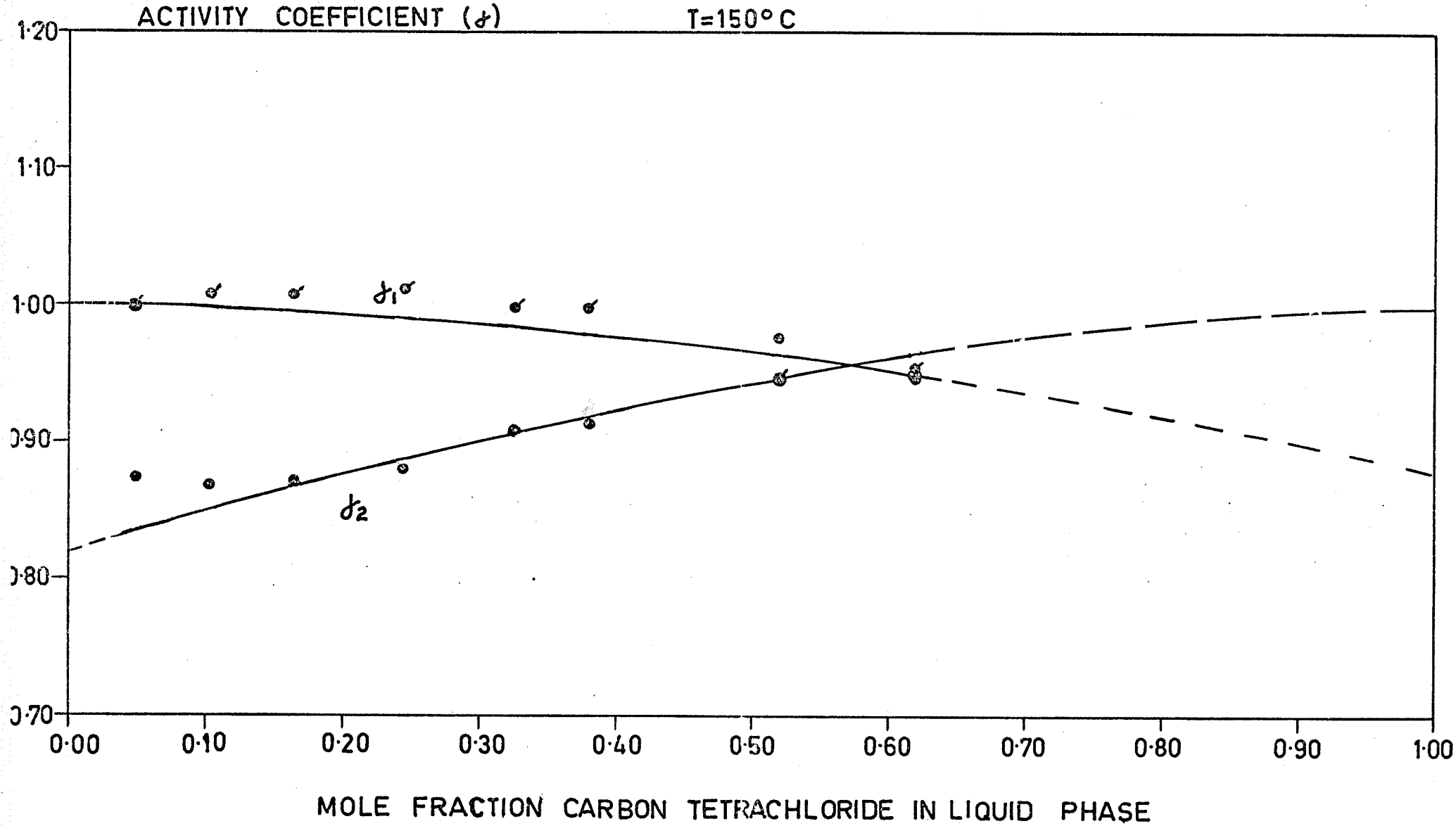
ACTIVITY COEFFICIENT (γ)
T=150° C
1·20
1·10
1·00
0·90
0·80
0·70
γ1
γ2
0·00
0·10
0·20
0·30
0·40
0·50
0·60
0·70
0·80
0·90
1·00
MOLE FRACTION CARBON TETRACHLORIDE IN LIQUID PHASE

FIGURE XXXV. Activity Coefficients versus Mole Fraction Carbon Tetrachloride in Liquid Phase for the System Benzene-Carbon Tetrachloride at 200°C.

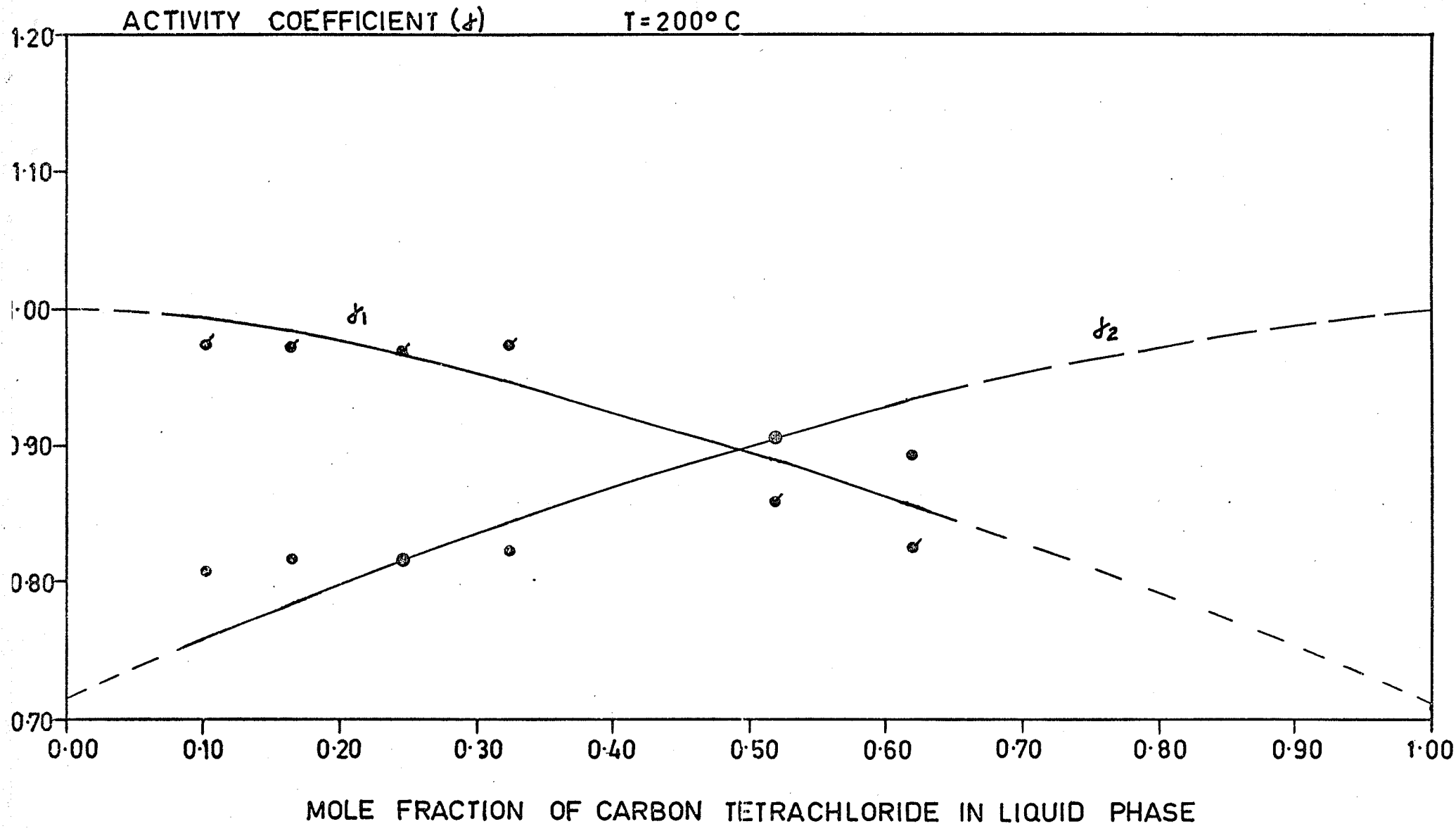
ACTIVITY COEFFICIENT (γ)
T = 200° C
1·20
1·10
1·00
0·90
0·80
0·70
γ1
γ2
0·00
0·10
0·20
0·30
0·40
0·50
0·60
0·70
0·80
0·90
1·00
MOLE FRACTION OF CARBON TETRACHLORIDE IN LIQUID PHASE

FIGURE XXXVI. Activity Coefficients versus Mole Fraction Carbon Tetrachloride in Liquid Phase for the System Benzene-Carbon Tetrachloride at 250°C.

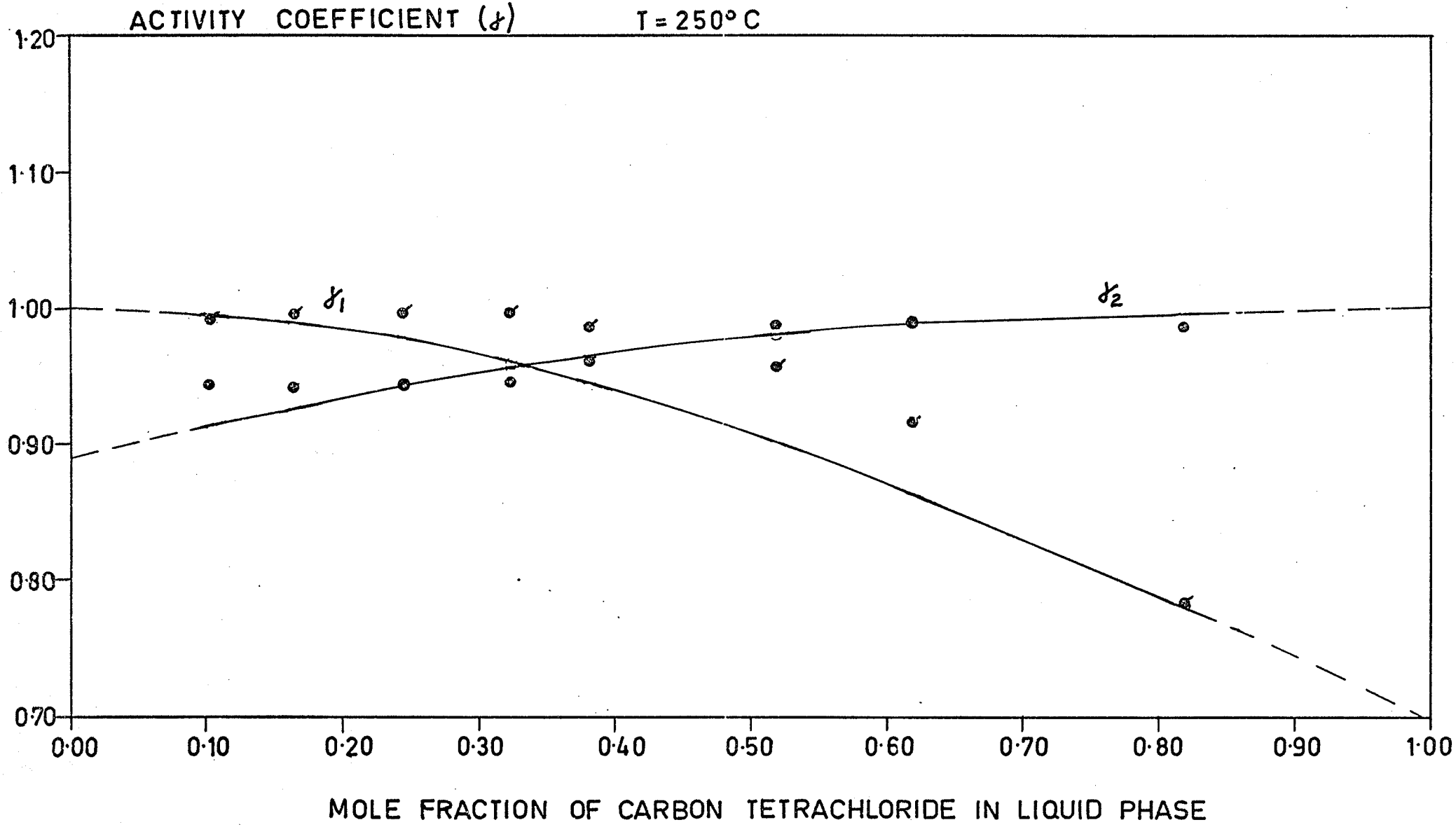
ACTIVITY COEFFICIENT (γ)
T = 250° C
1·20
1·10
1·00
0·90
0·80
0·70
γ1
γ2
0·00
0·10
0·20
0·30
0·40
0·50
0·60
0·70
0·80
0·90
1·00
MOLE FRACTION OF CARBON TETRACHLORIDE IN LIQUID PHASE

FIGURE XXXVII. Activity Coefficients versus Mole Fraction Carbon Tetrachloride in Liquid Phase for the System Benzene-Carbon Tetrachloride at 270°C.

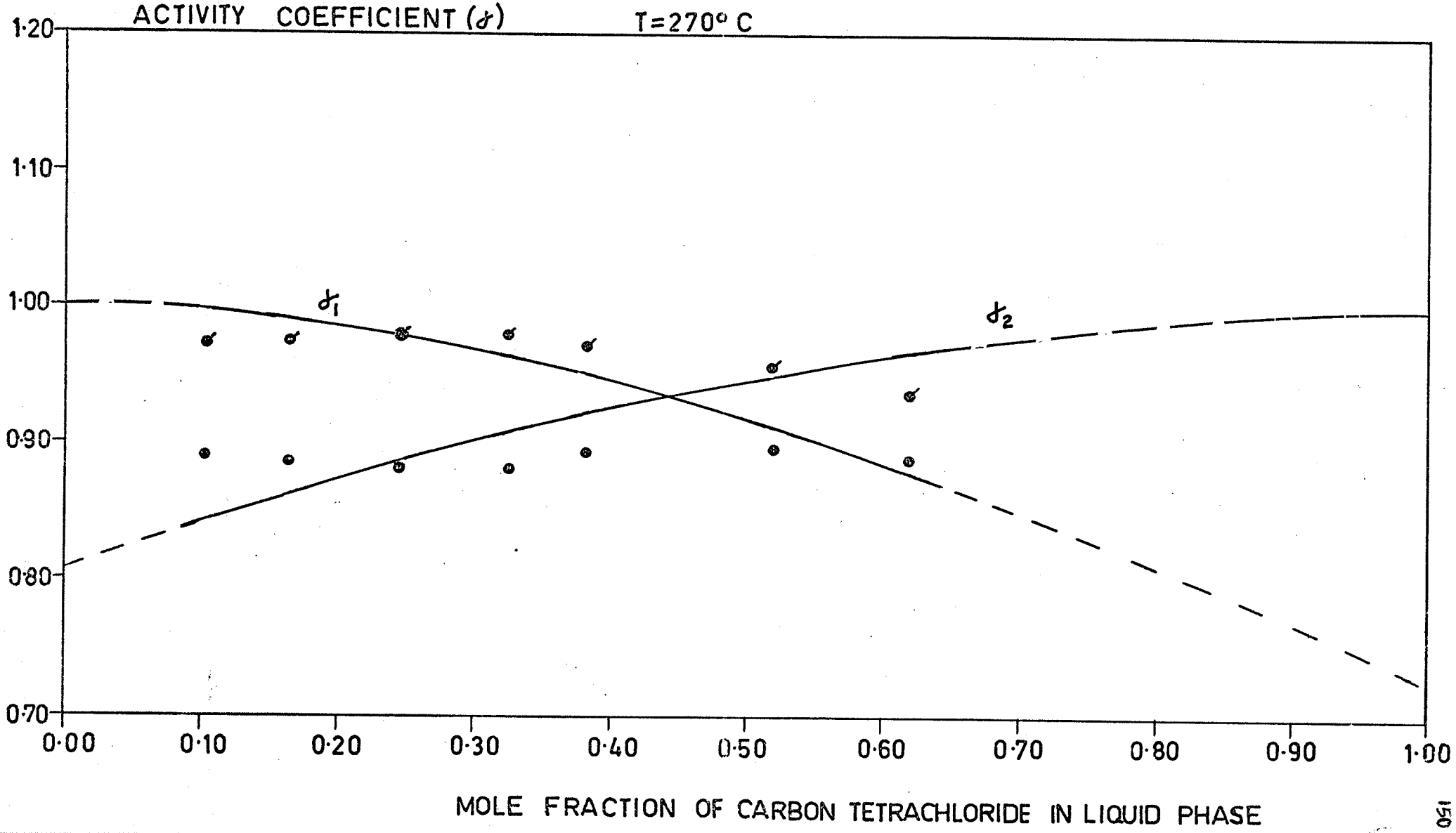
ACTIVITY COEFFICIENT (γ)
T=270° C
1·20
1·10
1·00
0·90
0·80
0·70
γ1
γ2
0·00
0·10
0·20
0·30
0·40
0·50
0·60
0·70
0·80
0·90
1·00
MOLE FRACTION OF CARBON TETRACHLORIDE IN LIQUID PHASE

V (C) General Discussion

In liquid mixtures, deviations from ideal behaviour can be interpreted in terms of intermolecular forces operating within the mixture. It is convenient to distinguish between strong attractive (chemical) forces leading to formation of chemical species and weak attractive (physical) forces frequently called van der Waals forces. Accordingly, the theory of liquid solutions has followed two distinct paths: (1)The work of Kortüm and Buchholz-Meisenheimer (108) which interprets solution non ideality in terms of chemical forces while neglecting physical forces and (2) the work initiated by van Laar (109) who interprets solution non ideality in terms of physical forces alone.

In the first case, it was assumed that in a mixture of "apparent" components A and B the "true" molecular species in the mixture may not only be molecules A and B but may also include molecules A_2, A_3 ....., B_2, B_3 ....., AB, A_2B .....etc. Van Laar, on the other hand, denied the existence of any molecular species other than A and B and explained deviations from Raoult's law in terms of differences among intermolecular forces acting among A-A, A-B and B-B.

It is now accepted that the above views are extreme representations of the actual situation; the borderline between chemical and physical forces is arbitrary and in many cases, designation of a mixture as "chemical" or "physical" is a matter of convenience only. However, while it is reasonable to assume that chemical forces are absent from simple solutions of saturated non-polar liquids, it is

not reasonable to neglect chemical forces in liquid mixtures where hydrogen bonding or charge-transfer complexing is appreciable. And it is not strictly correct to neglect physical forces entirely in "chemical solutions". A physically more reasonable description of liquid solutions should make allowance for both chemical and physical forces. Work in this direction has been carried out by Scatchard (110) and Harris and Prausnitz (111).

It has been shown (109) that positive deviations from Raoult's law are favored by differences in "internal pressure" or molecular attractive force and that negative deviations are favored by a tendency to compound formation between the two components or by a marked difference in size.

The system Acetone-Chloroform investigated in the present project shows a negative deviation from Raoult's law, and as pointed out earlier, Campbell and Kartzmark (82) have proven the existence of a 1:1 compound in the solid phase in this system. They proposed hydrogen bonding in the compound

$$(CH_3)_2CO \cdots\cdots\cdots H - C(Cl)_2 - Cl$$

Many theoretical and semi-theoretical treatments have been given for this system (112,113). Although there is no doubt about the presence of hydrogen bonding as evident from the results of ultraviolet spectroscopy (113) and proton magnetic resonance (114), complications arise when one attempts to construct a theory, because of the fact that both acetone and chloroform are known to associate in the pure state.

Table XIII shows that the one parameter model of the van Laar equation is not successful in reproducing activity coefficients for the system Acetone-Chloroform at temperatures of 150°, 160°, 170° and 180°C, that is, at temperatures where both components can exist as liquids. The dilated van Laar model of Chueh et al (50) is based on the assumption that the non ideality of liquid mixtures is due to the interaction of solute molecules with each other in the environment of the solvent molecules and not to interactions between the solute and solvent molecules. I am not too certain whether such a model would apply to the system Acetone-Chloroform. And furthermore, Prausnitz and Chueh's theory (50) applies mostly to non-polar or slightly polar components; both acetone and chloroform are polar compounds.

The solution model of Prausnitz et al would not strictly apply to the system Acetone-Carbon tetrachloride. Table XIV shows that the one parameter model of the van Laar equation is fairly successful in reproducing activity coefficients for the temperatures 150° and 200°C. The two parameter model applied at temperatures where one of the components (acetone) is supercritical, is apparently not very successful - See Table XV . The same conclusion was obtained by Chatterjee (80) who used the two parameter model for the system Acetone-Benzene at temperatures higher than 200°C.

The system Benzene-Carbon tetrachloride, consisting of two non-polar components, should be the ideal system to test the solution model of Prausnitz et al (50). It has been shown (115) that the deviation of the physical properties from the rule for mixtures in the above system can be ascribed to the association of the carbon tetra-

chloride. Table XVI shoes that the one parameter solution model of the van Laar equation gives satisfactory results for the activity coefficients for the tmperatures 150^{o}, 200^{o}, 250^{o} and 270^{o}C but why the activity coefficients are so far away from unity I cannot explain. I expected the activity coefficients for this system to be nearly one at all concentrations. Interaction between the benzene molecules and carbon tetrachloride molecules would, in my opinion, explain partially this discrepancy.

An extension of the solution model of Prausnitz et al (50) which gives consistently good results for mixtures of non-polar or slightly polar components, must be made to polar components to make it more general. And finally, since certain simplifying assumptions must be made in all theories of liquid mixtures as a consequence of insufficient knowledge about intermolecular forces, and also because of the lack of extensive experimental data, any general theory must await accurate and extensive experimental data on equilibrium properties of mixtures, especially those containing polar components.

SUMMARY

This thesis has dealt with the following thermodynamic properties of the systems (1)Chloroform-Acetone, (2)Carbon Tetrachloride-Acetone, and (3)Benzene-Carbon Tetrachloride: - gas $\rightleftharpoons$ liquid critical temperatures, vapor $\rightleftharpoons$ liquid equilibrium compositions and saturation vapor pressures. The gas $\rightleftharpoons$ liquid critical temperatures were measured for each binary system over the whole concentration range using the disappearance of the meniscus method. The vapor $\rightleftharpoons$ liquid equilibrium compositions were determined for each binary system using a glass apparatus with a steel bomb. Measurements were made at temperatures ranging from 100°C to 270°C. The saturation vapor pressures were measured using a closed air-manometer and the pressure calculated from the equilibrium volume of compressed air using van der Waals equation.

The experimental data were treated thermodynamically to yield the non-idealities in each of the two phases in the vapor $\rightleftharpoons$ liquid equilibria. An equation of state suggested by Redlich and Kwong was found to be very satisfactory and simple in the calculations of the fugacity coefficients of both components in the vapor phase. The dimensionless constants Ωa and Ωb in the Redlich-Kwong equation were re-evaluated from the saturated volumetric properties of each pure component. The Redlich-Kwong equation, modified by Prausnitz and Chueh, and containing a binary interaction constant, was found to be very satisfactory for the binary mixtures. Liquid-phase non-idealities were obtained from a modified van Laar equation. The one-parameter solution model was used for all three systems at temperatures lower than 200°C and it was found to be fairly successful. For the system

Acetone-Carbon tetrachloride at 250^{o} and 270^{o}C the two-parameter solution model was used but even then the results were not quite satisfactory.

To show the effect of pressure on liquid phase properties, the partial molal liquid volumes were calculated using a liquid phase equation of state coupled with an extension to mixtures, of the corresponding-states correlation of Lyckman et al. The pressure correction (Poynting correction) to the activity coefficient in the liquid phase was then calculated from the partial molal volumes. To show the dependence of activity coefficients on compositon, they have been plotted as functions of the composition of one component in the liquid phase.

The present study shows that the solution model of Prausnitz et al has to be extended to include polar components to make it more general. Finally, because the calculations involved in the computer programs depend so much on the characteristic energy between two dissimilar molecules, more work has to be done to evaluate these potentials.

APPENDIX

The programs SYMFIT, HENRYS, FITTING and the subroutines VOLPAR, PHIMIX and CUBEQN used in the data are given in Appendix D of the monograph by Prausnitz and Chueh (50). The information for the input data used in these programs was obtained as follows:

Tc, Pc and Vc for the four pure components were obtained from Chatterjee (80). They are given below:

Substance	Tc(^{o}C)	Pc(atm)	Vc(cc/gmole)
Acetone	235.0	46.96	213.5
Benzene	288.5	48.22	260.1
Chloroform	263.2	52.59	243.56
Carbon Tetrachloride	283.15	44.98	279.6

The acentric factor ω was calculated from equation (81)

$$\omega = - \log P_R \Big|_{T_R = 0.7} - 1.00 \qquad (81)$$

and the vapor pressure of the pure components. The values obtained were 0.309, 0.192, 0.211 and 0.207 for acetone, carbon tetrachloride, benzene and chloroform respectively.

The dimensionless constants Ωa, Ωb in the Redlich-Kwong equation were obtained by fitting the Redlich-Kwong equation (24) to the volumetric data of the pure saturated vapor and pure saturated liquid.

	Liquid Phase		Vapor Phase	
	Ωa	Ωb	Ωa	Ωb
Acetone	0.3900	0.0745	0.4600	0.0940
Benzene	0.4100	0.0787	0.4450	0.0904
Chloroform	0.4071	0.0847	0.4176	0.0872
Carbon Tetrachloride	0.4172	0.0868	0.4276	0.0841

The universal values commonly used are $\Omega_a = 0.4278$ and $\Omega_b = 0.0867$.

The corrections to geometric mean for Tc_{12}, K_{12} for the vapor and for the liquid were obtained from equation (36) and Table V. The same value was used for both the vapor and liquid. The value of K_{12} used was 0.01 for the three binary systems.

The critical binary constant $2\tau_{12}/(Tc_1 + Tc_2)$ was 0.008 for the Acetone-Chloroform system, -0.033 for the Carbon Tetrachloride-Acetone system and -0.0030 for the Benzene-Carbon Tetrachloride system. The correlating parameter for critical volumes $2\nu_{12}/(Vc_1 + Vc_2)$ estimated from the generalized chart (50) was -0.0350 for the Acetone-Chloroform system, -0.1240 for the Acetone-Carbon Tetrachloride system and -0.040 for the Benzene-Carbon Tetrachloride system.

BIBLIOGRAPHY

1. C. de la Tour, Ann.Chim. (3) 21, 127 (1822)

2. T. Andrews, Phil.Trans. 159, 575 (1869)
   Proc.Roy.Soc.(London) 18-42 (1869)

3. J.D. Van der Waals, Doctoral Dissertation, Leiden, The Netherlands, 1873.

4. G. Woolsey, J.Chem.Educ. 16, 60 (1939)

5. O. Maass, Chem.Rev. 23, 17 (1938)

   S.G. Mason, S.N. Naldrett and O.Maass, Can.J.Research 18B 103 (1940)

   S.N. Naldrett and O.Maass, Can.J.Research 18B, 118 (1940)

6. Cailletet and Colardeau, Compt.rend. 108, 1280 (1889)

7. Hannay and Hogarth, Proc.Roy.Soc.(London) 30, 178 (1880)

8. Hagenbach, Drude Ann. 5, 276 (1901)

9. J.P. Kuenen, Die Zustandsgleichung der Gase und Flüssigkeiten und die Kontinuitäts theorie-Vieweg und Sohn, Braunschweig (1907)

10. A.W. Porter, Phil.Mag. 7, 624 (1929)

11. J.E. Mayer and S.F. Harrison, J.Chem.Phys. 6, 87, 101 (1938)

12. J.E. Mayer and M.G. Mayer, "Statistical Mechanics", John Wiley and Sons, Inc., New York 1960 (Chapter 14)

13. M.A. Weinberger and W.G. Schneider, Can.J.Chem 30, 422 (1952)

    K.E. MacCormack and W.G. Schneider, Can.J.Chem. 29, 699 (1951)

    W.G. Schneider and H.W. Habgood, J.Chem.Phys. 21, 2080 (1953)

14. S.G. Whiteway and S.G. Mason, Can.J.Chem. 31, 569 (1953)

15. "Symposium on Critical Phenomena in Magnetism", J.Appl. Phys. 37, No. 3, 1172 (1966)

16. "Proceedings of the International Conference on Phenomena near Critical Points, Washington, 1965", NBS Misc. Publication No. 273, (1966)

17. O.K. Rice, Chem.Rev. 44, 69 (1949)

18. O.K. Rice, "Thermodynamics and Physics of Matter", edited by F.D. Rossini, Princeton University Press, Princeton, N.J. 1955.

19. J.S. Rowlinson, "Liquids and Liquid Mixtures", Butterworths Scientific Publications, London 1959.

20. R. Clausius, "Die Kinetische Theorie der Gase", F. Vieweg und Sohn, Braunschweig, 1889, Chap. II.

21. Rankine, from J.P. Joule and W.Thomson, "On the Thermal Effects of Fluids in Motion, Part II", Phil. Trans. 144, 336-7 (1854)

22. J.D. Van der Waals, "Over de Continuitet van den Gas en Vloeisoffoestand", Leyden 1873; tr. Threlfall and Adair, 1890, cf.

H.V. Jüptner, "Verdampfungsstudien,II", Z.Physik.Chem. 63 579-618 (Heft 5, 1908) and "Verdampfungsstudien V", Z.Physik.Chem. 73, 343-82 (Heft 3, 1910)

23. M.E. Fisher, J.Appl.Physics 38, 981 (1967)

24. M.E. Fisher, Rept.Progr.Phys. 30, 615 (1967) The Institute of Physics and Physical Society, London.

25. P. Heller, Rept.Progr.Phys. 30, 731 (1967) The Institute of Physics and Physical Society, London.

26. J.V. Sengers and A.Levelt-Sengers, Chem.Eng.News 46, No. 25, 104 (1968)

27. L. Onsager, Phys.Rev.65, 117 (1944) and Physical Society Cambridge Conference Report p.137 (1947)

28. M. Fierz, Helv.Phys.Acta. 24, 357 (1951)

29. J.De Boer, Changement de Phases, C.R. Deuxieme Reunion de Chimie Physique, Paris p. 8 (1952)

30. M.E. Fisher, Lectures in Theoretical Physics VII C (University of Colorado Press, Coulder) p. 1-159 (1965)

31. J.W. Essam and M.E. Fisher, J.Chem.Phys. 38, 802 (1963)

32. E.A. Guggenheim, J.Chem.Phys. 13, 253 (1945)

33. O.K. Rice, J.Chem.Phys. 23, 164 (1955)

34. O.K. Rice, J.Chem.Phys. 23, 169 (1955)

35. F.E. Murray and S.G. Mason, Can.J.Chem. 30, 550 (1952)

36. H.L. Lorentzen, Acta.Chem.Scand. 7, 1335 (1953)

37. B.Widom and O.K.Rice, J.Chem.Phys. 23, 1250 (1955)

38. B. Widom, J.Chem.Phys. 43, 3898 (1965)

39. B.W. Davis and O.K. Rice, J.Chem.Phys. 47, 5043 (1967)

40. O.K.Rice and D.R. Thompson, J.A.C.S. 86, 3547 (1964)

41. G.N.Lewis and M. Randall, "Thermodynamics and the Free Energy of Chemical Substances", New York, McGraw-Hill Book Co., 1923.

42. J.J.Van Laar, Z.Physik.Chem. 72, 723-51 (1910)
Z.Physik Chem. 83, 599-608 (1913)

43. M. Margules, Sitzber.Akad.Wiss.Math.Naturw. Klasse II 104 1243-78 (1895)

44. G. Scatchard and W.J. Hamer, J.A.C.S. 57, 1805-9 (1935)

45. J. A. Beattie, Chem.Rev. 44, 144 (1949)

46. J. M. Prausnitz,Am.Inst.Chem.Engrs.Journal 5, 3 (1959)

47. J.J. Martin and C.Y. Hou, A.I.Ch.E.Journal 1, 142 (1955)

47A. J. Martin, Ind.And Eng.Chem. 59, 34 (1967)

48. K.K. Shah and G. Thodos, Ind. and Eng.Chem. 57, 30 (1965)

49. O. Redlich and J.N.S. Kwong, Chem.Rev. 44, 233 (1949)

50. P.L. Chueh and J.M. Prausnitz, Ind.andEng.Chem. 60, 35 (1968)
"Computer Calculations for High Pressure Vapor Liquid Equilibria", Prentice Hall 1968.

51. M. Benedict, G.B. Webb and L.C. Rubin, J.Chem.Phys. 8, 334 (1940)
J.Chem.Phys. 10, 747 (1942), Chem.Engr.Progr. 47, 419 (1951)

52. O. Redlich, F.J. Ackerman, R.D. Gunn, M. Jacobson and S. Lau,
a. Ind. and Chem.Eng. (Fundametals) 4, 369 (1965)
b. (Correction) Ind.Eng.Chem.(Fundamentals) 6, No. 4 619 (1967)

53. K.S. Pitzer, in "Thermodynamics", by G.N. Lewis, M.Randall, K.S. Pitzer and Leo Brewer, Appendix 1, McGraw Hill, New York 1961.

54. J. M. Prausnitz and R.D. Gunn, A.I.Ch.E., Journal 4, 430 (1958)

55. P.L. Chueh and J. M. Prausnitz, A.I.Ch.E., Journal 13, 1099 (1967)

56. B.E.F. Fender and G.D. Halsey, J.Chem.Phys. 36, 1881 (1962)

57. E. M. Dantzler, C.M. Knobler and M.L. Windsor, J.Phys.Chem. 72, 676 (1968)

58. J. Joffe, Ind.Eng.Chem. 40, 1738 (1948)

59. T. W. Leland, P.S. Chappelear and B.W. Gamson, Am.Soc.Chem. Engs. Journal 8, 482 (1962)

60. K.S. Pitzer and R.J.Curl, J.Am.Chem.Soc. 79, 2369 (1957)

61. J.P. O'Connell and J.M. Prausnitz, Ind.Eng.Chem. Process Design Develop 6, 245 (1967)

62. J. M. Prausnitz and R.D. Gunn, Am.Inst.Chem.Engrs., Journal 4, 430 (1958)

63. J. M. Prausnitz, Am.Inst.Chem.Engrs. Journal 5, 3 (1959)

64. P. L. Chueh and J.M. Prausnitz, Am.Inst.Chem.Engrs. Journal 13, 896 (1967)

65. M. Orentlicher and J.M. Prausnitz, Can.J.Chem. 45, 595 (1967)

66. E.A. Guggenheim, Thermodynamics, North-Holland Publishing Company, Amsterdam.

67. K. Wohl, Trans.Am.Inst.Chem.Engrs. 42, 215 (1946)

68. N.K. Muirbook, Dissertation, University of California, Berkeley, 1964.

69. E. W. Lyckman, C.A. Eckert and J.M. Prausnitz, Chem.Eng.Sci. 20, 703 (1965)

70. K.S. Pitzer, D. Lippman, R.F. Curl Jr., C.M. Huggins and D.E. Petersen, J.Am.Chem.Soc. 77, 3433 (1955)

71. J.M. Prausnitz, C.E. Eckert, R.V.Orye and J.P. O'Connell, Computer Calcuations for Multicomponent Vapor-Liquid Equilibria, Englewood Cliffs, N.J., Prentice Hall Inc. 1967.

72. W.B. Kay, Ind.Eng.Chem., 28, 1014 (1936)

73. J. Joffe, Ind.Eng.Chem. 39, 837 (1947)

74. W.E. Stewart, S.F. Burkhardt, and D.Voo, Paper presented at A.I.Ch.E. Kansas City Meeting (May 18, 1959).

75. R.C. Reid, and J.K. Sherwood, "The Properties of Gases and Liquids" 2nd Edition, New York, McGraw Hill Book Co.Inc. 1958.

76. F.J. Ackerman and O. Redlich, J.Chem.Phys. 38, 2740 (1963)

77. P.C. Davis, A.F. Bertuzzi, T.L. Gove, and F. Kurata, J.Petrol. Technol. 6, 37 (1954)

78. C.K. Eilerts et al., "Phase Relations of Gas-condensate Fluids", Vol. I Monograph no.10, U.S. Bureau of Mines 1957.

79. J.R. Sutton, "Advancess in Thermophysical Properties at Extreme Temperatures and Pressures", p.76, New York, American Society of Mechanical Engineers, 1965.

80. R. M. Chatterjee, "Orthobaric Volumes and Vapor Pressure of Certain Pure Liquids and Vapor Liquid Equilibria in a Binary Mixture up to the Critical Region", Ph.D. thesis, Winnipeg, 1968.

81. A.N. Campbell, E.M. Kartzmark and H.Friesen, Can.J.Chem. 39, 735 (1961)

82. A.N. Campbell and E.M. Kartzmark, Can.J.Chem. 38, 652 (1960)

83. J.V. Zawidzki, Z.Physik.Chem. 35, 129 (1900)

84. H. Rock and W. Schroder, Z.Physik.Chem. (Frankfurt) 11, 41 (1957)

85. R. M. Chatterjee, "Exesss Volumes, Vapor Pressures, and Vapor Compositions of the Systems Acetone-Chloroform, and Acetone-Chloroform-Benzene.", M.Sc. thesis, Winnipeg 1965.

86. S. Young, "Distillation Principles and Processes", 1922, London, MacMillan.

87. G. Scatchard, S.E. Wood, and J.M. Mochel, J.A.C.S. 62, 712 (1940)

88. R. T. Fowler and S.C. Lim, J.Appl.Chem. 6, 75 (1956)

89. A.N. Campbell and W.J. Dulmage, J.A.C.S., 70, 1723 (1948)

90. G.C. Gerrits, Proc.Acad.Sci.Amst. 7, 167 (1904)

91. W.H.Severns, A.Sesonske,R.H.Perry and R.L. Pigford, J.Am.Inst. Chem.Engrs. 1, 401 (1955)

92. I.Brown and F.Smith, Aust.J.Chem. 10, 423 (1957)

93. S.R.M.Ellis and L.M. Rose, Birmingham University Chemical Engineer, 14,(2) 45 (1963).

94. F. Schwers, Bull.Class.Sci.Acad.Roy.Belgique p.55 (1912)

95. J.Rosin, Reagent Chemicals and Standards, 2nd Edition, New York, Van Nostrand 1946.

96. A.N. Campbell, E. M. Kartzmark and J.M. Gieskes, Can.J.Chem. 41, 407 (1963)

97. W. Reinders and C.H. de Minjer, Rec.Trav.Chim. 59, 207 (1940)

98. I.Brown and F. Smith, Aust.J.Chem. 15, 9 (1962)

99. K.A.Kobe and R. E. Lynn, Chem.Rev. 52, 117 (1953)

100. H.C. Van Ness, "Classical Thermodynamics of Non-electrolyte Solutions", Pergamon Press, New York (1964)

101. S.B. Adler, Leo Friend, R. L. Pigford and G.M. Rosselli, A.I.Ch.E. Journal 6, 104 (1960)

102. P.L. Chueh, N.K. Muirbrook and J.M. Prausnitz, A.I.Ch.E. Journal 11, 1097 (1965)

103. O. Redlich and A.T. Kister, Ind.Eng.Chem. 40, 345 (1948)

104. E.F.G. Herington, Nature 160, 610 (1947)

105. E.W. Lyckman, C.A.Eckert and J.M. Prausnitz, Chemical Engineering Science, 20, 685 (1965)

106. W. Swietoslawski and A. Kreglewski, Bull.de l'Acad.Plonaise des Sciences Cl III-Vol.II, No. 4 (1954) p. 187.

107. J.P. Kuenen and W.G. Robson, Phil.Mag. 3, 149, 622 (1902)

108. G.F.A. Kortüm and H.Buchholz-Meisenheimer, "Die Theorier der Distillation und Extraktion von Flussigkeiten", Springer Verlag, Berlin 1952.

109. J.H. Hildebrand and R.L. Scott, "Solubility of Non-electrolytes", 3rd edition, Chap. Xi, Dover, New York 1964.

110. G. Scatchard, Chem.Rev. 44, 7 (1949)

111. H.G. Harris and J.M. Prausnitz, Iα EC Fundamentals Vol. 8 No. 2, 180-188 (1969)

112. J.A. Barker and F.J. Smith, J.Chem.Phys. 22, 375 (1954)

113. A. Munster, Trans.Faraday Soc. 46, 165 (1950)

114. C.M. Huggins, G.C. Pimentel and J.N. Shoolery, J.Chem.Phys. 23, 1244 (1955)

115. A. Schulze, Z.Physik.Chem. 86, 309-33 (1913)